Aus dem
Lübecker Institut für Experimentelle Dermatologie
Direktor: Prof. Dr. Dr. Enno Schmidt

INVESTIGATING PEMPHIGUS VULGARIS PATHOGENESIS USING A HUMAN SKIN ORGAN CULTURE MODEL

Inauguraldissertation
zum Erwerb des Doktorgrades
der Universität zu Lübeck

- Aus der Sektion Medizin –
vorgelegt von

Hanna Asmussen
aus Bremen

Lübeck 2020

1. Berichterstatterin/Berichterstatter:	Prof. Dr. med. vet. Jennifer Hundt
2. Berichterstatterin/Berichterstatter:	Prof. Dr. rer. nat. Lars Redecke
Tag der mündlichen Prüfung:	21.12.2021

Zum Druck genehmigt. Lübeck, den 21.12.2021

Promotionskommission der Sektion Medizin

DECLARATION

I declare that I have prepared this dissertation without assistance of third parties and have not utilised any personal, technical or factual resources without declaration in the text. Any concepts or quotations applicable to these sources are clearly attributed to them.

This dissertation has not been submitted in the same or a similar version to any other authority.

22.06.2020, Hanna Asmussen

TABLE OF CONTENTS

1 LISTS

1.1 LIST OF ABBREVIATIONS

°C	Degree Celsius
ACN	Acetonitrile
BP	Bullous pemphigoid
BSA	Bovine serum albumin
C18	Octadecyl carbon chain
Ca^{2+}	Calcium
CAA	2-Chloroacetamide
$CaCl_2$	Calcium chloride
cAMP	Cyclic adenosine monophosphate
cm	Centimetre(s)
CO_2	Carbon dioxide
DAPI	4′,6-Diamidin-2-phenylindol
ddH_2O	Double-distilled water
DEJ	Dermal-epidermal junction
dH_2O	Distilled water
DIF	Direct immunofluorescence
DIFC	Desmosome–intermediate filament complex
DMSO	Dimethyl sulfoxide
DP	Desmoplakin
DPBS	Dulbecco’s phosphate-buffered saline
Dsc	Desmocollin
Dsg	Desmoglein
E. coli	*Escherichia coli*
e.g.	*Exempli gratia*
EDTA	Ethylenediaminetetraacetic acid
EGFRK	Epidermal growth factor receptor kinase
ELISA	Enzyme-linked immunoabsorbent assay
ERK	Extracellular signal-regulated kinase
ETA	Exfoliative toxin A
FA	Formic acid
Fab	Antigen binding fragment
FBS	Fetal bovine serum
Fc	Crystallisable fragment
Fig.	Figure
Fv	Variable fragment
g	The relative centrifugal force
g	Gram(s)
Ge	Gel electrophoresis
GuHCl	Guanidine hydrochloride
h	Hour(s)
H + L	Heavy + light

H_2O	Water
HA	Haemagglutinin
HaCaT	Human adult low calcium high temperature keratinocytes
HCl	Hydrochloride
HE	Haematoxylin-Eosin
HEPES	4-(2-Hydroxyethyl)piperazine-1-ethanesulfonic acid
HLA	Human leukocyte antigens
HPG-ALD	Hyperbranched polyglycerol-aldehydes
HSOC	Human skin organ culture
HSP	Heat shock protein
IDP	Inner dense plaque
IgA	Immunoglobulin A
IgG	Immunoglobulin G
IIF	Indirect immunofluorescence
iRT	Indexed retention time
iTRAQ	Isobaric tags for relative and absolute quantitation
IVIg	Intravenous immunoglobulin
kDa	Kilodalton
LC	Liquid chromatography
M	Molar
m / z	Mass-to-charge ratio
m^2	Square metre(s)
mAb	Monoclonal antibody
MAPK	Mitogen activated protein kinase
MEK	MAPK / ERK kinase
MeOH	Methanol
MeV	Multi experiment viewer
mg	Milligram(s)
min	Minute(s)
mL	Millilitre(s)
mM	Millimolar
mm	Millimetre(s)
MMP	Matrix metalloprotease
mRNA	Messenger ribonucleic acid
MS	Mass spectrometry
ms	Millisecond(s)
mTOR	Mammalian target of rapamycin
n	Number
$NaBH_3CN$	Sodium cyanoborohydride
NaOH	Sodium hydroxide
NC	Negative control
NE	Neutrophil elastase
NH_4HCO_3	Ammonium hydrogen carbonate
NH_4HCO_4	Ammonium bicarbonate
NHEK	Normal human epidermal keratinocytes
nL	Nanolitre(s)
nm	Nanometre(s)
O.C.T.	Optimal cutting temperature

ODP	Outer dense plaque
PBS	Phosphate-buffered saline
PCT	Pressure cycling technologies
PF	Pemphigus foliaceus
PG	Plakoglobin
pH	The decimal logarithm of the reciprocal of the hydrogen ion activity
PKC	Phosphokinase C
PKP	Plakophilin
PLC	Phospholipase C
psi	Pound-force per square inch
PV	Pemphigus vulgaris
Rho	Ras homolog
rpm	Revolutions per
s	Second(s)
scFv	Single chain variable fragment
SDS	Sodium lauryl sulfate
SEM	Standard error of the mean
STAGE	Stop and go extraction
TAILS	Terminal amine isotope labelling of substrates
TBS	Tris-buffered saline
TCEP	Tris(2-carboxyethyl) phosphine hydrochloride
TFA	Trifluoroacetic acid
TMT	Tandem mass tag
TRIS	Tris(hydroxymethyl)aminomethane
VF	Visual field
µL	Microlitre(s)
µM	Micromolar
µm	Micrometre(s)

1.2 LIST OF FIGURES

1.3 LIST OF TABLES

2 INTRODUCTION

2.1 STRUCTURE OF THE HUMAN SKIN

2.1.1 GENERAL

With approximately 1.5–2 m^2 surface area and a percentage share of 7–8 % of the total body weight, the skin is by far the human's largest organ with various purposes. Its main passive function is protection. Protection from the cold, the heat, from loss of water, from mechanical influences such as pressure and friction, from toxic substances and also from germs. Additionally, the skin has active functions including the protection against infiltrated pathogenic germs (bacteria and viruses) and allergens. It is also able to take up active components, to perspire and release sebum and also to regulate the body temperature via perfusion. Furthermore, the skin enables us to register our surroundings by providing sensory perception (*e.g.*: pressure, temperature and pain).

The human skin has three classified layers: epidermis, dermis and subcutis (**FIG. 1**).

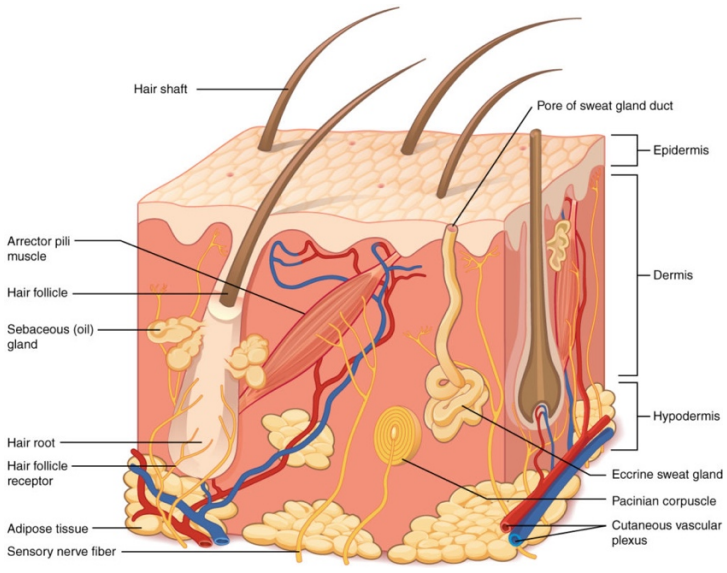

FIG. 1: STRUCTURE OF THE HUMAN SKIN
The human skin is composed of three layers: the epidermis, mainly made of closely packed keratinocytes, the dermis, made of connective tissue housing several structures such as sweat glands and hair follicles, and the subcutis (= hypodermis) which is made of fatty and loose connective tissue. Adapted from (OpenStax 2013).

2.1.2 EPIDERMIS

The epidermis consists of mostly keratinised, stratified squamous epithelium, primarily built by keratinocytes (approximately 90 % of all cells). Along the basal membrane of the epidermis pigmented cells (melanocytes) can be found, as well as the tissue resident macrophages of the skin (Langerhans cells) and sporadic Merkel cells.

The epidermis is divided into four different layers according to the differentiation status and morphology of the keratinocytes. The *stratum corneum* is the outermost layer, composed of cornified anucleate keratinocytes. This layer provides most of the protection against mechanical stressors, hence, it is especially pronounced on the insides of the hands and also the sole of the foot. The next layer in a descending order is the *stratum granulosum* which contains granulated keratinocytes losing their nuclei. The *stratum spinosum* shows big polygonal keratinocytes with pointed protrusions. In this layer, the keratinocytes are attached to each other by cell-cell adhesion structures called desmosomes.

The lowermost layer of the epidermis is the *stratum basale*. It is made up of one layer of basal keratinocytes containing the stem cells for the epidermal regeneration. Differentiation of one keratinocyte takes approximately four to six weeks from the *stratum basale* to the *stratum corneum*.

The *stratum basale* is attached to the basal membrane and a part of the dermal-epidermal junction (DEJ). The DEJ constitutes the connection between the epidermal and dermal layers of the human skin (**FIG. 2**):

The basal keratinocytes of the epidermis are attached to the *lamina lucida* of the basal membrane by hemidesmosomes. Microfilaments (laminin 332, integrin α6β4 and collagen type XVII) connect the hemidesmosomes to the *lamina densa* by running through the *lamina lucida* of the basal membrane. The basal membrane is a porous filter, allowing cell and fluid exchange and is attached to the dermis by collagen type I and VII and anchoring fibrils (Fenner and Clark 2016).

Defects in the DEJ are important factors for the development of skin blistering diseases (Sterry and Czaika 2018).

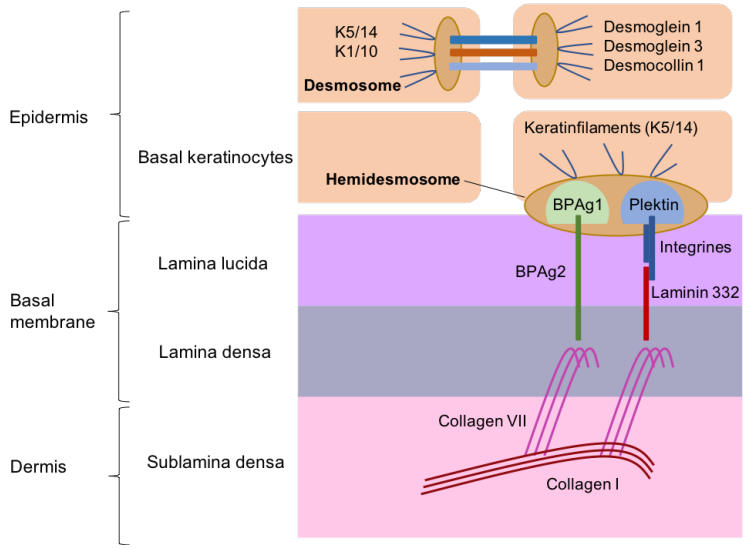

FIG. 2: STRUCTURE OF THE DERMAL-EPIDERMAL JUNCTION ZONE
The dermal-epidermal junction is the interface between the epidermis and the dermis. Listed here are several components that might lead to skin blistering in case of dysfunction. BPAg2 = bullous pemphigoid antigen 2; K = Keratin

2.1.2.1 DESMOSOMES

Desmosomes are the structures which are responsible for strong intercellular adhesion in epithelia and the cardiac muscle and for maintaining the integrity of the epidermis. They are composed of three regions: the extracellular core, the outer dense plaque (ODP) and the inner dense plaque (IDP) (**FIG. 3**). Transmembrane glycoproteins called desmosomal cadherins make up the extracellular core and provide adhesion by binding to the extracellular N-terminal of their opposing counterpart. Intracellularly, the desmosomal cadherins interact with plakoglobin (PG) and plakophilin (PKP) which are both armadillo proteins. The binding site between the cadherins and PG and PKP builds the ODP. On the opposite side, PG and PKP bind to desmoplakin (DP) which connects to the cytoskeletal intermediate filaments and is located within the cytoplasmic IDP.

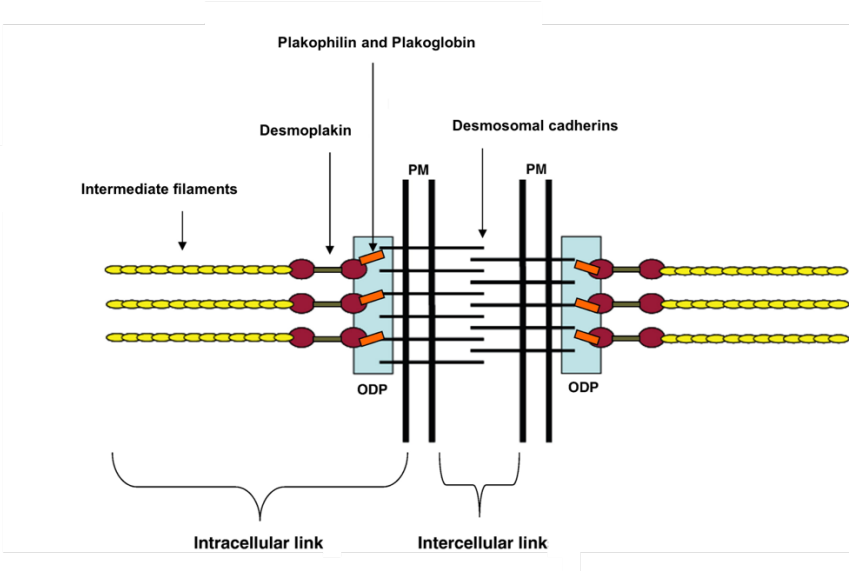

FIG. 3: SCHEMATIC DESMOSOMAL STRUCTURE
The human desmosome is made of one intercellular link created by desmosomal cadherins and two intracellular links between the intermediate filaments and desmoplakin and between desmoplakin and the armadillo proteins plakophilin and plakoglobin. ODP = Outer dense plaque; PM = plasma membrane. From (Garrod and Chidgey 2008).

There are two types of desmosomal cadherins: desmoglein (Dsg) with four isoforms (Dsg 1, Dsg 2, Dsg 3, Dsg 4) and desmocollin (Dsc) with three isoforms (Dsc 1, Dsc 2, Dsc 3). The desmosomal cadherins contain four calcium (Ca^{2+}) -dependent cadherin repeats (EC 1, EC 2, EC 3, EC 4) of approximately 110 amino acids each in their extracellular domains. In addition to the extracellular domains, cadherins have a membrane-proximal extracellular anchoring domain (Nose, Tsuji *et al.* 1990). The different isoforms of Dsg and Dsc are being expressed differently depending on the location (Evangelista, Culton *et al.* 2015). Dsg 1 and Dsc 1 are the predominant desmosomal cadherins in the skin, with the highest expression in the upper epidermal layers, whilst Dsg 3 and Dsc 3 are expressed in the lower epidermal layers (**FIG. 4**). Dsg 4 can be found in hair follicles and Dsg 2 is located in every tissue with desmosomes.

2.1.3 DERMIS

The dermis is structured in two layers: the *stratum papillare* which is closer to the epidermis and made from loose connective tissue containing elastic fibres and collagen type I and III and the *stratum reticulare* which is made of a dense

connective tissue and provides the skin's elasticity. It is also responsible for the variable thickness of the skin depending on the body region. The primary cell type of the dermis is the fibroblast which can produce collagen, elastin and other proteins. The dermis has a distinct vascular and nervous network. It contains many structures such as blood and lymph vessels and sensory receptors for pain, pressure and mechanical stress (**FIG. 1**). Eccrine perspiratory glands that can be found in the dermis are responsible for thermoregulation, whilst apocrine glands mostly found in the dermis of the axilla, around the mammilla and the anogenital area, produce a fatty exudate. Moreover, hair follicles and sebaceous glands are present.

2.1.4 SUBCUTIS

The subcutis (= hypodermis) is the cushion between the dermis and the underlying muscular and skeletal components. It mostly consists of adipocytes and connective tissue. Its main functions are the insulation to prevent heat loss, cushioning to protect underlying structures and the stored fat can provide an energy reserve.

2.2 PEMPHIGUS VULGARIS

2.2.1 GENERAL

Pemphigus vulgaris (PV) is a subtype of the autoimmune skin blistering disease pemphigus which is mediated through autoantibodies. Diseases of the pemphigus group are characterised by suprabasilar blistering of the skin. There are two major types of pemphigus disease, one being PV with nearly 80 % of all pemphigus cases and the other one being pemphigus foliaceus (PF). The less frequent subgroups include paraneoplastic pemphigus and immunoglobulin A (IgA) -pemphigus.

2.2.2 EPIDEMIOLOGY

The incidence of the PV depends on the population (Alpsoy, Akman-Karakas *et al.* 2015). For Germany, the estimated incidence is approximately 0.5 cases per one million people per year (Bertram, Brocker *et al.* 2009), whilst in other European

countries this number can be as much as sixteen times as high (Michailidou, Belazi *et al.* 2007). On average, the disease manifests between the age of 45 and 60 years and it preferentially affects the female sex (Alpsoy, Akman-Karakas *et al.* 2015; Shah, Seiffert-Sinha *et al.* 2015)

2.2.3 AETIOLOGY

PV is an autoimmune skin blistering disease meaning immunoglobulin G (IgG) autoantibodies against the desmosomal structure proteins Dsg 1 and Dsg 3 can be found in PV patients. The binding of the IgG autoantibodies to Dsg 1 and Dsg 3 causes the keratinocytes to separate from each other, this process is called acantholysis.

There is a known association between several human leukocyte antigens (HLA) class II alleles and a higher susceptibility to PV (Sinha 2011), but the exact correlation is still unclear.

Several triggers are currently being discussed including drugs such as angiotensin-converting-enzyme inhibitors, certain antibiotics and diuretics. Also, impairment of the skin through ultraviolet radiation, certain dietary factors or virus infections may trigger PV outbreak (Ruocco, Ruocco *et al.* 2013).

2.2.4 CLINICAL SYMPTOMS

Due to intraepidermal blistering of the skin in PV the blisters have very thin roofs causing them to easily rupture and result in an enanthema and erosions (**FIG. 4**). In active disease, PV patients show a positive Nikolsky sign which means shearing of healthy-appearing skin with sideward friction can mechanically induce further erosions. These erosions can be seen on mucous membranes and also on the skin (**FIG. 4**) whilst in PF the erosions are limited to the skin.

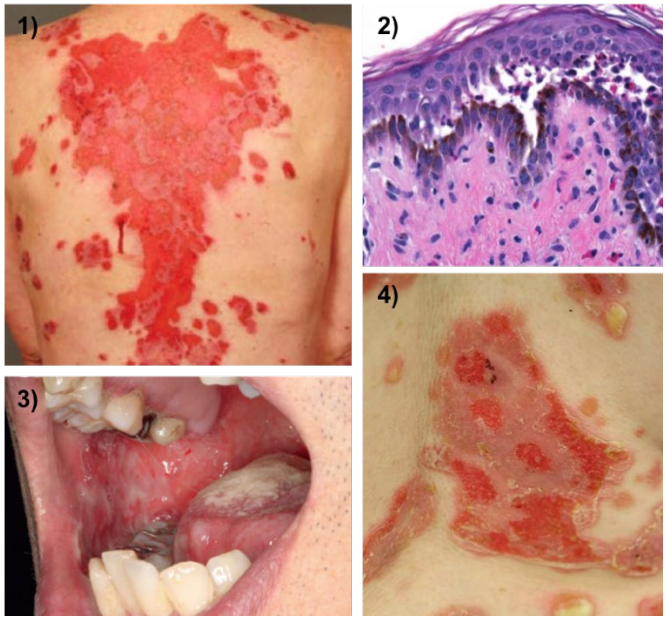

FIG. 4: CLINICAL CHARACTERISTICS OF PEMPHIGUS VULGARIS
1) Large erosions on the back of a pemphigus vulgaris patient.
2) Split formation just above the basal cell layer within the epidermis.
3) Erosions on buccal mucosa around the teeth and also tongue.
4) Flaccid, superficial blisters and erosions.
Pictures modified from (Hammers and Stanley 2016) (1, 2), (Kasperkiewicz, Ellebrecht *et al.* 2017) (3) and (Didona, Maglie *et al.* 2019) (4).

PV can manifest as a mucosal-dominant, mucocutaneous or the less frequent exclusively cutaneous type depending on the anti-Dsg antibody profile (Amagai, Tsunoda *et al.* 1999). Accordingly to the location of the erosions, patients may present with symptoms such as burning pain, dysphagia or hoarseness (Mahmoud, Miziara *et al.* 2012). All these symptoms reduce the quality of life of PV patients profoundly.

2.2.5 PATHOMECHANISMS

2.2.5.1 DESMOGLEIN COMPENSATION THEORY

The Dsg compensation theory was proposed in 1999 by Amagai and Stanley: when co-expressed in the same cell, Dsg 1 and Dsg 3 compensate one another meaning the existence of one Dsg type is adequate to maintain the sound condition of the mucosa or skin (Amagai, Koch *et al.* 1996; Amagai 1999). This model is based on the findings that showed the difference in distribution of Dsg between skin and

mucosa (**FIG. 5**). Dsg 1 is expressed weakly in the mucous membranes throughout all layers whilst it is very strongly expressed in the skin, especially in the superficial layers of the epidermis. Dsg 3 on the other hand is pronounced only in the basal layers of the skin and expressed very strongly in all layers of the mucosa (Pan, Liu *et al.* 2011).

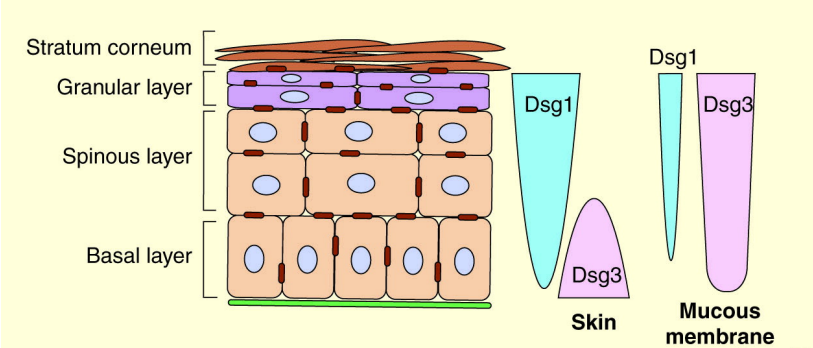

FIG. 5: DISTRIBUTION OF DESMOGLEIN 1 AND 3 IN THE SKIN AND MUCOUS MEMBRANES

Desmoglein (Dsg) 1 is expressed throughout all layers of the epidermal skin, especially in the more superficial layers. Dsg 3 can only be found in the basal layer of the epidermis. Contrarywise in the mucous membranes, Dsg 3 is expressed very strongly throughout all layers whilst Dsg 1 is only weakly pronounced and even weaker around the basal than the more superficial layers. Adapted from (Ishii and Green 2001).

The known antigen for PF is Dsg 1 which is expressed in the superficial layers of the epidermis. In case of dysfunction of Dsg 1, erosions in the superficial layers of the skin can be seen in PF patients, where there is no co-expression of Dsg 3. No lesions can be found in the basal layer where Dsg 3 is pronounced and compensates the dysfunction of Dsg 1. Dsg 3 is expressed in all layers of the mucous membranes and can compensate a possible Dsg 1 dysfunction, hence, PF patients show only superficial skin lesions, but no lesions in the mucosa (**FIG. 6**).

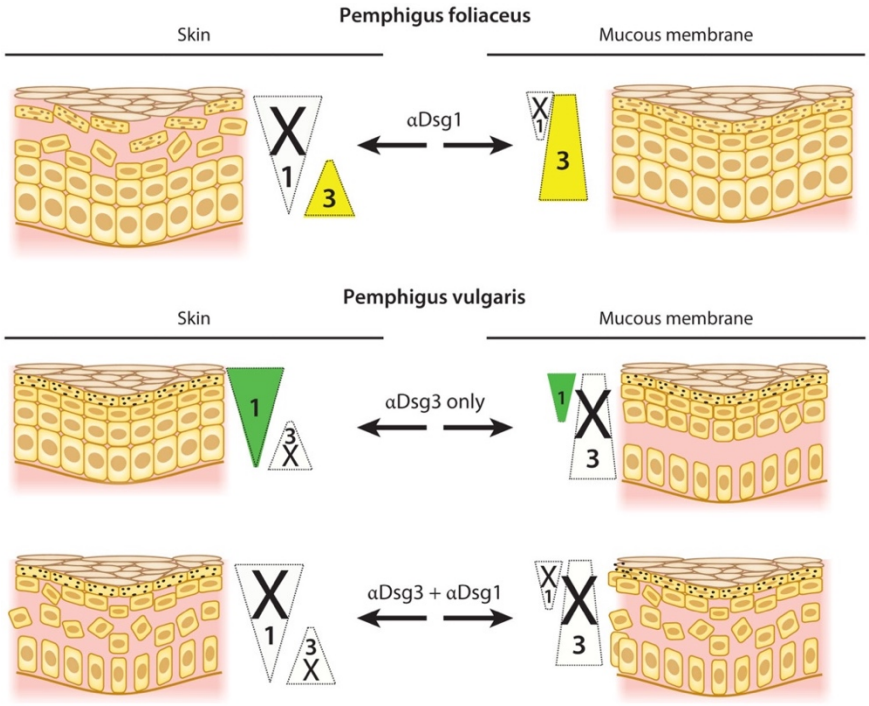

FIG. 6: DESMOGLEIN COMPENSATION THEORY
The distribution pattern of desmoglein in the skin and mucous membranes can explain the corresponding blister formation in pemphigus diseases. Adapted from (Hammers and Stanley 2016).

For PV, the different clinical types of presentation can also be explained with this model. Patients showing the mucosal-dominant type *e.g.* express mainly the antigen Dsg 3. A Dsg 3 dysfunction alone cannot lead to blister formation within the skin because of the co-expression and compensation of Dsg 1. However, in the mucous membranes the low concentration of Dsg 1 is not sufficient enough to compensate the Dsg 3 dysfunction causing blisters. The same theory can be applied to the cutaneous and mucocutaneous type of PV.
In conclusion, this theory states that the distribution of the anti-Dsg autoantibodies determines the pemphigus typing for PV and PF (Mahoney, Wang *et al.* 1999).

2.2.5.2 DIRECT STERIC HINDRANCE MODEL

This model states that the anti-Dsg 1 and anti-Dsg 3 autoantibodies are directly responsible and also sufficient for the blister formation in PV.
The direct pathogenicity of PV antibodies has been established by several studies. Early on, it could been shown that the passive transfer of IgG from PV patients into

mice can induce the disease (Anhalt, Labib *et al.* 1982). The amino-terminal EC1 and EC2 domains contain important structures for adhesive interactions and precisely these domains are most often targeted by pemphigus autoantibodies (Boggon, Murray *et al.* 2002, Harrison, Brasch *et al.* 2016). Anti-Dsg 3 monoclonal antibodies (mAbs) cloned from both mice and PV patients bind directly to structures mediating *trans*-adhesion (Tsunoda, Ota *et al.* 2003) without relying on transduction of signalling (Heupel, Zillikens *et al.* 2008); (Saito, Stahley *et al.* 2012). Besides, the anti-Dsg 3 mAbs also bind to structures mediating *cis*-adhesion (Di Zenzo, Di Lullo *et al.* 2012).

PV outbreak does not require compliment activation like other autoimmune bullous diseases. It has also been shown that monovalent antibody fragments are sufficient to cause blistering of the skin, indicating that the fragment crystallisable (Fc)-mediated effects are not needed for disease development (Ishii, Lin *et al.* 2008; Payne, Ishii *et al.* 2005).

Furthermore, pemphigus antibodies show a Ca^{2+} stabilised confirmation, just like the adhesive property of cadherins. This suggests that the antibodies bind to just these important adhesive domains (Kamiya, Aoyama *et al.* 2013).

2.2.5.3 DESMOGLEIN NONASSEMBLY DEPLETION HYPOTHESIS

In addition to the direct steric hindrance model explained above, other models with explanations for the loss of cell-cell adhesion have been proposed. These models are most likely not exclusive but may contribute to the pathophysiology of PV.

One of these models is called the Dsg nonassembly depletion hypothesis. The model explains the loss of cell adhesion with the ability of the PV anti-Dsg autoantibodies to cluster and crosslink. This leads to the internalisation of nonjunctional Dsg preventing newly synthesised Dsg from being integrated into the desmosome. Hence, the desmosome is depleted of Dsg and can no longer provide integrity of the skin. The clustering of Dsg 1 and Dsg 3 by the corresponding autoantibody can be detected in patients with PV and PF (Oktarina, van der Wier *et al.* 2011; Van der Wier, Pas *et al.* 2014) and similar events were also shown in cell culture (Aoyama, Owada *et al.* 1999; Jennings, Tucker *et al.* 2011).

Further, monoclonal monovalent anti-Dsg 3 PV antibodies can stop Dsg integration into newly formed desmosomes (Mao, Choi *et al.* 2009).

2.2.5.4 SIGNALLING PATHSWAYS INVOLVED IN PEMPHIGUS

Besides the Dsg nonassembly theory there are several signalling pathways thought to be involved in pemphigus pathogenesis. These pathways are most likely complementing each other and also not opposing but supporting the theories described above.

The signalling pathways involved with PV pathogenesis described in the literature include p38 mitogen activated protein kinase (MAPK) (Cipolla, Park *et al.* 2017), Ras homolog (Rho) GTPases, cyclic adenosine monophosphate (cAMP) (Spindler, Vielmuth *et al.* 2010), the regulator gene c-myc (Williamson, Raess *et al.* 2006), epidermal growth factor receptor kinase (EGFRK) (Bektas, Jolly *et al.* 2013), mammalian target of rapamycin (mTOR) (Pretel, Espana *et al.* 2009), heat shock protein 27 (HSP 27) (Berkowitz, Diaz *et al.* 2008), phospholipase C (PLC) and protein kinase C (PKC) (Sajda and Sinha 2018).

There are also studies suggesting that signalling molecules may be involved in desmosomal homeostasis (Sharma, Mao *et al.* 2007).

2.2.6 DIAGNOSTICS

Histologically, in pemphigus the basal keratinocytes and the cells directly above it loose cell-cell adhesion. This leads to the formation of a suprabasilar intraepidermal blisters which can be seen in a Haematoxylin-Eosin (HE) overview staining of a lesional biopsy specimen.

Immunohistologically, IgG can be found bound to the cell surface within the epidermis. As the hallmark of diagnostics for distinction between intra- and subepidermal blistering the cell surface-bound IgG antibodies can be shown as a honeycomb-like pattern in the direct immunofluorescence (DIF) staining of a biopsy from perilesional skin (**FIG. 7**).

Indirect immunofluorescence (IIF) staining on monkey oesophagus functions as a semi-quantitative screening for anti-Dsg antibodies in the serum of a PV patient by showing the intercellular surface staining of IgG antibodies (**FIG. 7**).
Since there is a known correlation between the levels of serum autoantibodies and the intensity of the disease, enzyme-linked immunoabsorbent assays (ELISA) are used to monitor and predict disease activity (Hertl, Jedlickova *et al.* 2015).

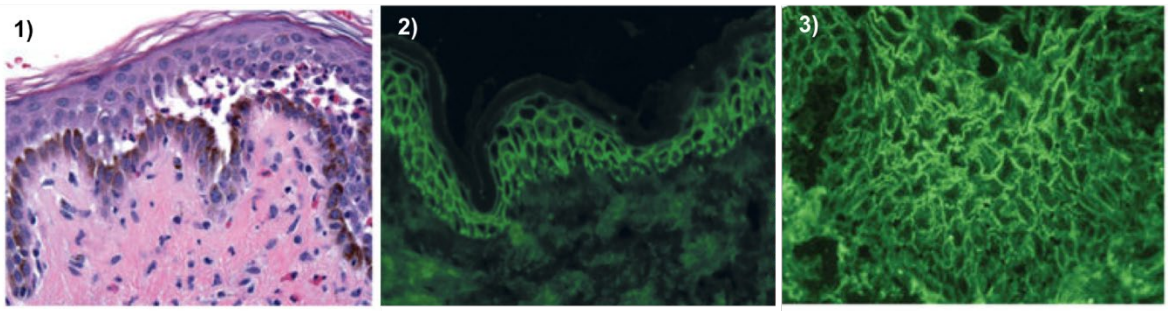

FIG. 7: PEMPHIGUS VULGARIS DIAGNOSTICS
1) Histology of pemphigus vulgaris (PV) showing intraepidermal blistering just above the basal keratinocytes.
2) Direct immunofluorescence staining of perilesional skin showing deposits of immunoglobulin G intercellularly.
3) Indirect immunofluorescence staining of PV autoantibodies on monkey oesophagus.
Modified from (Hammers and Stanley 2016) (1, 3), (Schmidt, Kasperkiewicz *et al.* 2019) (2).

2.2.7 TREATMENT

The current treatment guidelines in Germany (AWMF-S2k-Leitlinie „Diagnostik und Therapie des Pemphigus vulgaris / foliaceus und des bullösen Pemphigoids“ 2019) for PV suggest the intravenous application of prednisolone as the first-line therapy. The use of topic corticosteroids or the alternative off-label use of topic calcineurin inhibitors is also recommended. In case of insufficient clinical improvement, the prednisolone therapy can be supported by adding azathioprine, mycophenolate mofetil or mycophenolic acid. In case of moderate to severe disease development, several other options are available: rituximab (a monoclonal anti-CD20 antibody), intravenous immunoglobulins (IVIg), immunoapharesis, cyclophosphamide or dapsone in addition to prednisolone application. The current treatment options for PV consisting mostly of general immunosuppressant drugs with severe side effects, target the innate and adaptive immune system very unspecifically. Thus, there is great need for the development of new and more specific treatments.

2.2.8 PROGNOSIS

The mortality rate for patients with PV is currently 5-10 %. It was reduced from nearly 100 % by introducing the immunosuppressant therapy options.

2.3 SINGLE CHAIN VARIABLE FRAGMENT

Small antibody fragments, called single chain variable fragment (scFvs) can be used as an alternative to conventional antibodies. ScFvs are fusion proteins consisting of single variable regions of antibody heavy and light (H + L) chains connected by a short, flexible linker peptide (10-25 amino acids) or a disulfide bond (Ahmad, Yeap *et al.* 2012) (**FIG. 8**). The scFv is the most used form of recombinant antibodies due to its low molecular mass (approximately 30 kDa) and simple structure.

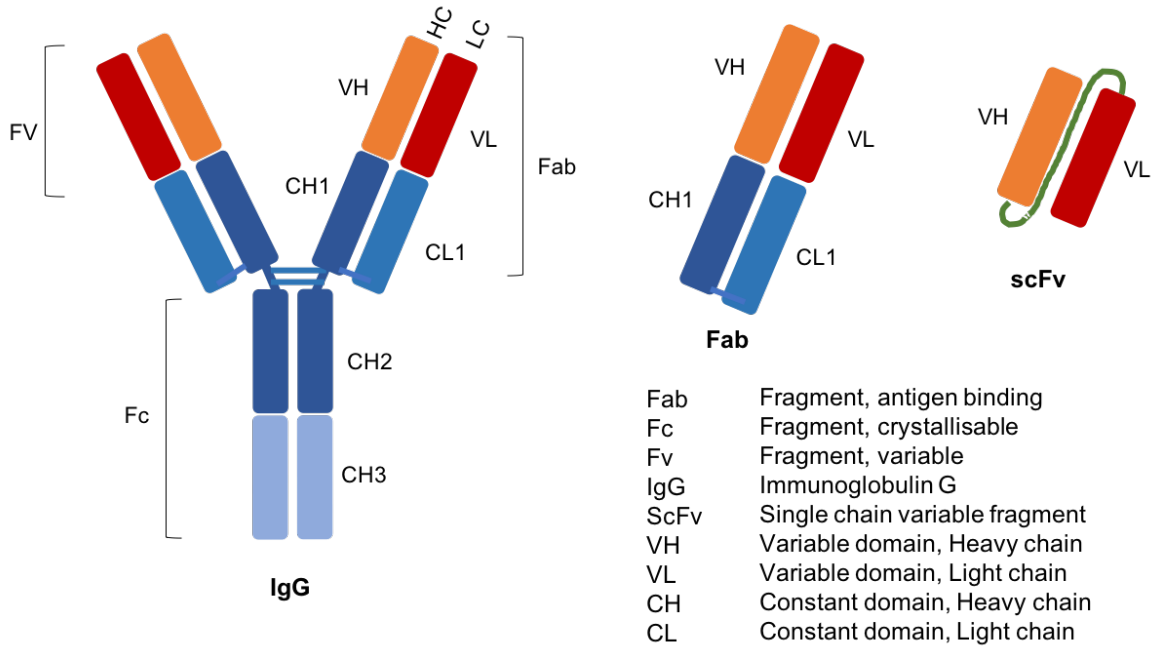

FIG. 8: STRUCTURE OF THE SINGLE CHAIN VARIABLE FRAGMENT
The single chain variable fragment (scFv) format consists of the variable domains of the heavy and the light chain of the antigen binding fragment of an IgG antibody.

The coding deoxyribonucleic acid for specific scFvs is selected by antibody phage display, followed by production in *Escherichia coli* (*E. coli*) and protein purification on a metal affinity column (Barbas, Burton *et al.* 2001; Hammers and Stanley 2014).

Protein engineering can be performed to improve the properties of the scFv (*e.g.* increase or alteration of specificity).

Using scFvs has several advantages over the use of mAbs. Firstly, the phages are very stable and can be stored for years in a normal fridge. Secondly, the production of scFvs is quick and inexpensive using *E. coli* and thirdly, properties of a scFv can be easily modified by protein engineering.

In my thesis, I used an anti-Dsg 1 / anti-Dsg 3 scFv called Px4-3 which was kindly provided by Dr. Dr. Christoph Hammers (Department of Dermatology, Allergology and Venereology, University Medical Centre Schleswig-Holstein, Lübeck). This scFv can be produced as mentioned above by using antibody phage display with the serum of a PV patient with both anti-Dsg 1 and anti-Dsg 3 antibodies (Payne, Ishii *et al.* 2005; Hammers, Chen *et al.* 2015). It targets the desmosomal structures Dsg 1 and Dsg 3 just like an IgG autoantibody (150 kDa) from PV patients and can induce acantholysis in otherwise healthy skin. This effect was shown in both human and murine skin (Burmester, Emtenani *et al.* 2019). The cross-reactivity of Px4-3 to both tissues shows promise regarding possible future mouse models for PV.

2.4 HUMAN SKIN ORGAN CULTURE

The human skin organ culture (HSOC) model similar to the procedures used today was first described in 1965 by Sarkany (Sarkany, Grice *et al.* 1965) and has been developed ever since. HSOC uses full thickness human skin, reflecting the *in vivo* structure of the skin and is therefore more physiologically relevant than cell culture experiments employing *e.g.* human adult low calcium high temperature keratinocytes (HaCaT) cells, and also more relevant than other commercially available 3D “skin equivalent” assays (Zhou, Zhang *et al.* 2018). The full HSOC is now also a standardised test system for PV. By culturing the skin is in an air-liquid interface instead of suspending the model in serum containing media, the physical conditions of intact skin are mimicked. This model also allows assessment of pharmacological substances on human skin *in vitro* and is also a standardised test system for PV (Burmester, Emtenani *et al.* 2019).

2.5 PROTEOMICS

Proteomics constitute the technologies for identification and quantification of the overall protein content of a cell, tissue or an organism (proteome).

When trying to understand a physiological or pathological event, we need to look at the effectors of biology, with proteins being the chief actors of biological functions. Protein abundance and function does not depend on the analogous messenger ribonucleic acid (mRNA) levels alone, but also on post-translational regulation on the protein level. This means, that the same mRNA can be translated into a variety of protein isoforms with different functions. Due to its resulting size and variety it is difficult to fully analyse the proteome. Advances in the development of liquid chromatography tandem mass spectrometry (LC-MS / MS) techniques, made this currently the most practical method for global protein identification as this high-throughput technology is able to collect immense amounts of data at once (Hammers, Tang *et al.* 2018).

During their lifetime all proteins undergo at least one form of proteolysis an irreversible post translational modification affecting protein activity, function and localization, which is catalysed by proteases. Proteases are functional enzymes that proteolytically cleave the peptide backbone of a protein. One protease function is the degradation of proteins *e.g.* in the digestive tract or the lysosome of a cell. Proteolysis can dramatically alter the function of a protein and misregulated proteolysis is often associated with diseases. Substrate cleavage is often incomplete though, meaning that substrates are only partially processed and neo-N-terminal fragments have a very low concentration. Due to this, many cleaved proteins escape detection in a classical whole proteome LC-MS analysis. These newly generated protein N-termini are detectable through terminal amine isotope labelling of substrates (TAILS), a form of quantitative proteomics allowing distinction between several experimental groups.

Classical proteomic studies, as well as TAILS, have been applied to dermatological research and successfully characterised the plasma membrane proteome of human epidermal keratinocytes (Blonder, Terunuma *et al.* 2004), as well as their secretome (Schlage, Egli *et al.* 2017). Furthermore, recent research shows the impact of proteases on pemphigoid diseases (Hiroyasu, Turner *et al.* 2019) identifying several

matrix metalloproteases (MMPs) and also neutrophil elastase (NE) to be expressed in the human bullous pemphigoid (BP) blister fluid. A study scrutinising the antibody response in pemphigus by proteomic analysis of circulating pemphigus antibodies suggests that it is much more diverse than previously described in genetic studies of B cells encoding autoantibodies (Chen, Zheng *et al.* 2017). However, the influence of proteases on PV pathogenesis are not yet investigated sufficiently.

2.6 RESEARCH OBJECTIVES

The objective of this study is to investigate the split formation in the HSOC model induced by the anti-Dsg 1 / anti-Dsg 3 binding scFv in more detail.

Firstly, I wanted to determine the time point of blister formation onset after injection of the scFv by performing time course organ culture experiments with skin samples from different patients.

Secondly, I explored changes in proteome composition by analysing the samples from the time course experiments with quantitative LC-MS / MS. The obtained data was investigated for known candidate proteins associated with signalling pathways known to be involved with PV pathogenesis during split formation in the HSOC and the abundance of those candidates over time.

Lastly, since it was shown, that substrate proteolysis plays an important role in PV pathogenesis, I also investigated abundance changes over time of the N-terminome of the skin during blister formation by TAILS and mapped identified cleavages in the parent proteins to distinguish internal substrate processing.

3 MATERIAL

3.1 DEVICES

Device	Manufacturer	Catalogue number
Barocycler 2320 EXT	Pressure BioSciences	#2320-EXT
Bioruptor® Pico sonication device	Diagenode	#B01060010
Biosafety Cabinet	Nu Aire	#NU-140
Centrifuge 5415 R	Eppendorf	#Z605212
Centrifuge Heraeus Fresco™ 17	Thermo Fisher Scientific	#75002420
Centrifuge Heraeus Multifuge X3R	Thermo Fisher Scientific	#521-2844P
CO_2 incubator	Thermo Fisher Scientific	Model Hercacell 150
Cryostat	Leica Biosystems	#CM3050S
EASY-nLC™ 1200 system	Thermo Fisher Scientific	#LC140
Freezer -20 °C	Liebherr-International	#LGPV6520
Freezer -80 °C	Thermo Fisher Scientific	#TSX400V
Fridge 4 °C	Liebherr-International	#KS95
Fully automated glass coverslipper	Leica Biosystems	#CV5030
Microcentrifuge MiniStar	VWR	#521-2844P
Microscope	Keyence	#BZ9000 BIOREVO
Microtome	Reichert-Jung	Model 1140 / Autocut
Paraffin stretch bath	Medax	#24900
Q Exactive™ Hybrid-Quadrupol-Orbitrap mass spectrometer	Thermo Fisher Scientific	#IQLAAEGAAPFALGMAZR
Scale analytical balance ME204	Mettler Toledo	#30029066

Spectrophotometer/ Fluorometer (Nanodrop)	DeNovix	DS-11 FX
ThermoMixer® C	Eppendorf	#5382000015
Tissue Embedding Console System	Sakura Finetek	Model Tissue-Tek® TEC™ 5
Tissue infiltration machine	Leica Biosystems	#ASP300S
Vortex Genie 2	Scientific Industries Inc.	#SI-0236
Vortex IKA MS 3 basic	IKA	#0003617000
Water cooler 230V	Diagenode	#B02010002

3.2 CONSUMABLES

Item	**Manufacturer**	**Catalogue number**
0.2 µm Filtropur	Sarstedt	#83.1826.001
96-well microplate: *Nunclon* ™ Delta Surface	Thermo Fisher Scientific	#167008
Amicon Ultra-0.5 centrifugal filter units, 30 kDa	Merck (Millipore)	#UFC5030BK
Cellstar® 15 mL tubes	Greiner bio-one	#188271
Coverslides	Roth	#H878.2
Disposable sterile scalpels	Swann Morton	#0503
Empore™ Octadecyl C18 47 mm extraction disks	Supelco	#66883-U
Eppendorf™ Research™ Plus Pipettes 0,5-10 µL	Eppendorf	#3123000020

2-20 µL 10-100 µL 100-1000 µL		#3123000039 #3123000047 #3123000063
Fat pen	DAKO	#S2002
Insulin syringe 1 mL	Becton Dickinson	#324827
Low protein binding tubes 1.5 mL	Eppendorf	#0030108116
Micro-tubes for PCT	Pressure BioSciences Inc.	#MT-96
Microtome and cryostat blades type 819	Leica Biosystems	#14035838382
Paraffin cassettes	Medite	#47-1306-00
Pasteur pipettes	Labsolute	#7691064
PCT-µ-pestles (30 µL)	Pressure BioSciences Inc.	#MT-96
Pipetboy 2	Integra	#155017
Pipette tips: 0,1-10 µL 5-300 µL 100-1250 µL	Thermo Fisher Scientific	 #02-707-438 #02-707-411 #02-707-408
Reaction tube	Eppendorf	#CLS3450
Safe-lock tubes 1.5 mL 0.5 mL 2 mL	Eppendorf	 #003013328 #0030121023 #0030123344
Sterile forceps	Thermo Fisher Scientific	#12-000-131
Sterile petri dish	Sarstedt	#821.472
Sterile surgical blade	Swann-Morton	#0501
SuperFrost slides	Thermo Fisher Scientific	#J1800AMNZ
Tissue Tek Cryomold	Sakura Finetek	#4566
Tissue Tek O.C.T. compound	Sakura Finetek	#4583

Transwell plates, 6-well culture (24 mm diameter insert with 0.4 µm pore size)	Sigma Aldrich	#CLS3450
Wet chamber	A. Hartenstein	#IK20

3.3 REAGENTS

Reagent	**Manufacturer**	**Catalogue number**
Acedic acid	Merck	#100063
Acetonitrile	Sigma Aldrich	#34851
Ammonia solution	Merck	#1054222500
BSA	Sigma Aldrich	#A-7906
CAA	Sigma Aldrich	#C0267
$CaCl_2$	Acros Organics	#349610025
cOmplete™ Mini, EDTA-free protease inhibitor cocktail	Roche	#04693159001
DAPI Fluoromount-G®	Southern Biotech	#0100-20
DMSO	Sigma Aldrich	#D8418
DPBS 1x	Gibco	#14190-094
EDTA	Sigma Aldrich	#EDS
Eosin	Waldeck	#18425
Ethanol 100 %	Roth	#K928.4
Ethanol 70 %	Chemsolute	#2202.5000
Ethanol 96 %	Chemsolute	#2209.5000
Eukitt®	Fluka	#03989
Formalin solution, neutral buffered, 10 %	Sigma-Aldrich	#HT501128
GuHCl	Sigma Aldrich	#G3272

Haematoxilin solution according to Papanicolaou	Merck	#1092532500
HCl	Sigma Aldrich	#H1758
HPG-ALD-polymer for proteomics	Flintbox	#08-038
HEPES	Sigma Aldrich	#H3375
iRT kit	Biognosys	#Ki-3002-1
LiChrosolv® Acetone for liquid chromatography	Merck	#1000202500
LiChrosolv® MeOH	Merck	#1060072500
NaOH	Sigma Aldrich	#S5881
NH_4HCO_4	Sigma Aldrich	#A6141
Normal goat serum	DAKO	#X0907
Quick start bovine serum albumin standard	Bio-Rad	#5000206
Quick Start Bradford 1x, dye reagent	Bio-Rad	#500-0205
Sodium cyano-borohydride solution (5 M in 1 M NaOH)	Sigma Aldrich	#296945
TBS	Bio-Rad	#1706435
TCEP	Sigma Aldrich	#C4706
TMTsixplex™ isobaric label reagent set	Thermo Fisher Scientific	#90061
Trifluoroacetic acid	Sigma Aldrich	#T6508
Trypsin gold, mass spectrometry grade	Promega	#V5280
Tween 20	Euroimmun	#F170323DI
Water with 0.1 % formic Acid	Merck	#1590132500
Williams Medium E	Gibco	#22551-022
Xylene	Chemsolute	#326.2500

3.4 ANTIBODIES

Antibodies	Manufacturer	Catalogue number
Alexa Fluor 594 goat anti-rat IgG (H + L)	Lifetechnologies	#A11007
Anti-HA mAB high affinity 0.1 µg / µL, rat	Roche	#12013819001
Cy™3-conjugated AffiniPure goat anti-mouse IgG (H + L), clone: polyclonal	Jackson ImmunoResearch	#115-165-146
Goat anti-mouse IgG (H + L) Alexa Fluor 488, clone: polyclonal)	Thermo Fisher Scientific	#A11029
Mouse anti-human desmoglein 1, clone: monoclonal 27B2	Origene	#AM26377PU
Mouse anti-human desmoglein 3, clone: polyclonal 5G11	Origene	#SM2037PS

3.5 SOFTWARE

Software	Manufacturer
BZ-II Analyzer	Keyence, Osaka, Japan
BZ-II Viewer	Keyence, Osaka, Japan

End Note X9.3.2.	Clarivate Analytics, Philadelphia, United States
FLUOstar Omega, Multi-user Reader and MARS Data Analysis Software	BMG Labtech, Ortenberg Germany
GraphPad Prism 8	GraphPad Software Inc., La Jolla, United States
Image J 1.52a	Wayne Rasband, Bethesda, United States
Microsoft Office 2019 for Mac	Microsoft Corporation, Redmond, United States
Mutiple experiment viewer (MeV) 4.8.1.	J. Craig Venter Institute, La Jolla, United States
PANTHER classification system 15.0	Gene Ontology Consortium, Los Angeles, United States
Proteome discoverer 2.2	Thermo Fisher Scientific, Waltham, United States
Venny 2.1	Juan Carlos Oliveros, BioinfoGP Service, Centro Nacional de Biotecnología

4 METHODS

4.1 HUMAN SKIN ORGAN CULTURE

4.1.1 SET-UP AND EXECUTION

The acantholysis associated with PV can be induced in the HSOC by injecting a bispecific anti-Dsg 1 / anti-Dsg 3 scFv (Burmester, Emtenani *et al.* 2019).
The scFv used for the following experiments was kindly provided by Dr. Dr. Christoph Hammers (Department of Dermatology, Allergology and Venereology, University Medical Centre Schleswig-Holstein, Lübeck).

For the model I used skin derived from healthy patients undergoing elective plastic surgery (**TABLE 1**). The approval of the ethics committee of the University of Lübeck for this proceeding is on hand under the proposal number 06-109 (see chapter ***8.1 ETHICS APPROVAL***). Skin sections for this model should be chosen from unscathed areas meaning no scars, no tattoos and no liver spots.

TABLE 1: INFORMATION ABOUT THE SKIN DONORS

Year of birth	Sex	Sampling location	Experiment
1971	Female	Abdomen	1st 24 h
1963	Male	Face lift	1st 11 h
1967	Female	Abdomen	2nd 24 h
1975	Female	Upper arm	3rd 24 h 2nd 11 h
1971	Female	Thigh	3rd 11 h

The HSOC was started 24 hours (h) after the extraction of the skin at the latest. Until then the skin was kept in William's Medium E and cooled at 4 °C.
Using a sterile scalpel, I trimmed the skin into six approximately 1 x 1 cm large skin sections including all three skin layers and injected 60 µg of the scFv diluted in phosphate-buffered saline (PBS) intradermally into each section (**FIG. 9**).

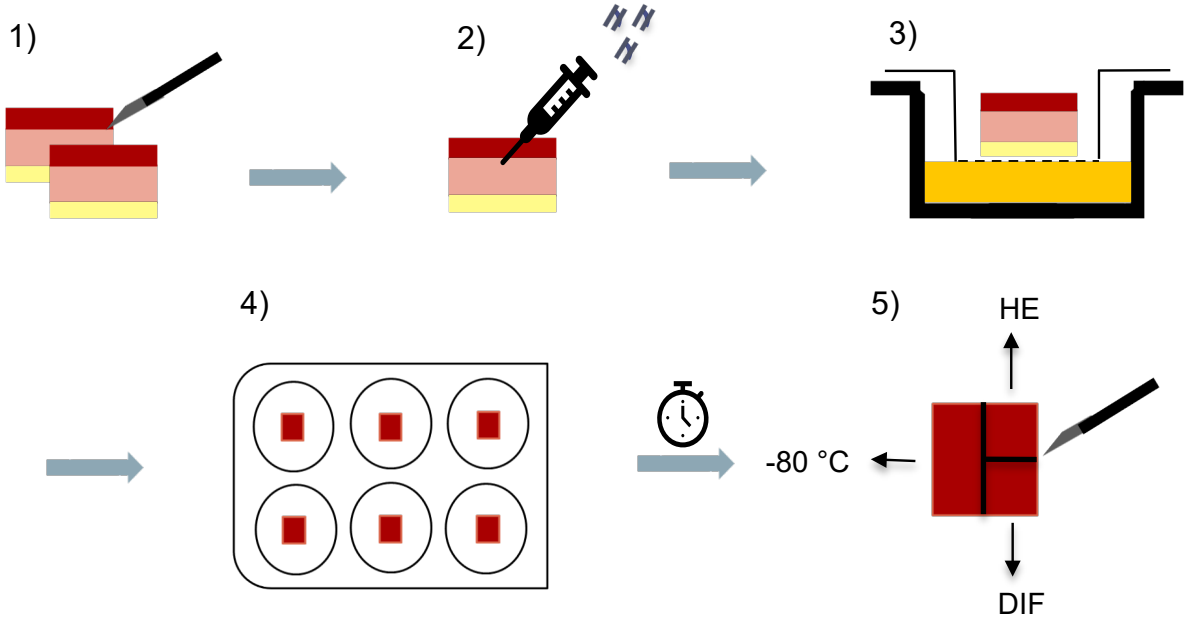

FIG. 9: SET-UP OF THE HUMAN SKIN ORGAN CLUTURE

1) The skin is cut into approximately 10 x 10 mm large squares containing all three skin layers (epidermis, dermis, subcutis).
2) Intradermal injection of the short chain variable fragment (scFv) and intravenous immunoglobulin g (IVIg) as a negative control (NC).
3) The skin samples are placed in the prepared transwell plates with preheated William‘s Medium E.
4) The transwell plate is placed in the incubator (37 °C, 5 % CO_2).
5) After a defined amount of time the skin samples are cut into different sections with a sterile scalpel. Half a sample is frozen at -80 °C for proteome analysis. One quarter is frozen in Tissue Tek O.C.T. compound for immunofluorescence staining and the other quarter is embedded in formalin solution for Haematoxylin-Eosin (HE) staining.

As a negative control (NC) 30 µL of IVIg (0.25 µg / µL) diluted in 20 µL of PBS were injected intradermally. It is important not to inject more than 50 µL of liquid into one skin section at once. Also, a BP scFv (60 µg of 3-14G) diluted in 20 µL of PBS was used in a separate experiment as a second NC to ensure the specificity of Px4-3.

The prepared skin sections were placed into transwell plates, containing 1 mL of preheated William’s Medium E per transwell (**FIG. 10**) and put into the incubator (37 °C, 5 % CO_2) for a defined amount of time.

After incubation, the samples were cut into smaller sections: a quarter of the skin section for HE staining, another quarter for immunofluorescence staining and half a skin section was immediately frozen at -80 °C for proteome analyses.

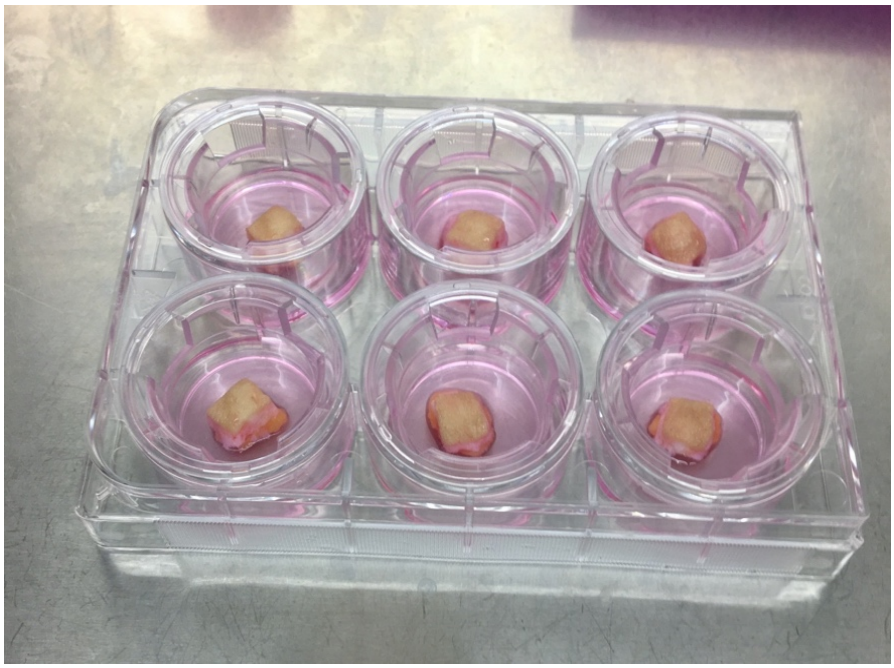

FIG. 10: TRANSWELL PLATE EQUIPPED WITH THE SKIN SAMPLES
The transwell plate is prepared with 1 mL William‘s Medium E per well and the skin samples sized approximately 1 x 1 cm are lying within the inlets ready for incubation.

Since the aim of the project was to identify the time point at which the split formation within the epidermis starts, we set up a time course experiment. We knew that after 24 h there is a visible split formation, so we arranged one experiment looking at defined time points within the first 24 h after injection of the scFv. After performing the first 24 h experiment, we realised we needed to take a closer look into the first 12 h after injection of the scFv, so we set up another experiment over the course of 11 h and performed n=3 for each one (**FIG. 11**). The first three organ cultures (1st, 2nd 24 h experiment, 1st 11 h experiment) were performed by Nick Feldmann.

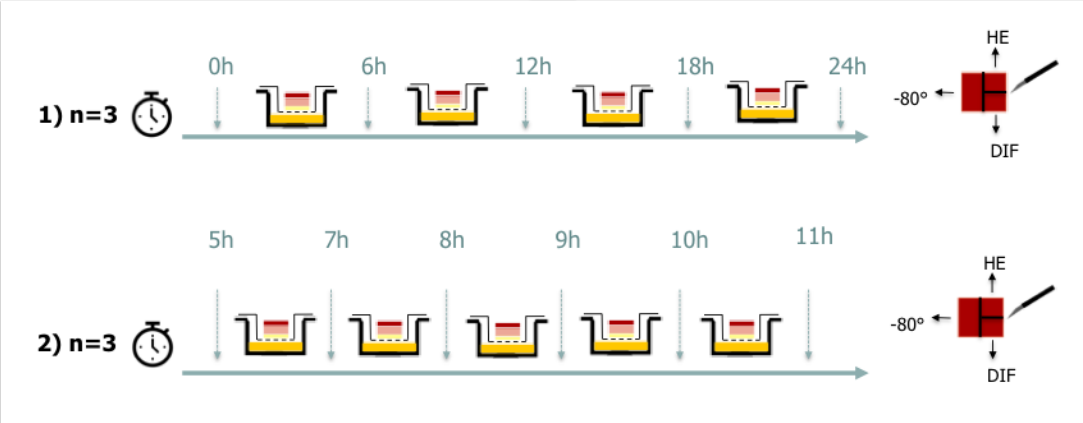

FIG. 11: SET-UP OF THE TIME COURSE EXPERIMENTS

1) The 24 hours (h) set-up: After every 6 h, one sample is removed from the transwell plate for further processing.
2) The 11 h set-up: After 5 h the first sample is removed, then after 7, 8, 9, 10 and 11 h the other samples are removed.

4.1.2 HAEMATOXYLIN-EOSIN STAINING

The HE staining was performed to receive an overview of the sample's tissue structure and as the base for analysing the split formation within the samples over time.

For the HE staining a quarter of each skin sample was placed in a paraffin cassette and put into formalin solution for fixation after marking the corner of the sample opposite the cutting edge. This allowed me to recognise the edge that I would need to cut later on.

The samples were fixated for at least 24 h before being dehydrated overnight.

On the following day, I embedded my samples in paraffin. The resulting blocks was put on a microtome and cut into 4 µm thick slices. The slices were then affixed to microscope slides and dried over night at 37 °C.

For the actual HE staining the slides were put into xylene (xylene 1) for 20 minutes (min) to deparaffinise and subsequently bathed in two more xylene baths (xylene 2, xylene 3). Next, the slides were slued in a descending row of ethanol (100 % ethanol, 96 % ethanol, 70 % ethanol) in order to rehydrate the slides. They were then washed in water and incubated in haematoxylin for 5 min (bluing). Afterwards, they were washed again, slued in acetic acid alcohol, washed in water and then slued in ammonia water two to three times. Another thorough wash step followed before the slides were placed in eosin for 30 to 90 seconds (s) (depending

on the maturity of the eosin). In an ascending ethanol row (in reverse order from xylene 1 to 96 % ethanol) the slides were dehydrated and covered with a cover slide.

4.1.3 SEMI-QUANTITATIVE HISTOMORPHOMETRY

To analyse the split formation within the skin sections over time I took non-overlapping pictures along the complete epidermis with the *BZ-II-Viewer* of all HE stained slides in x100 magnification. A scale bar of 100 µm was inserted into each picture. Every picture corresponds to one visual field (VF). Afterwards the pictures were imported into *Image J 1.52a* where the scale bar was set using the scale bar that was already in the picture. The complete epidermal length of each VF was measured using the segmented line just above the basal cell layer. I subtracted 200 µm from the first and also from the last VF of each skin sample (from the edge of the sample) to reduce possible mistakes induced by cutting artefacts (**FIG. 12**). Afterwards, I measured the split length for each VF measuring also just above the basal cell line of the split leaving out the same 200 µm from both edges of each sample as described above. Both results were transferred into a table and the percentage split formation was calculated for each VF.

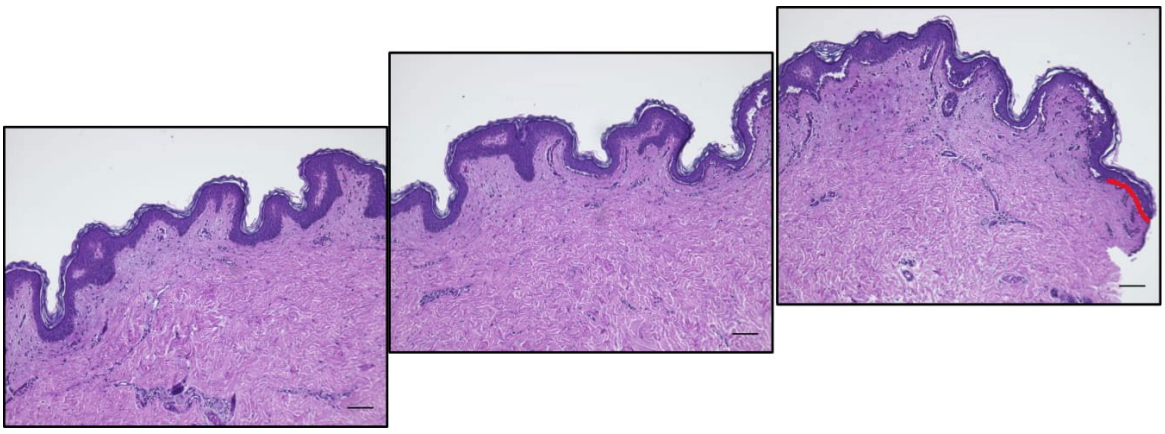

FIG. 12: TAKING PICTURES FOR SEMI-QUANTITATIVE HISTOMORPHOMETRY
To analyse the split formation non-overlapping pictures along the epidermis are taken (as shown in the exemplary pictures above).
The picture on the right shows the right edge of the skin sample – to reduce mistakes due to cutting artefacts, 200 µm are measured from the edge (shown in red) and substracted from the total epidermal length of that visual field. In this area the split formation is also not measured.

4.1.4 STATISTICS

The software *GraphPad Prism 8* was used for the statistical analysis of the semi-quantitative histomorphometry. The values for the split formation (percentage) of the relevant experiment and the relevant point of time within this experiment were transferred into *GraphPad Prism*. The data is non paired and consists of six groups per experiment. I performed a test for normal distribution before continuing with either a One-way ANOVA (normally distributed data) or a Kruskal Wallis Test (non normally distributed data). In this experiment's case, the data was non normally distributed. Afterwards, I performed the appropriate post-hoc test (Dunn's multiple comparisons test) and looked at the significance of the data in comparison to the NC (0h).

The identified p values were labelled significant when $p \leq 0.05$.

* $p \leq 0.05$

** $p \leq 0.01$

*** $p \leq 0.001$

**** $p \leq 0.0001$

4.1.5 DIRECT IMMUNOFLUORESCENCE STAINING

TABLE 2: SOLUTIONS AND ANTIBODY DILUTIONS TO PREPARE FOR DIRECT IMMUNOFLUORESCENCE STAINING

Washing buffer (1 litre)	100 mL 10x Tris-buffered saline (TBS)
	500 µL 2M Calcium chloride ($CaCl_2$)
	900 mL NanoPure distilled water (dH_2O)
	Tween20
Blocking buffer	0.5 g Bovine serum albumin (BSA)
	Dilute in washing buffer to a final volume of 50 mL and sterile filter solution with 0.2 µm Filtropur
Secondary antibody	Rat anti-haemagglutinin (HA)-peroxidase-monoclonal antibody

	(mAb), high affinity, 0.1 µg / µL 1:100 dilution with blocking buffer
Tertiary antibody	Alexa Fluor 594 goat anti-rat IgG heavy + light (H + L) 1:200 dilution with blocking buffer

The skin sections frozen at -80 °C in Tissue-Tek O.C.T. Compound were cut into 6 µm thick slices on a cryostat and affixed to microscope slides. Until further usage, the slides were stored at -80 °C.

For the staining, the slides were taken out of the freezer and left to dry at room temperature for 3 to 5 min. Each cryosection was encircled with a fat pen, ensuring the antibody dilutions for the staining to stay on each section. In order to avoid the drying up of the sections, washing buffer was immediately pipetted onto the encircled sections and all slides were put into a wet chamber. Next, I performed the proper washing step, using washing buffer two times for 3 min. Afterwards, the sections were incubated with blocking buffer (15 min at room temperature) to reduce unspecific bindings. After discarding the blocking buffer, the secondary antibody in dilution with blocking buffer was pipetted onto the sections and left to incubate (60 min at room temperature). Meanwhile the tertiary antibody was centrifuged whilst being protected from light [4 °C, 5 min, 5000 revolutions per minute (rpm)] before the amount necessary for the dilution was taken from the top of the tube. The antibody dilution was prepared protected from light.

A thorough washing step followed the incubation of the secondary antibody (three times for 3 min each at room temperature) before the tertiary antibody dilution was added to the sections protected from light. Incubation time for the tertiary antibody dilution was 30 min (at room temperature), followed by the last washing step (three times 3 min at room temperature, protected from light). Subsequently, nuclei were visualised with 4′,6-Diamidin-2-phenylindol (DAPI) Fluoromount-G and the slides left to dry protected from light for at least 60 min.

The stained slides (**FIG. 13**) were stored at -20 °C in a slide folder for approximately 24 h before the pictures of the staining were taken on the microscope.

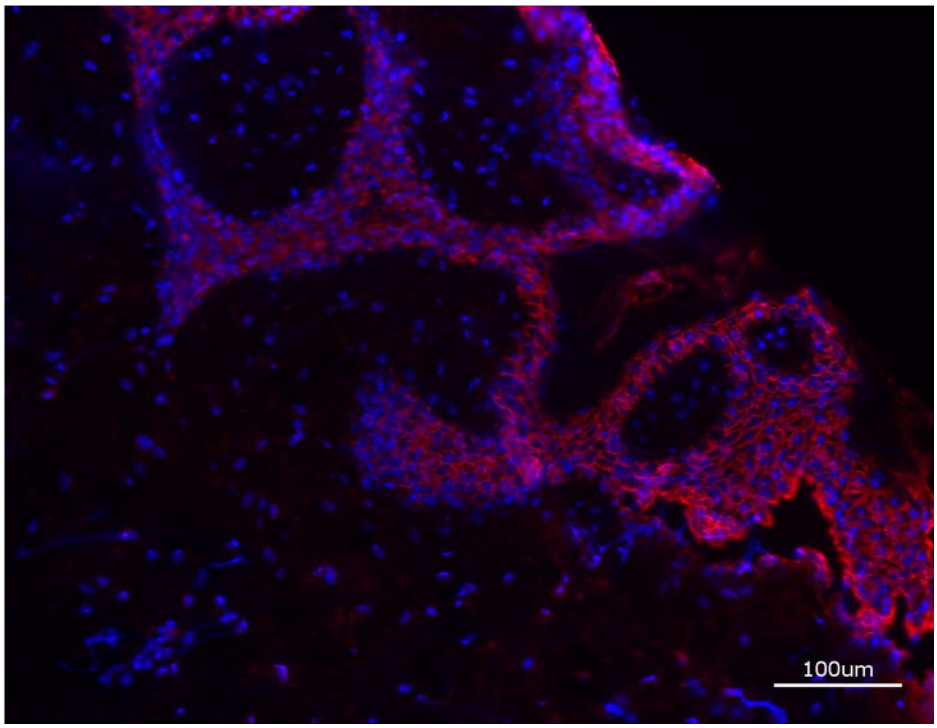

FIG. 13: BINDING PATTERN OF THE SHORT CHAIN VARIABLE FRAGMENT IN HUMAN SKIN

Direct immunofluorescence staining in samples from human skin organ culture shows the short chain variable fragment (scFv) (anti-desmoglein 1 / anti-desmoglein 3) (red) and 4′,6-Diamidin-2-phenylindol (DAPI) (blue). It visualises the binding pattern of the scFv on the keratinocyte surface.

4.1.6 INDIRECT IMMUNOFLUORESCENCE STAINING

In order to show the deposition of the target antigens of the scFv (Dsg 1 and Dsg 3) in the skin, IIF stainings were performed. Both antigens should be found within the epidermis. Dsg 1 should be expressed in the more superficial layers whilst Dsg 3 should be expressed in the lower epidermal layers just above the basal membrane. The following IIF stainings were kindly performed by Julia Möller as part of her internship in our lab working group.

4.1.6.1 STAINING OF DESMOGLEIN 1

TABLE 3: ANTIBODY DILUTIONS TO PREPARE FOR THE STAINING OF DESMOGLEIN 1

Primary antibody	Mouse anti-human desmoglein 1 antibody 1:100 dilution in phosphate-buffered saline (PBS)
Secondary antibody	Cy™3-conjugated AffiniPure goat anti-mouse IgG heavy + light (H + L) 1:200 dilution in PBS

The skin sections frozen at -80 °C in Tissue-Tek O.C.T. Compound were cut into 6 µm thick slices on a cryostat and affixed to microscope slides. Until further usage, the slides were stored at -80 °C. For the staining, the slides were taken out of the freezer and left to dry at room temperature for 10 min. The slides were then fixed in acetone for 20 min at -20 °C. Then, each cryosection was encircled with a fat pen ensuring the antibody dilutions for the staining to stay on each section. Each section was washed twice with PBS for 5 min. The sections were then preincubated with 100 µL of a dilution made from 10 % normal goat serum in PBS per section for 20 min at room temperature. Without washing the slices, the normal serum was dropped and the primary antibody pipetted onto the sections (100 µL / section). 2 % normal serum (serum from the same species as secondary antibody: goat) was added and the sections incubated over night at 4 °C. On the next day, the slides were washed three times with PBS for 5 min each. Next, the 100 µL per sections of the secondary antibody (Cy™3-conjugated AffiniPure goat anti-mouse IgG H + L) and 2 % normal serum (goat) were pipetted onto the sections and then left to incubate for 45 min at room temperature. The slides must be covered from light at all times after the secondary antibody is added (light sensitive). Another washing step (3 x PBS for 5 min) follows the incubation of the secondary antibody. Subsequently, the sections were embedded in DAPI Fluoromount-G and the slides left to dry protected from light for at least 60 min.

The stained slides were stored at -20 °C in a slide folder for approximately 24 h before the pictures of the staining were taken on the microscope.

4.1.6.2 STAINING OF DESMOGLEIN 3

TABLE 4: ANTIBODY DILUTIONS TO PREPARE FOR THE STAINING OF DESMOGLEIN 3

Primary antibody	Mouse anti-human desmoglein 3 antibody 1:50 dilution in phosphate-buffered saline (PBS)
Secondary antibody	Goat anti-mouse IgG heavy + light (H + L) Alexa Fluor 488 1:200 dilution in PBS

The skin sections frozen at -80 °C in Tissue-Tek O.C.T. Compound were cut into 6 µm thick slices on a cryostat and affixed to microscope slides. Until further usage, the slides were stored at -80 °C. For the staining, the slides were taken out of the freezer and left to dry at room temperature for 10 min. The slides were then fixed in acetone for 20 min at -20 °C. Then, each cryosection was encircled with a fat pen ensuring the antibody dilutions for the staining to stay on each section. Each section was washed twice with PBS for 5 min. The sections were then preincubated with 100 µL of a dilution made from 10 % normal goat serum in PBS per section for 20 min at room temperature. Without washing the slices, the normal serum was dropped and the primary antibody pipetted onto the sections (100 µL / section). As a NC one slide was not prepared with the primary antibody. 2 % normal serum (serum from the same species as secondary antibody: goat) was added and the sections incubated over night at 4 °C. On the next day, the slides were washed three times with PBS for 5 min each. Next, the secondary antibody (100 µL / section) and 2 % normal serum (goat) were pipetted onto the sections and then left to incubate for 45 min at room temperature. The slides must be covered from light at all times after the secondary antibody (goat anti-mouse IgG H + L Alexa Fluor 488) is added (light sensitive). Another washing step (3 x PBS for 5 min) follows the incubation of the secondary antibody. Subsequently, the sections were embedded in DAPI Fluoromount-G and the slides left to dry protected from light for at least 60 min. The stained slides were stored at -20 °C in a slide folder for approximately 24 h before the pictures of the staining were taken on the microscope.

4.2 PROTEOME ANALYSIS

4.2.1 PROTEIN EXTRACTION FROM HUMAN SKIN

The frozen samples from the time course experiments were transferred to the *Technical University of Denmark* to perform proteome analyses of the tissue. In order to do this, the proteins had to be extracted from the skin samples. I compared two different methods to achieve this.

TABLE 5: BUFFERS AND DILUTIONS TO PREPARE FOR PROTEIN EXTRACTION

50 mM HEPES	50 mM 4-(2-hydroxyethyl)-1-piperazineethanesulfonic acid (HEPES), pH 7.8
250 mM HEPES	250 mM 4-(2-hydroxyethyl)-1-piperazineethanesulfonic acid (HEPES), pH 7.8
Lysis buffer	4 M Guanidine Hydrochloride (GuHCl) in 250 mM 4-(2-hydroxyethyl)-1-piperazineethanesulfonic acid (HEPES), pH 7.8
200 mM TCEP	200 mM tris(2-carboxyethyl) phosphine hydrochloride (TCEP) dissolved in 50 mM HEPES
400 mM CAA	400 mM chloroacetamide (CAA) dissolved in 50 mM HEPES

4.2.1.1 PRESSURE CYCLING TECHNOLOGY TISSUE HOMOGENISATION DENATURATION

First, I used pressure cycling technology (PCT) to extract the proteins from the tissue. For this method, I weighed 3 mg of tissue by cutting it with a sterile scalpel from the cutting edge of the sample and placed it into a PCT micro tube. The PCT micro tube was placed in a 1.5 mL microcentrifuge tube to ease handling. I added

30 µL of lysis buffer (**TABLE 3**) with protease inhibitor and sonicated the vials for 10 min in an ultrasonic bath in ice water. Afterwards, I took the PCT micro tubes out of the microcentrifuge tubes, capped them with 96 µ-pestles, loaded the tubes onto the Barocycler® cartridge distributed evenly in each barrel and placed the cartridge in the Barocycler®. The tissue was then homogenised in the Barocycler®. The settings on the Barocycler® for homogenisation of tissue depend on the type and size of the sample. My data was obtained with the following settings: 2 rounds of 60 cycles at 33 °C with 45,000 pound-force per square inch (psi) for 20 s and no pressure for 10 s.

The µ-pestles were released and 1:20 (volume / volume) 200 mM tris(2-carboxyethyl) phosphine hydrochloride (TCEP) (**TABLE 3**) was added to the lysis buffer. Also 1:10 (volume / volume) of 400 mM chloroacetamide (CAA) (**TABLE 3**) was added to the lysis buffer before the PCT micro tubes were placed in 1.5 mL microcentrifuge tubes and the samples incubated on a shaker at 21 °C for 30 min at 600 rpm. Afterwards, I quickly spun the PCT micro-tubes upside down in a 1.5 mL protein low binding microcentrifuge tube and then removed the PCT tubes. The 1.5 mL protein low binding microcentrifuge were then spun at room temperature for 10 min at 13,000 *g* so that I could transfer the supernatant to a new 1.5 mL protein low binding microcentrifuge tube. 250 mM 4-(2-hydroxyethyl)-1-piperazineethanesulfonic acid (HEPES) (**TABLE 3**) was added to a final concentration of 2.5 M Guanidine Hydrochloride (GuHCl) and an aliquot of 2 µL was taken for determining the protein concentration using the Bradford protein assay.

4.2.1.2 SONICATION TISSUE HOMOGENISATION DENATURATION

The Biorupter® as a method for protein extraction was our second attempt to extract larger amounts of protein at once. This is possible due to the fact, that a larger amount of tissue can be processed at once.

I collected 10 mg tissue samples from the cutting edge of the frozen samples from the time course experiments and cut them into approximately 1 x 1 mm small cubes using a sterile scalpel. The cubes were transferred into a 0.5 mL microcentrifuge tube. I then added 100 µL lysis buffer (**TABLE 5**) and sonicated the samples in the Biorupter® for 60 cycles at 30 sec ON and 30 sec OFF, temperature 37 °C.

To reduce disulphide bonds I added 200 mM TCEP (**TABLE 5**) to 100 µL of sample to final concentration of 10 mM. Alkylation of disulphide bonds was achieved by adding 400 mM CAA (**TABLE 5**) to the sample to a final concentration of 40 mM. The samples were incubated on a heating block for 30 min at 37 °C and 300 rpm. Afterwards, the microcentrifuge tubes were centrifuged at room temperature for 10 min at 13,000 *g* and the supernatant was then transferred to a new 1.5 mL microcentrifuge tube. Next 250 mM HEPES (**TABLE 5**) was added to a final concentration of 2.5 M GuHCl and an aliquot was taken to measure the protein concentration using the Bradford protein assay.

4.2.1.3 BRADFORD PROTEIN ASSAY

The Bradford protein assay was used to measure the protein concentration in the samples extracted from the skin tissue. The bovine serum albumin (BSA) standard is diluted in the same buffer the samples are dissolved in in this case, 2.5 M GuHCl, 250 mM HEPES, pH 7.8. Standard dilutions need to be prepared in the following concentrations: 0.1, 0.2, 0.5, 0.8, 1, 1.5, 1.8, 2 mg / mL, double-distilled water (ddH_2O) was used as a blank. All samples were analysed in duplicates using 2 µL of sample diluted in 9 µL of the 2.5 M GuHCl, 250 mM HEPES, pH 7.8. Next, 5 µL of each standard plus the blank and the sample are pipetted into a 96-well microplate in duplicates. Then, 250 µL of the dye reagent was added into each well and everything mixed using a microplate mixer. The microplate was incubated at room temperature for approximately 5 min, not for longer than 10 min, before it was placed in the plate reader and read at 595 nm. Using the *MARS data analysis software*, the concentration was determined.

4.2.2 TERMINAL AMINE ISOTOPIC LABELLING OF SUBSTRATES

TAILS is a method of quantitative proteomics allowing the discovery of cleaved proteins and peptides within the samples from the time course experiments. This set-up combines a negative selection procedure with differential isotopic labelling allowing identification of proteolytic cleavage events (Kleifeld, Doucet *et al.* 2010).

To combine several samples in one experiment, I performed tandem mass tag (TMT)-6-plex labelling (**TABLE 6**). I combined five time points from one of the time course experiments to be analysed. As a sixth channel I created a reference sample made up of equal amounts of all the other time points in the analysis. The available TMT channels for each experiment are 126, 127, 128, 129, 130 and 131.

TABLE 6: ALLOCATION OF TANDEM MASS TAG CHANNELS

	126	**127**	**128**	**129**	**130**	**131**
24 h experiments	0 h	6 h	12 h	24 h	NC	Reference
11 h experiments	5 h	7 h	8 h	9 h	10 h	Reference

The TAILS experiment was performed following published protocol (Madzharova, Sabino *et al.* 2019). In short, 50 µg of each above indicated sample were transferred into a clean microcentrifuge tube and a reference channel was created using 10 µg protein / sample all mixed in one microcentrifuge tube. The protein concentration was adjusted to 0.5 µg / µL and each tube was filled up to 100 µL volume using 2.5 M GuHCl, 250 mM HEPES, pH 7.8. Then, in order to distinguish abundances of peptides between different samples, the different time points were isotopically labelled using TMT reagents. Aliquots of 200 µg of each TMT label were dissolved in dimethyl sulfoxide (DMSO) by pipetting in a volume equivalent to the volume of the sample (100 µL). To differentially label the proteins within the different samples, the TMT reagents were added to the samples in a protein to TMT weight ratio of 1:4 and a final DMSO concentration of 50 %. The labelled samples were mixed by pipetting and left to incubate for 60 min at room temperature (**FIG. 14**) The 60 min of labelling should be counted precisely for each condition to reduce quantification errors deriving from different labelling times. To quench the labelling reaction and get rid of all the excess labels, 20 µL of ammonium hydrogen carbonate (NH_4HCO_3) were added to a final concentration of 100 mM NH_4HCO_3 and the samples were incubated for 30 min at room temperature. Afterwards, all TMT labelled samples were combined in a 15 mL conical tube and mixed by vortexing. To clean up the proteome, proteins were precipitated with 10 mL of ice-cold acetone and 1.4 mL of ice-cold methanol (MeOH), followed by an incubation for at least 2 h at -80 °C. The sample was centrifuged at 4,700 rpm for 20 min at 4 °C. Then, the supernatant was carefully discarded, the pellet resuspended in 5 mL ice-cold MeOH and once more

centrifuged at 4,700 rpm for 10 min at 4 °C. Afterwards, the supernatant was discarded and the pellet was air dried with the tube upside down underneath a fume hood for approximately 15-20 min. The dried pellet was resuspended in 60 µL 100 mM sodium hydroxide (NaOH) and transferred to a new clean microcentrifuge tube. To adjust the protein concentration to 1 µg / µL (assuming no protein loss), 100 mM HEPES (pH 7.8), 30 µL of 1 M HEPES (pH 7.8) and 210 µL ddH_2O were added. The proteins were digested overnight with trypsin at a 1:10 ratio (protease / protein) on a heating block at 350 rpm, at 37 °C.

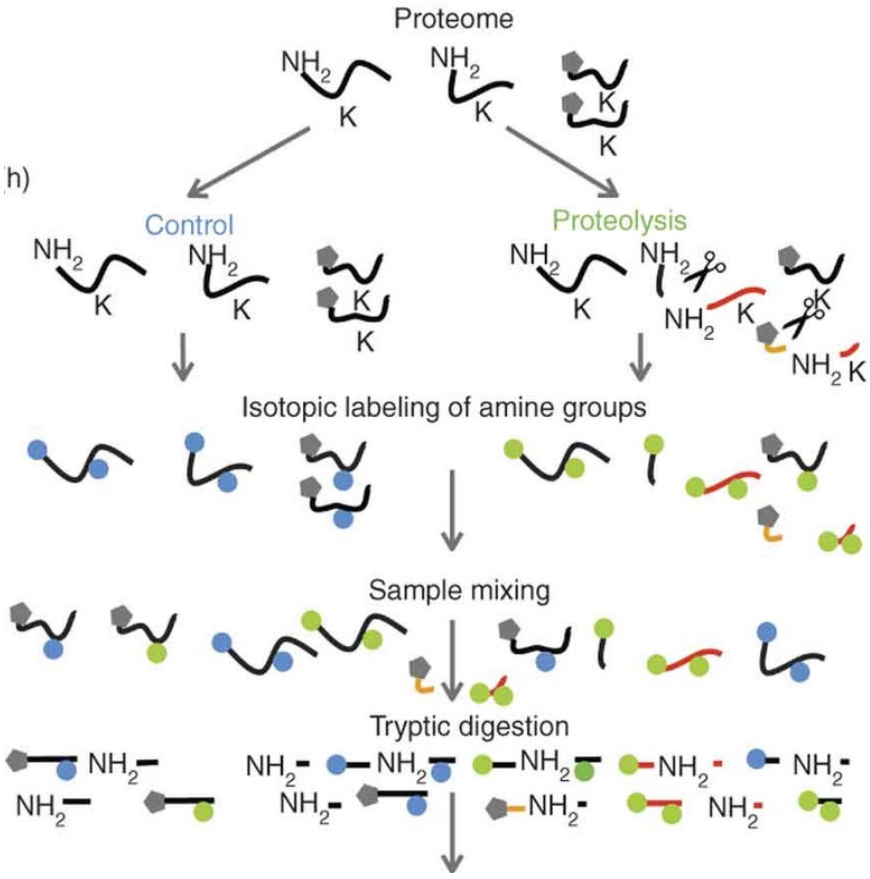

FIG. 14: TERMINAL AMINE ISOTOPIC LABELLING OF SUBSTRATES (TAILS)
In theory, proteolytic peptides will have been generated in the samples from the human skin organ culture injected with the single chain variable fragment in comparison to the negative control (NC) sample injected with intravenous immunoglobulins.
The isotopic labelling of amine groups with tandem mass tags (TMT) allows the peptides that originated from one sample to be distinguished from the other samples (in this case the other points of time and the NC). Afterwards, the samples are pooled together before trypsin digestion. The labelled N-termini of the original proteins remain blocked whilst new internal tryptic peptides have a free N-terminus. Modified from (Kleifeld, Doucet *et al.* 2010).

I removed 10 % (= 30 µL) of the peptide solution for whole proteome analysis (preTAILS sample) and stored it at -20 °C. The pH of the remaining peptide solution was adjusted to pH 6-7 with 2 M HCl. Then, a fourfold excess (weight / weight) of a hyperbranched polyglycerol-aldehydes (HPG-ALD) polymer and 5 M sodium cyanoborohydride ($NaBH_3CN$) were added to a final concentration of 50 mM $NaBH_3CN$. The solution containing the polymer was incubated overnight on a heating block at 0 rpm, at 37 °C. This polymer reacts with the newly generated tryptic peptides through their free N-terminus (**FIG. 15**). Native and protease-generated N-termini of original peptides as well as lysine side chains are blocked by the TMT labels and can therefore not react with the HPG-ALD polymer. Thus, original N-terminal peptides can be negatively enriched by ultrafiltration. To do this, a 30 kDa Amicon Ultra 0.5 mL centrifugal filter unit was conditioned with 400 µL of ddH_2O and centrifuged at 10,000 *g* (the relative centrifugal force) for 4 min. The collecting tube was exchanged and the polymer solution added to the filter. The solution was centrifuged at 10,000 *g* for 10 min at room temperature to recover unbound peptides in the flow through. The polymer was washed by adding 30 µL of 100 mM NH_4HCO_3 to the filter and centrifuging at 10,000 *g* for 10 min. The flow through was collected in one tube (TAILS sample) and stored at -20 °C until further sample processing.

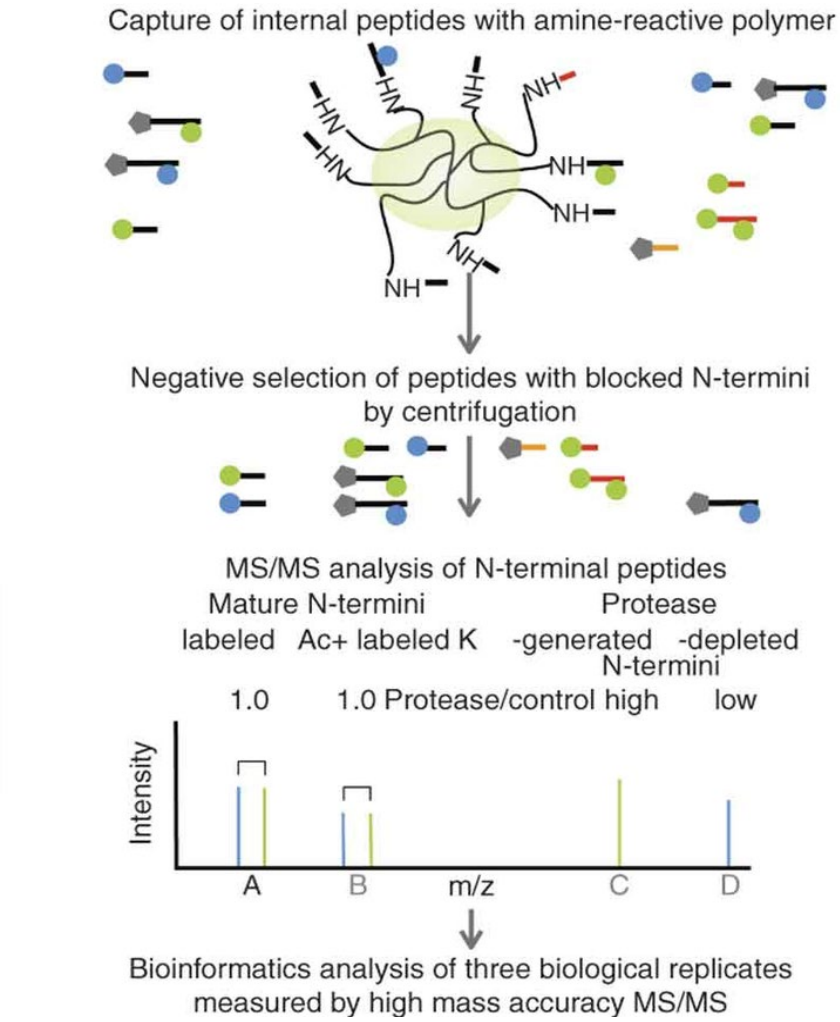

FIG. 15: THE POLYMER CAPTURES INTERNAL PEPTIDES
By adding a hyperbranched polyglycerol-aldehyde (HPG-ALD) polymer that reacts with the tryptic peptides, the peptides can then be pulled out of the sample by negative selection. The pull-out sample and a sample taken before the polymer pull-out are then run on a liquid chromatography-tandem mass spectrometer before undergoing statistical analysis. Modified from (Kleifeld, Doucet *et al.* 2010).

4.2.2.1 STAGE-TIP SAMPLE CLEAN-UP

After the isolation of peptides as described above, salts and buffers have to be removed for MS analysis using reversed phase resins. For this, octadecyl carbon chain (C18) matrix was used for capturing and separating peptides based on their hydrophobicity. The reverse phase column binds the peptides while salts and buffers are being washed off.

TABLE 7: BUFFERS AND SOLUTIONS TO PREPARE FOR THE CLEAN-UP

Buffer A	0.1 % Formic acid (FA)
Buffer B	80 % Acetonitrile (ACN), 0.1 % trifluoroacetic acid (TFA) in H_2O
Buffer A’	3 % ACN, 1 % TFA

The samples were acidified to < pH 2 with 20 % trifluoroacetic acid (TFA). STAGE (stop and go extraction) -tip columns were prepared in 200 µL pipette tips. One Empore™ C18 plug can bind approximately 5 µg protein. Since it is to be expected that after the HPG-ALD polymer pull-out up to 90 % of the sample is lost (resulting in ~27 µg sample maximum), 4 plugs were used allowing a maximum recovery of 20 µg protein.

I placed the C18 column in a 2 mL microcentrifuge tube with an adaptor and prewashed the columns once with 80 µL 100 % MeOH, once with 80 µL of Buffer B (**TABLE 7**) and twice with 80 µL Buffer A' (**TABLE 7**), by centrifugation at 1,000 *g* for 1 min. In parallel, the samples were centrifuged at 13,000 *g* for 10 min to get rid of non soluble material.
The microcentrifuge tube was then replaced with a clean 2 mL tube. I loaded the sample onto the column and centrifuged at 1,000 *g* for 2 min until the sample had passed through the column. Afterwards, the flow through was reloaded and centrifuged at 1,000 *g* for 2 min. The sample was then washed two times with 80 µL of Buffer A (**TABLE 7**) and centrifuged at 1,000 *g* for 1 min. The tube was replaced with a clean 1.5 mL protein low binding tube and the peptides were eluted three times by centrifugation at 1,000 *g* for 2 min with Buffer B (3 x 40 µL). The eluate was dried under vacuum at 45 °C for approximately 3 - 3.5 h.
Lastly, the sample in the protein low binding tube was resuspended in MS buffer [A*iRT= 2 % acetonitrile (ACN), 0.1 % with indexed retention time (iRT), 1:500 iRT volume / volume]. iRTs can be used as internal control peptides to assess the quality of the MS analysis. The protein concentration was measured using a Nanodrop and 500 ng of each sample were injected in the MS.

4.2.2.2 MASS SPECTROMETRY ANALYSIS

The samples were run on a Q Exactive™ Hybrid Quadrupole-Orbitrap™ MS coupled with an EASY-nLC™ 1200 system (**FIG. 15**), performed by Dr. Simonas Savickas. A data sheet on the MS settings is available (see chapter ***8.2 LC-MS PARAMETERS FOR TAILS ANALYSIS***).

4.2.2.3 STATISTICS

The data analysis of the original MS data was performed by the *Proteome Discoverer 2.2* software, transferring the data into *Microsoft Excel* tables for further analysis. *Proteome Discoverer* 2.2 normalised all data using the corresponding reference channel for each experiment. In *Microsoft Excel* the abundances were recalculated first as ratios to the NC and then as ratios to one another. This way, the comparison between the abundances was reduced to values between 0 and 1.

5 RESULTS

5.1 THE VARIABLE FRAGMENT Px4-3 CAUSES SPLIT FORMATION

In the HE stained sections we can see the split formation caused be the scFv over time. The split forms within the epidermis, just above the basal cell layer. In the NC injected with IVIg and also the NC injected with the BP scFv 3-14G, we do not see a split formation after 24 h of incubation, while we can already see the split formation after 7 h in the sample injected with the scFv (**FIG. 16**). The sample which was put into formalin solution immediately after injection of the scFv, without any incubation time, shows no split formation (**FIG. 16**).

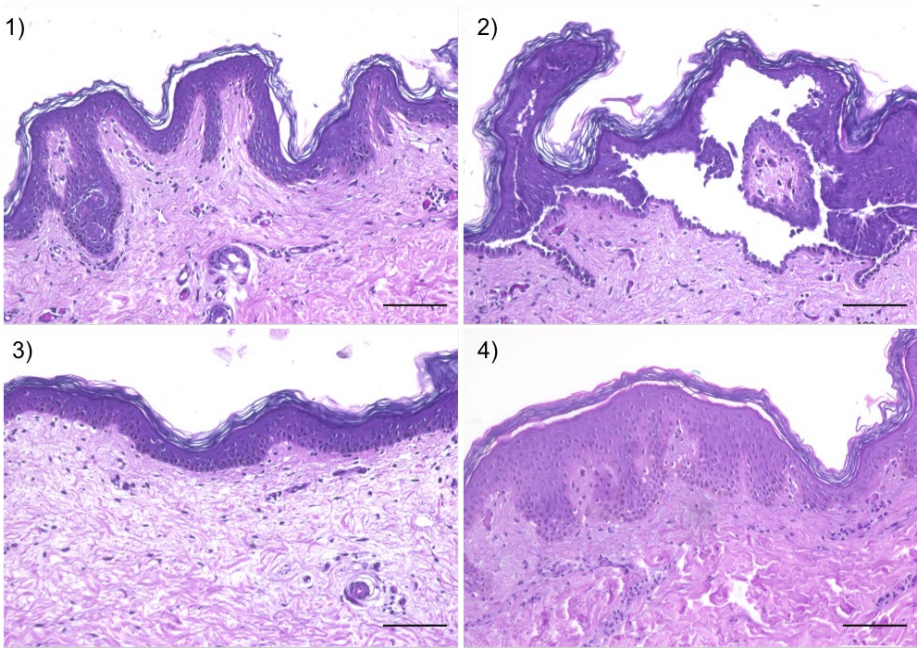

FIG. 16: THE VARIABLE FRAGMENT Px4-3 CAUSES SPLIT FORMATION

1) A section of full thickness human skin directly, 0 hours (h), after injection of the single chain variable fragment (scFv).
2) A section of full thickness human skin incubated with the scFv for 7 h showing intraepidermal blistering.
3) A section of full thickness human skin incubated with intravenous immunoglobulins as a negative control showing no intraepidermal blistering after 24 h.
4) A section of full thickness human skin incubated with a bullous pemphigoid scFv (3-14 G) as a negative control showing no intraepidermal blistering after 24 h.

Scale bars = 100 µm

5.2 SPLIT FORMATION STARTS BETWEEN 5 AND 7 HOURS

The aim of the time course experiments was to determine the point of time at which the split formation begins to occur within the skin. When looking at the HE stained sections, we can see a clear split formation after 7 h and in some samples the lesions can be found even earlier. The split formation progresses over time (**FIG. 17**) even though it does not necessarily get bigger but shows a more consistent appearance within the samples.

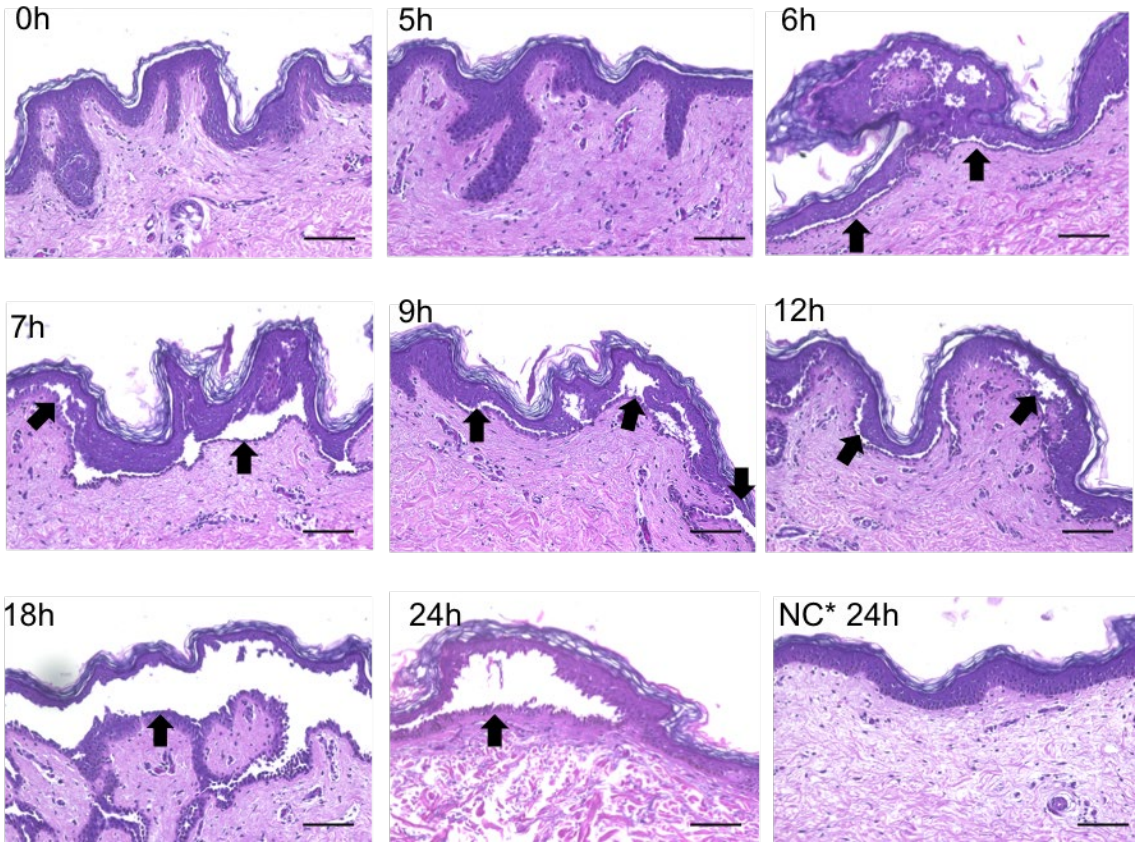

FIG. 17: EXEMPLARY OVERVIEW OF THE SPLIT FORMATION AFTER INJECTION OF THE SHORT CHAIN VARIABLE FRAGMENT Px4-3 OVER TIME
Over the course of 24 hours (h) we can see a split formation (black arrows) within the epidermis in these exemplary photos. The first split formation is visible after 6 h. The negative control (NC*) shows no split within the epidermal layer after 24 h. Scale bars = 100 µm

To quantify these results, the semi-quantitative histomorphometry was performed, measuring the exact length of each split for each sample. The first significant increase in split formation in comparison to the NC which showed no split formation at all occurs after 7 h (**FIG. 18**). In one of the HE sections I could also find a split

after 5 h, and in several samples after 6 h. This leads to the conclusion that the split formation starts somewhere between 5 and 7 h after injection of the scFv.

We cannot see a clear linear progression of the split formation over 24 h. The biggest difference of increased split formation is measured 18 h after injection of the scFv.

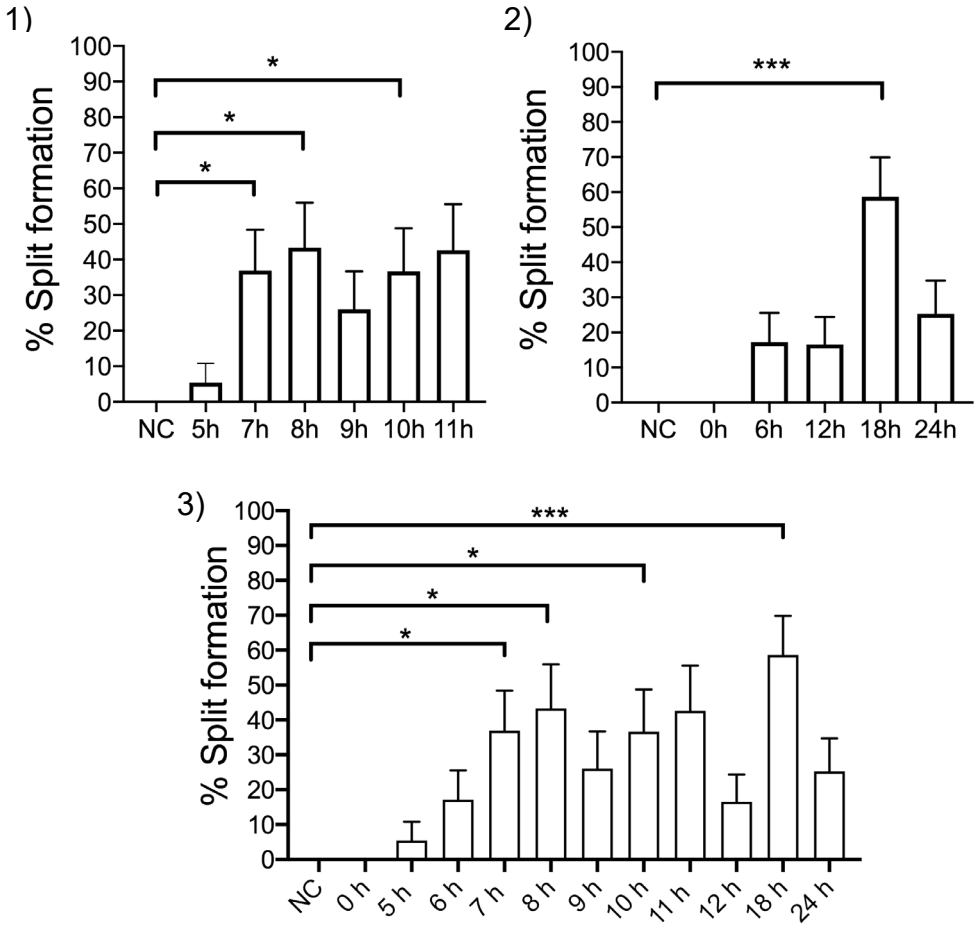

FIG. 18: FIRST SIGNIFICANT INCREASE IN SPLIT FORMATION OCCURS AFTER 7 HOURS

All results from the semi-quantitative histomorphometry were analysed by performing a Kruskal-Wallis test with Dunn‘s multiple comparisons post-hoc test.

1) Results from the 11 hours (h) experiments combined: n = 3, min. 9 – max. 15 VFs* per point of time. 89 VFs in total.
2) Results from the 24 h experiments combined: n= 3, min. 11 - max. 18 VFs per point of time. 91 VFs in total.
3) Results from all time course experiments combined: n = 6, min. 10 - max. 18 VFs per point of time. 172 VFs in total.

The graphs are showing the significance of the increase in split formation in comparison to the negative control (for significance levels see chapter ***4.1.4 STATISTICS***). Plot: mean with standard error of the mean (SEM). VFs = visual fields

5.3 THE VARIABLE FRAGMENT Px4-3 BINDS IN THE EPIDERMIS

The DIF staining was used to visualise the binding pattern of the scFv (in red) (**FIG. 19**). Red stained cells can only be seen in the epidermal skin layer which indicates the binding structures of the scFv. During the incubation time, the scFv is able to spread and bind to Dsg 1 and Dsg 3, causing acantholysis. Dsg 1 and Dsg 3 are part of the desmosomes which are localised right in between the keratinocytes creating the reticular binding pattern in the DIF (**FIG. 19**). The DIF shows cell nuclei in blue which can be seen in both, the sample injected with the scFv and the NC.

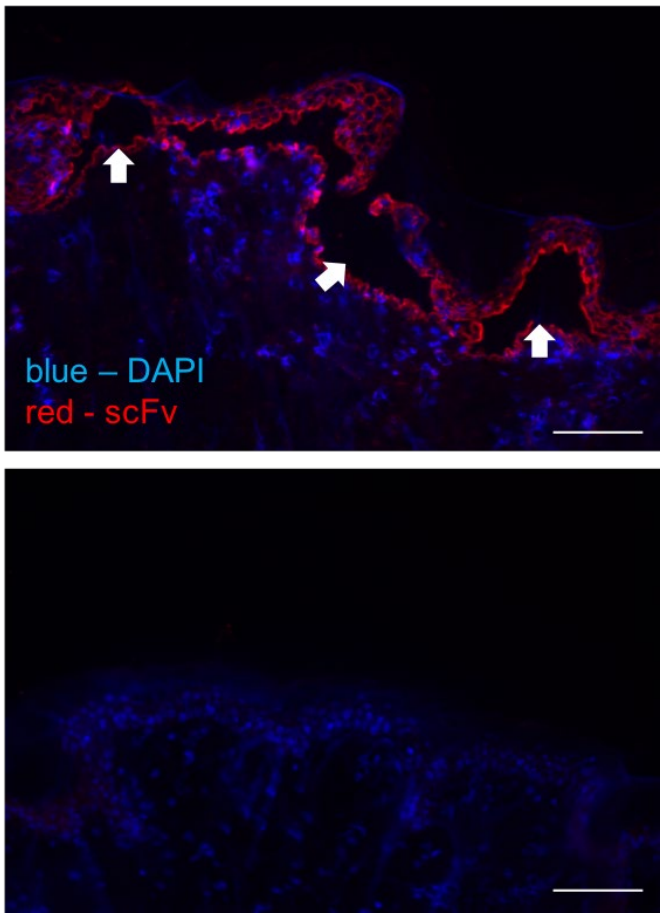

FIG. 19: THE SHORT CHAIN VARIABLE FRAGMENT Px4-3 BINDS TO THE EPIDERMIS

1) Specific staining of the short chain variable fragment (scFv) [anti-desmoglein (Dsg) 1 / anti-Dsg 3] (red) and 4′,6-Diamidin-2-phenylindol (DAPI) staining the cell nucleus (blue) in human skin. Red stained cell surfaces can be found within the epidermis only, not within the dermis. This visualises the binding pattern of the scFv to Dsg 1 and Dsg 3 of the keratinocytes. Several blisters are also shown in this staining (white arrows).
2) The sample injected with intravenous immunoglobulins as a negative control shows no staining of the scFv and no intraepidermal blistering.

Scale bars = 100 µm

5.4 BINDING PATTERN OF DESMOGLEIN 1 IN THE EPIDERMIS

In the IIF Dsg 1 staining we visualised the binding pattern of Dsg 1 within the epidermis. Like in the DIF staining of the scFv, the keratinocytes were stained using DAPI and therefore show up in a blue colour. As expected, Dsg 1 can be found around the keratinocytes forming a honeycomb like pattern (**FIG. 20**). Dsg 1 is spread throughout the epidermis with a focus on the more superficial layers.

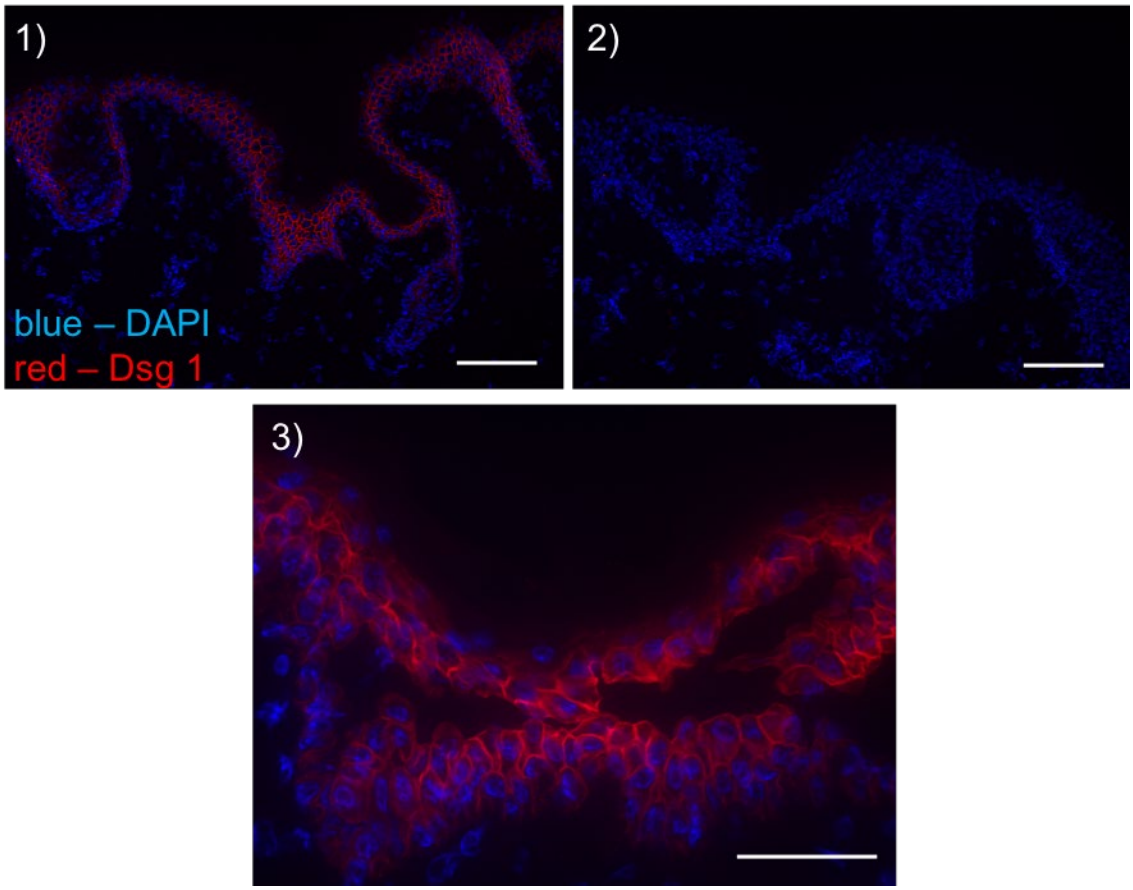

FIG. 20: BINDING PATTERN OF DESMOGLEIN 1 IN THE EPIDERMIS
Desmoglein (Dsg) 1 can be found in a honeycomb like pattern around the keratinocytes throughout all layers of the epidermis. The staining shows a higher amount of Dsg 1 in the outermost layers.
1) Dsg 1 staining of the 7 hours (h) sample; scale bar = 100 µm.
2) Negative control of the Dsg 1 staining without the secondary antibody of the 7 h sample; scale bar = 100 µm.
3) Dsg 1 staining of the 8 h sample; scale bar = 50 µm.

5.5 BINDING PATTERN OF DESMOGLEIN 3 IN THE EPIDERMIS

In the IIF Dsg 3 staining we visualised the binding pattern of Dsg 3 within the epidermis. The keratinocytes are stained with DAPI in a blue colour. Around the keratinocytes in a honeycomb like pattern we can find Dsg 3 stained in a bright green (**FIG. 21**). The staining also shows the distribution of Dsg 3 in the epidermis. Dsg 3 can be found mostly in the lower layers of the epidermis and not in the more superficial layers.

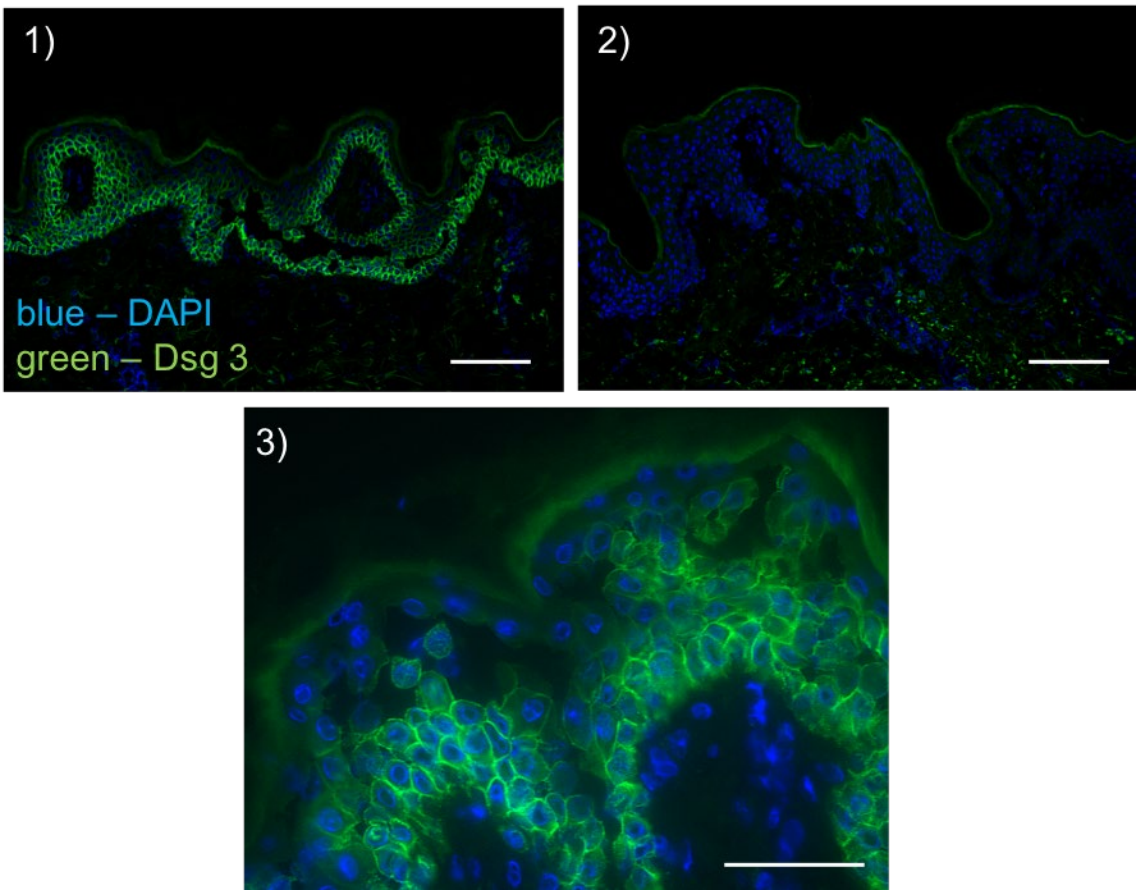

FIG. 21: BINDING PATTERN OF DESMOGLEIN 3 IN THE EPIDERMIS
The binding pattern of desmoglein (Dsg) 3 in the epidermis is also honeycomb like around the keratinocytes. Dsg 3 is clearly located in the lower layers of the epidermis and fades out towards more superficial layers.
1) Staining of Dsg 3 in the 8 hours (h) sample; scale bar = 100 µm.
2) Negative control of the Dsg 3 staining in the 8 h sample; scale bar = 100 µm.
3) Dsg 3 staining of the 7 h sample; scale bar = 50 µm.

5.6 TERMINAL AMINE ISOTOPIC LABELLING OF SUBSTRATES INCREASES PROTEOME COVERAGE

Autoimmune skin conditions, like PV pathogenesis, are associated with an increased protease activity and processing of proteins. In order to analyse changes in the proteome, as well as degradome composition and identify potential novel biomarkers for PV pathogenesis, the samples from the time course experiments were processed by TAILS. TAILS increases the overall proteome coverage by performing a classic whole proteome MS analysis and an additional N-terminal enrichment of protease generated peptides in parallel. In order to analyse quantitative changes in the proteome over time both time course experiments were analysed following the standard TMT-6-plex-TAILS workflow (see chapter ***4.2.2 TERMINAL AMINE ISOTOPIC LABELLING OF SUBSTRATES***) where a mix of equal amounts of the first five channels was used as a reference channel. The MS data was processed by *Proteome Discoverer 2.2*, and channels normalised by setting the reference channel to 100 %. The resulting values for each experiment were collected in tables for further data processing. The whole proteome analysis (preTAILS) identified comparable amounts of total quantifiable proteins and peptides in all 11 and 24 h experiments (**1st 24 h:** 1465 proteins, 6235 peptides; **2nd 24 h:** 1627 proteins, 6954 peptides; **3rd 24 h:** 1462 proteins, 6572 peptides, **1st 11 h** 1898 proteins, 8073 peptides; **2nd 11 h:** 1618 proteins, 7272 peptides; **3rd 11 h:** 1612 proteins, 7018 peptides).

TAILS identified quantifiable N-terminal proteins and peptides for each experiment that could not be identified in the conventional shotgun-like preTAILS analysis (**FIG. 22**, **FIG. 23**).

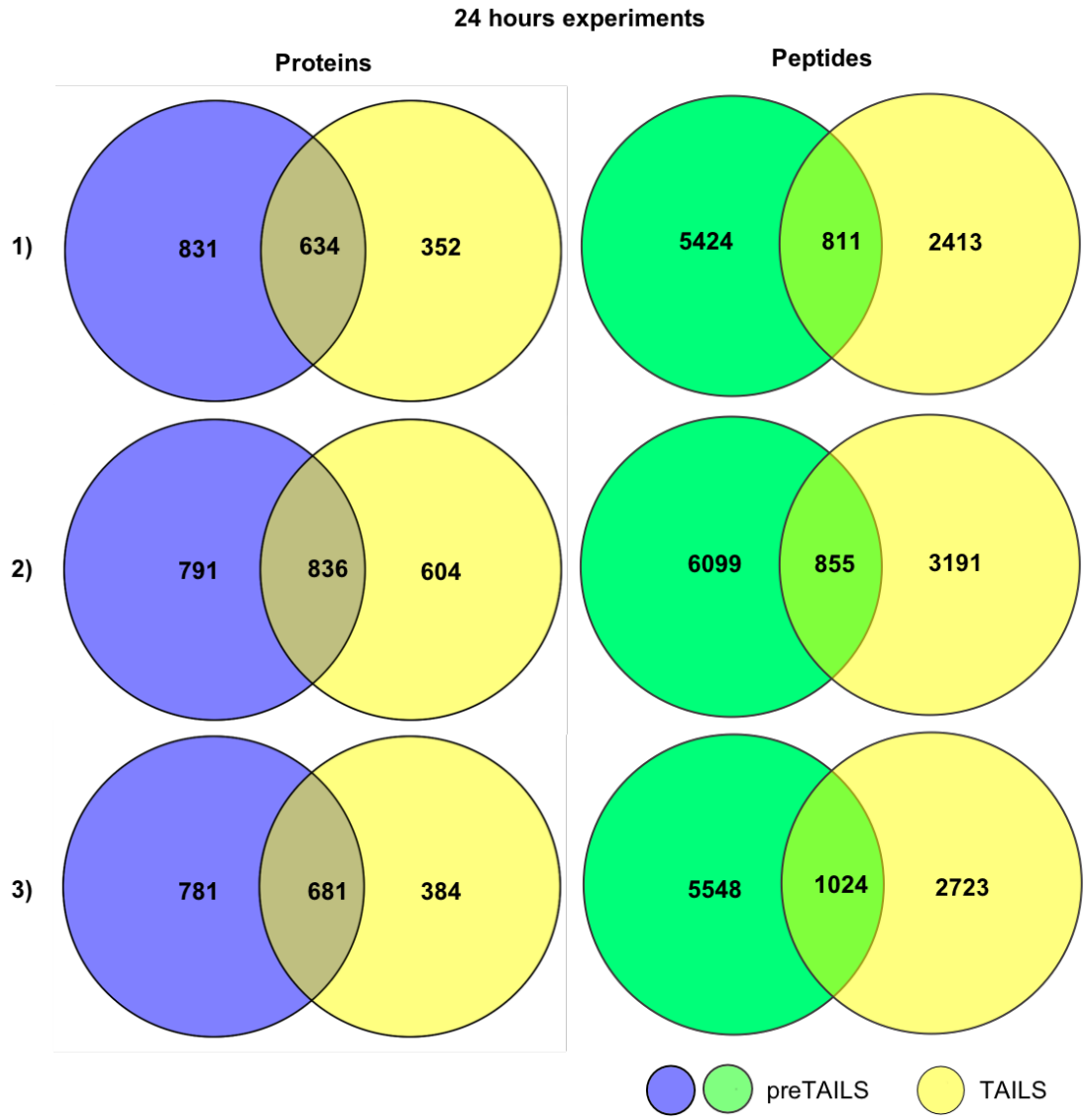

FIG. 22: TOTAL NUMBER OF UNIQUE QUANTIFIABLE PROTEINS AND PEPTIDES IDENTIFIED IN THE PROTEOME ANALYSES OF THE 24 HOURS EXPERIMENTS

Shown here are the unique numbers of proteins and peptides discovered in the 24 hours experiments from the three individuals 1) - 3) (see **TABLE 1**) that were quantifiable throughout all six channels. The preTAILS and TAILS samples and also the overlap between the two are shown for each individual.

The 24 h experiments (**FIG. 22**) resulted in similar numbers of proteins and peptides to the 11 h experiments (**FIG. 23**).

Similar to the whole proteome analysis, the TAILS analysis also identified comparable amounts of total quantifiable proteins and peptides in all 11 and 24 h experiments (**1st 24 h:** 986 proteins, 3224 peptides; **2nd 24 h:** 1440 proteins, 4046 peptides; **3rd 24 h:** 1065 proteins, 3747 peptides, **1st 11 h:** 1292 proteins, 4038 peptides; **2nd 11 h:** 1362 proteins, 4143 peptides; **3rd 11 h:** 1254 proteins, 7018 peptides).

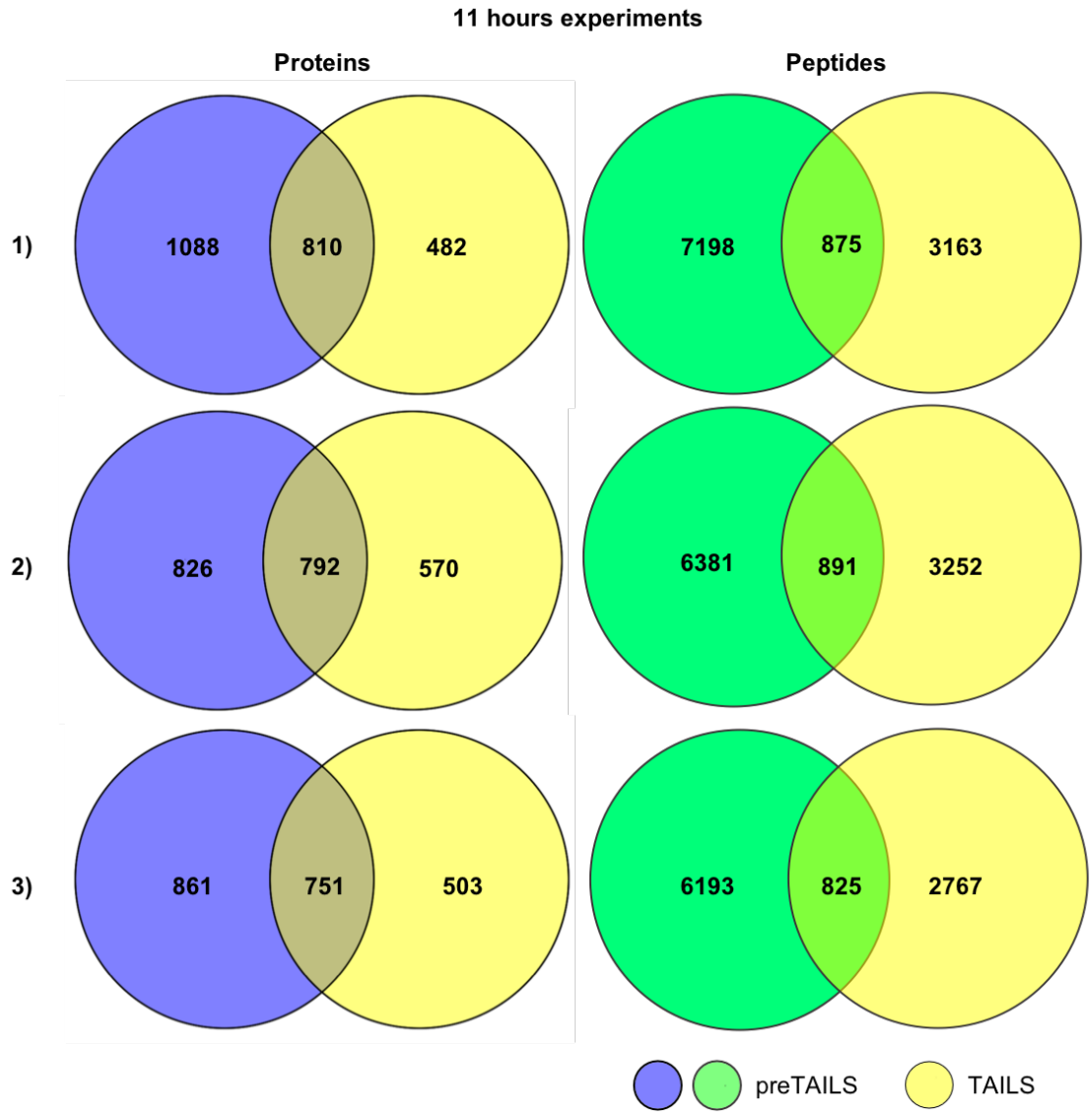

FIG. 23: TOTAL NUMBER OF UNIQUE PROTEINS AND PEPTIDES IDENTIFIED IN THE PROTEOME ANALYSES OF THE 11 HOURS EXPERIMENTS

Shown here are the numbers of unique and quantifiable proteins and peptides discovered in the 11 hours experiments from the three individual patients 1) - 3) (see **TABLE 1**). The preTAILS sample, the TAILS sample and also the overlap between the two are shown for each experiment.

In the next step, the numbers of unique, quantifiable protein hits were compared in between the 24 h (**FIG. 24**) and 11 h (**FIG. 25**) experiments for both the preTAILS and the TAILS analysis in order to determine the overlap of proteins / peptides between the different skin donors.

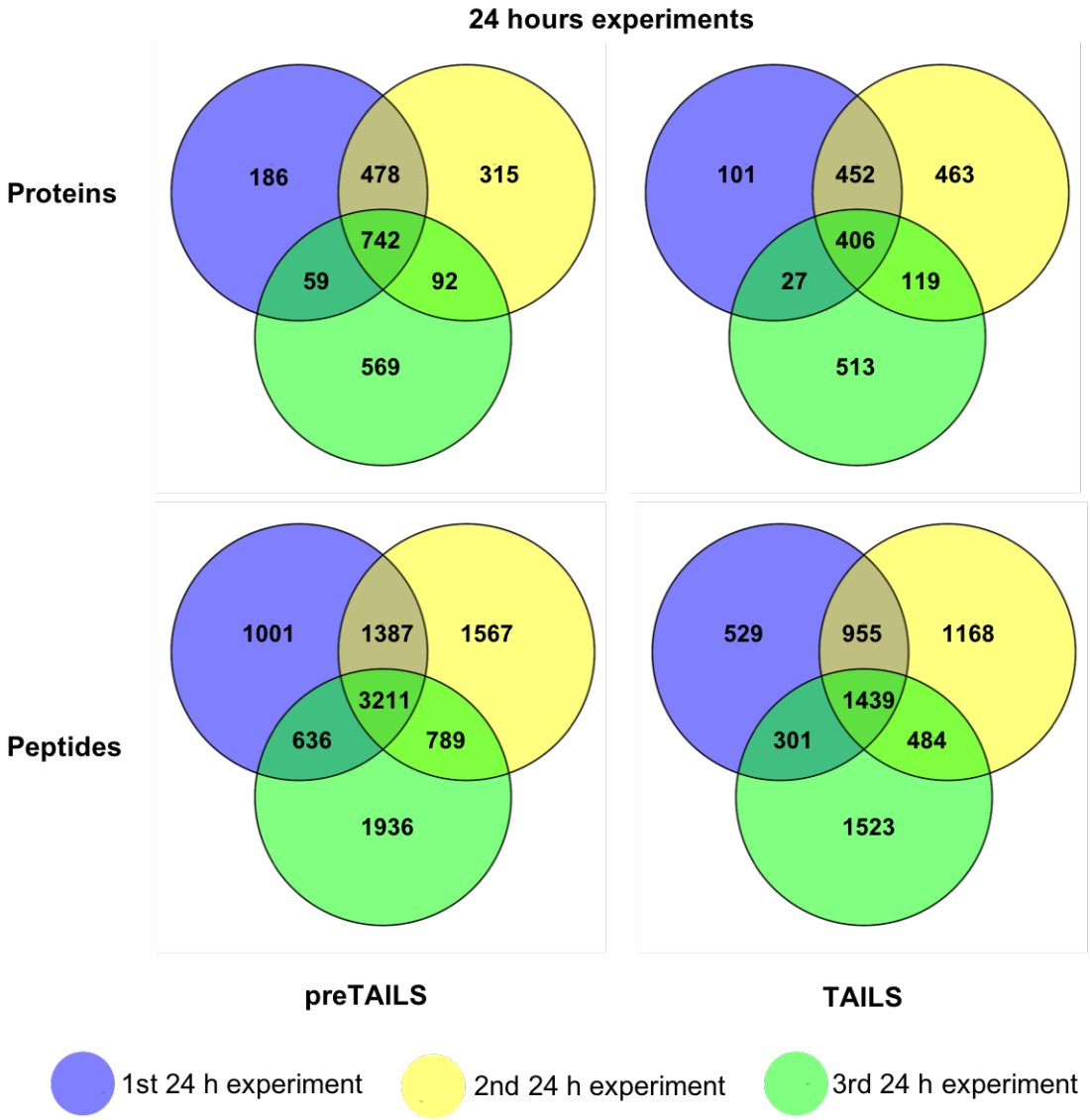

FIG. 24: PROTEOME COVERAGE OVERLAP IN ALL 24 HOURS EXPERIMENTS
The unique, quantifiable protein / peptide hits from each 24 hours experiment were compared between the three different skin donors.

The overlap between the three different skin donors used for the three 24 h experiments is 30.4 % for all unique protein hits identified in the preTAILS analysis. From the proteins detected in the TAILS analysis 19.5 % overlap between all three experiments. For the unique peptides detected in the preTAILS analysis the overlap between all three experiments is 30.5 % meaning one third of all unique peptides was identified within all three experiments. For the peptides detected in the TAILS analysis the intersection between all three patients is 22.5 %.

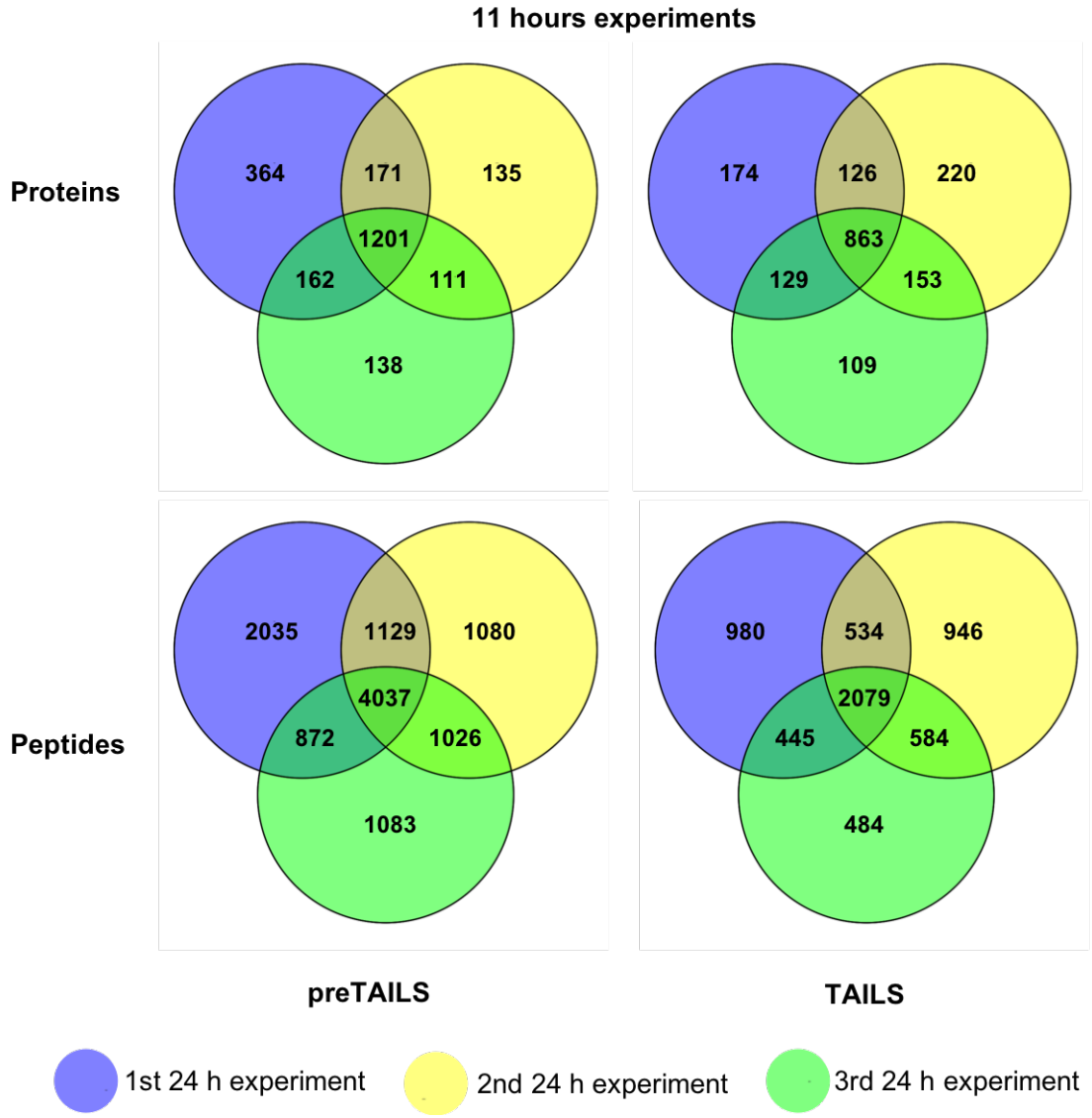

FIG. 25: PROTEOME COVERAGE OVERLAP IN ALL 11 HOURS EXPERIMENTS
The unique, quantifiable protein / peptide hits from each 11 hours experiment were compared between the three different skin donors.

Similar to the overlap of the proteome coverage discovered for the 24 h experiments, the overlap for all unique peptides from the 11 h experiments is 35.8 % for the preTAILS and 34.4 % for the TAILS analysis. The intersection for the proteins identified in the TAILS analysis of the 11 h experiments is 48.6 %. The proteins detected from the preTAILS samples even overlap by 52.6 % between all three experiments.

5.7 COMPOSITION OF PROTEINS AND THEIR FUNCTIONS

The functional classification of the proteins found in the samples was analysed using the *Panther classification system*. The resulting pie chart is shown in **FIG. 26**.

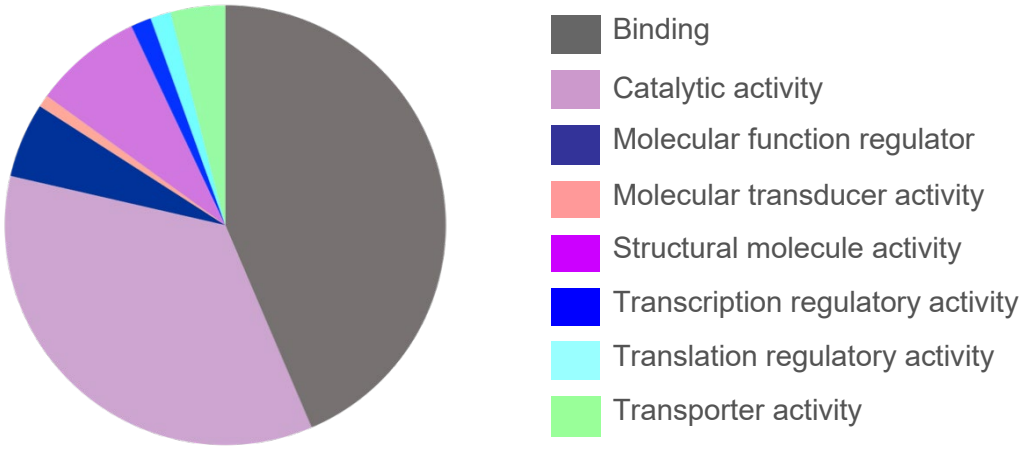

FIG. 26: MOLECULAR FUNCTIONS OF THE PROTEINS IDENTIFIED
Total proteins: 1242, total function hits: 949.
Shown here is the composition of molecular functions of the proteins identified in the preTAILS sample of the third 24 hours experiment.

Classification analysis coincided between the different experiments with comparable functions and values (see chapter ***8.3 COMPOSITION OF MOLECULAR FUNCTIONS***). The main two molecular functions of the proteins identified in all six experiments are catalytic activities and binding functions. In the particular experiment shown in **FIG. 26**, the proteins with binding functions consist of several subgroups. Interestingly, the largest subgroup being protein binding with 21.9 % (total number of 208 proteins), followed by organic cyclic compound binding with 20.6 % and heterocyclic compound binding with 20.1 %. In the other five experiments, the composition only varied around 0.3 %. The protein binding subclass includes functions such as cell adhesion molecule binding, enzyme binding but also HSP and complement binding. Several proteins with such functions were identified in the MS analysis and are known to be involved in PV pathogenesis. Thus, those will be further discussed in the following passages.

5.8 SCREENING OF PRESELECTED SKIN PROTEINS OVER THE COURSE OF TIME

TMT-labelling of proteins allows to monitor protein abundance changes between different conditions or time points. Thus, abundance data for proteins detected in all TMT-channels were analysed by hierarchical clustering to visualise if protein abundances change at a specific time point after scFv treatment. As already mentioned, protein abundances were normalised to the reference channel. For further processing and easier visualisation of the data the channel with the highest abundance was set to 1 for each separate protein, meaning a value of 1 is the highest possible value and all other values are adjusted in relation to this. In compliance with the observed pathological split formation (**FIG. 17**, **FIG. 18**), cluster analysis of all experiments also showed, that between 5 and 7 h protein abundances change and show upregulation for many proteins (**FIG. 27**). The clusters for the 5 and 7 h samples also differed the most from the remaining points of time. Clustering was performed according to the behaviour of the measured abundances over the course of time. Corresponding cluster patterns were found in the other experiments (see chapter ***8.4 FURTHER PROTEIN CLUSTER ANALYSIS RESULTS***). The cluster analysis was performed using the *ClustVis* webtool (Metsalu and Vilo 2015).

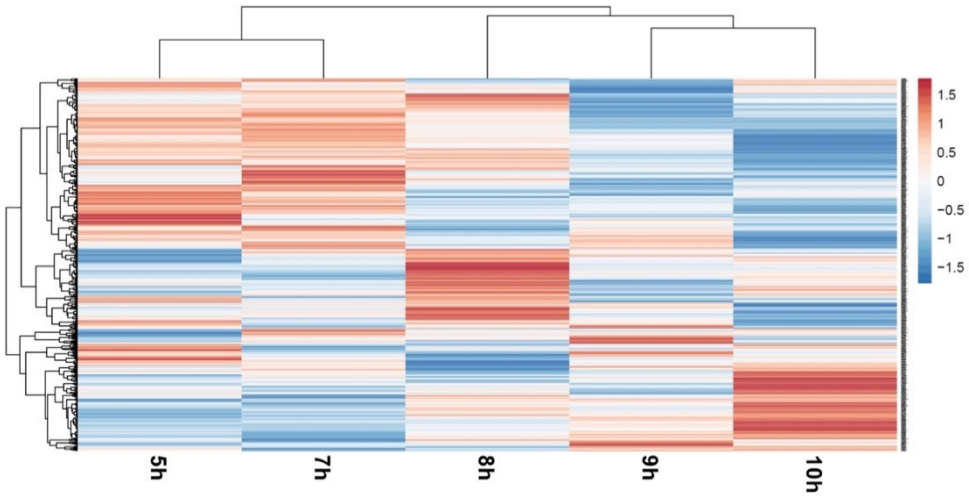

FIG. 27: CLUSTER ANALYSIS IDENTIFIED SIMILARITIES BETWEEN THE 5 AND 7 HOURS SAMPLES

The cluster analysis was performed with unique, quantifiable proteins identified in the preTAILS analysis of the second 11 hours (h) experiment. Shown here are the similarities between the 5 and 7 h samples in comparison to the other three time points. Several groups of proteins were identified that showed an upregulation in 5 and 7 h samples (shown in red).

The abundances over time of several candidate proteins associated to PV pathogenesis (see chapter ***8.5 SKIN PROTEINS INVOLVED IN PEMPHIGUS PATHOGENESIS***) were analysed in detail as well. Since the sample of the third 24 h experiment and the second 11 h experiment were derived from the same donor (see **TABLE 1**), data from those experiments was compared to each other. The data from the other experiments was also processed in the same pattern in order to compare the identified effects between all experiments (see chapter ***8.6 SKIN PROTEINS IDENTIFIED***). Since these tables still contain a large amount of protein hits and values, an extract of the tables created in correspondence with interesting, preselected skin proteins from the third 24 h experiment and the second 11 h experiment is shown in **FIG. 28**.

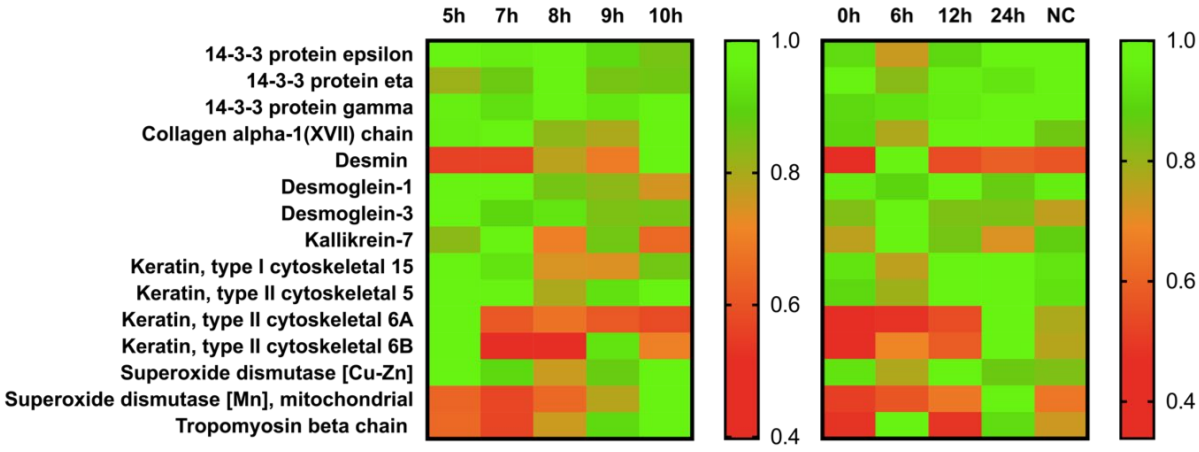

FIG. 28: PROTEINS AND INFLAMMATORY MARKERS CHANGE OVER THE COURSE OF 24 HOURS

Left: This heatmap shows an extract of the abundances measured in the preTAILS proteome analysis of the second 11 hours (h) experiment.
Right: This map shows the same skin proteins as the heatmap on the left but is created from the results of the third 24 h experiment. The selected skin proteins change over the course of 24 h.

In the two experiments, kallikrein 7, a known catalyst for the degradation of intercellular cohesive structures within the skin (Borgono, Michael *et al.* 2007), was analysed to show any up- or downregulation in comparison to the NC over time.
The highest abundance was measured after 6 h. In comparison to the NC which showed an abundance relation value of 12.5 % less. There is no linear development of the protein abundance for kallikrein 7 as the measured abundance levels peak at 6 h but decrease after this point to an even lower abundance than measured at 0 h.

When looking at the same protein in the second 11 h experiment we see the highest abundance after 7 h. Similar to the 24 h experiment, the levels measured after this point show a decline. The abundance measured for the 9 h sample is higher than the ones for the 8 h and 10 h samples.

Muscle related proteins, such as desmin and tropomyosin beta chain, both show an increased abundance after 6 h in comparison to the other points of time and also to the NC. The 6 h sample showed the highest abundance of all samples measured.
In the 11 h experiment the highest abundances were seen in the 10 h samples for both proteins whilst the lowest abundances were measured after 5 and 7 h. The contradicting results between the two experiments could be due to the separate measurements on the MS or the separate processing of the samples.

Interestingly, one of the main target antigens in PV pathogenesis and one of the targets of our scFv, Dsg 1, shows no significant up- or downregulation over the course of 24 h in comparison to the NC in the two experiments shown above. It also does not show any outstanding development over time in all other experiments.

For the other main target of the scFv, Dsg 3, the highest measured abundance belongs to the 6 h sample. The abundance of the NC sample is nearly 25 % lower than the abundance of the 6 h sample. All other points of time showed for Dsg 3 an approximately 10 % higher abundance than the NC and a nearly 15 % lower abundance than the 6 h sample. In the 11 h experiment these results are confirmed. The highest abundance was measured for the 5 h sample whilst all other points of time show abundances approximately a 10 to 15 % lower than of the value measured at 5 h.
However, in the other experiments the results for Dsg 3 do not coincide with the results from the two experiments mentioned above. In the first 24 h experiment, Dsg 3 was not identified in the MS analysis. In the second 24 h experiment, the highest abundance for Dsg 3 was measured in the 24 h sample and similar values were measured for the sample at 0 h and the NC sample. In the other two 11 h experiments, Dsg 3 could be found and the highest abundances were measured for 5 and 7 h. Nonetheless, there was no significant difference in comparison to the NC samples and also no linear decrease over time.

For further analysis a list of proteins which are known to be related or suspected to modulate PV pathogenesis was compiled (see chapter ***8.5 SKIN PROTEINS INVOLVED IN PEMPHIGUS PATHOGENESIS***). This list operates as the foundation for the following proteome analyses. A table showing all proteins from the list that I was able to identify within each experiment was created for each of the six HSOCs (see chapter ***8.6 SKIN PROTEINS IDENTIFIED***). Because the proteome shows a huge variety between each individual and also varies slightly between each run on the MS, the proteins found in each sample may also vary.

The mitochondrial superoxide dismutase, an enzyme catalysing the neutralisation of radicals in the cell, was found to increase its levels over 24 h in the samples injected with the scFv whilst the levels in the NC did not increase in the same way. This effect can be seen in two of three 24 h experiments (the mitochondrial form of this enzyme could not be found in the second 24 h experiment). Furthermore, the second 11 h experiment shows increased levels of the superoxide dismutase after 10 h. In the first and third 11 h experiment the levels did not change over the course of 10 h.

Not showing an increased incidence or upregulation in comparison to the NC were substrates reducing cellular stress such as several HSPs and regulatory proteins of the 14-3-3 family that could be identified in the proteome analyses.

5.9 UPREGULATION OF N-TERMINAL-ENRICHED PEPTIDES BETWEEN 5 AND 7 HOURS

In the time course experiments I could show that the split formation occurs between 5 and 7 h after injection of the scFv. This leads to the question which proteins and peptides are upregulated at this point of time and if they might be related to the pathogenesis of the split formation.

The following data was also analysed by comparing the pull-out TAILS results from the third 24 h experiment and the second 11 h experiment as they were both performed using skin from the same donor (see **TABLE 1**). Both set-ups should be comparable because the proteome of both samples should have been very similar before injection of the scFv although one must keep in mind that the hits recognised by the MS may also vary during different runs.

All peptides of the TAILS analysis from these two experiments were clustered using *MeV 4.8.1* software calculating a Pearson correlation and k-means. After creating 10 general clusters (3rd 24 h experiment: 1285 peptides in total, 2nd 11 h experiment: 1579 peptides in total), the clusters peaking around 5 to 7 h were merged to a total of 456 peptides for the 24 h experiment and 774 peptides for the 11 h experiment and then clustered once more. The four most suitable clusters were then combined to a total 329 peptides for the 24 h experiment (see chapter ***8.7 CLUSTERED PEPTIDE HITS AT 6 HOURS)*** and 298 for the 11 h experiment (see chapter ***8.8 CLUSTERED PEPTIDE HITS AT 5-7 HOURS***) (**FIG. 29**).

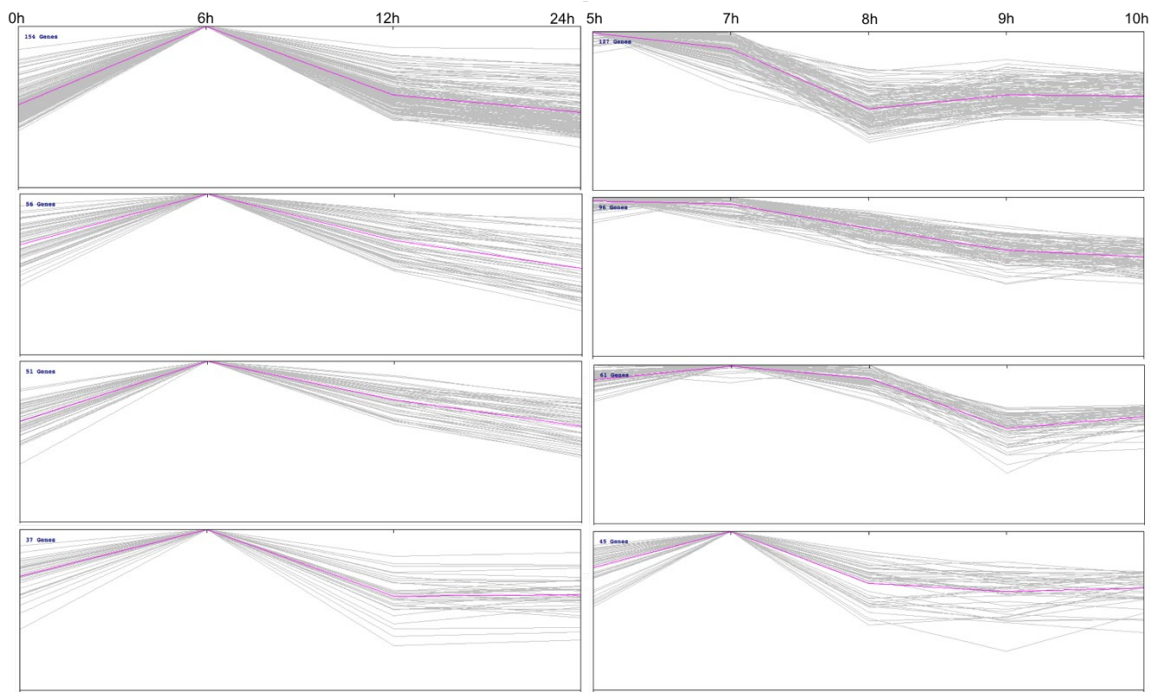

FIG. 29: PEPTIDES SHOWING AN UPREGULATION BETWEEN 5 AND 7 HOURS AFTER PX4-3 INJECTION

The graphs show the clusters created from all peptides identified in the TAILS analysis of the third 24 hours (h) experiment and the second 11 h experiment.
Left: In the 24 h experiment 298 peptides in total are expressed most frequently after 6 h of incubation time followed by a decreasing incidence after this point.
Right: In the 11 h experiment in total 329 peptides are expressed most frequently between 5 and 7 h of incubation time followed by a downregulation after this point.

These peptides were compared to each other but only two identical peptides were found between the two experiments in all four clusters: [R].QLEEAEEEAQR.[A], belonging to the myosin 9 protein, and [SG].DTSVVLSMDNNR.[NCSY], belonging to keratin type II (cytoskeletal 5, 6A, 6B).

I compared the levels of keratin type II (cytoskeletal 5, 6B and 6A) between all three 11 h experiments. It showed that the levels of these proteins were elevated after 5 to 7 h in all three experiments. This effect was particularly visible for 6A and 6B, but also for 5. In the first two 24 h experiments the effects on the regulation of keratin type II (cytoskeletal 5, 6A and 6B) varied a lot more. They even showed elevated levels of the proteins after 24 h in comparison to the third 24 h experiment which showed the upregulation after 6 h and was used for the clustering shown above.
Interestingly, the exact sequence [SG].DTSVVLSMDNNR.[NCSY] belonging to keratin type II (cytoskeletal 5, 6A, 6B) could also be found in the TAILS samples of

all other experiments. In every case, except for the first 11 h experiment, the highest abundance for this peptide was measured either at 6 h or 7 h. In the first 11 h experiment the highest abundance was measured for the 10 h sample. Curiously though, this peptide sequence could only be found in the pull-out TAILS samples and not in the preTAILS samples meaning it is a N-terminal original peptide from the sample and was not created by trypsin.

Myosin 9 was not listed on the skin protein register used to create the heatmaps but can be found in all the raw protein files from the proteome analyses. In the TAILS sample of the first 11 h experiment the sequence [R].QLEEAEEEAQR.[A] could be found. It showed the highest abundance value for the 8 h sample which would still be compatible with the clusters above. However, the exact peptide sequence found in the two clusters mentioned above could not be found in the other three experiments.

In the last step, all peptides from the clustered TAILS analysis (see chapters ***8.7 CLUSTERED PEPTIDE HITS AT 6 HOURS*** and ***8.8 CLUSTERED PEPTIDE HITS AT 5-7 HOURS***) were N-terminal annotated and their position within the corresponding master protein was mapped in cooperation with Dr. Philipp Kastl (Technical University of Denmark, Copenhagen). Over 90 % of all annotated peptides were internal peptides meaning they were not produced during the trypsin digest but by proteases that were active during the incubation of the scFv in the skin samples. The mapping of the exact position of the peptides within the master proteins will allow further research concerning the cleavage sites and the proteases that are able to cleave at exactly the sites identified.

6 DISCUSSION

6.1 SUMMARY OF ALL RESULTS

The aim of this study was to investigate the split formation in the HSOC regarding the point of time at which the blister formation occurs. The split formation first occurs between 5 and 7 h after injection of the scFv. This was answered by performing time course experiments using the HSOC.
In addition to the time course experiments, DIF and IIF stainings were performed proving the binding patterns of the scFv to be corresponding with the binding patterns of Dsg 1 and 3. The distribution of Dsg 1 and 3 within the epidermis is also conformable with the literature research done beforehand (Amagai, Koch *et al.* 1996). This shows that the scFv really targets both structures and mimics the effect of PV autoantibodies against both antigens in the skin.

Furthermore, the proteome of the samples from the time course experiments was analysed. The identified proteins were compared with proteins known to be involved in PV pathogenesis (see chapter ***8.6 SKIN PROTEINS IDENTIFIED***). By performing a TAILS experiment, I was able to increase the proteome coverage in comparison to a normal shot-gun like preTAILS analysis (**FIG. 22**, **FIG. 23**). This allows a more in-depth analysis of peptides created during the incubation of the scFv rather than during the trypsin digest of the TAILS experiment itself.
Regarding the development of the proteins identified, I was able to detect a number of proteins and also peptides that showed an upregulation between 5 and 7 h after injection of the scFv (**FIG. 27**, **FIG. 29**). The relevance of the discovered proteins, peptides and their behaviour over time will be debated in the following sections of this discussion.
Both methods, the HSOC and the TAILS analysis were performed in different facilities and using human tissue. Both methods provide unique results that would not have been achieved using alternative methods. They need to be challenged and investigated carefully in regard to possible sources of error and any disruptive

factors. The potential sources of error will be specified and evaluated in the following sections.

6.2 ADVANTAGES AND DISADVANTAGES OF THE HUMAN SKIN ORGAN CULTURE MODEL FOR PEMPHIGUS VULGARIS

The HSOC model is a very elegant method for testing substances *in vitro* as it mimics most physiological circumstances in the human skin. This is due to the fact that all three skin layers are preserved and the air-liquid interface of the human skin is imitated nicely in the transwell plates.

The main advantages of the HSOC for PV are its simplicity and stability. In comparison to a cell culture that consumes more time and is much more susceptible to infections and contaminations, this HSOC runs over the course of 24 h after injecting the scFv into the samples. No further management is necessary and the incubation time will probably be reduced in the future due to the findings of my work.

Furthermore, in the model for PV using the scFv, both main targets of physiological PV antibodies are targeted at once without the reliance on unphysiological substances such as exfoliative toxin A (ETA). ETA is used in several PV mouse models for cleaving Dsg 1 to disable the compensatory binding.
The HSOC model for PV could also be performed using serum from PV patients. However, not all patients show antibodies against both Dsg in their serum which is making the acquisition of such a serum difficult. One would also need to determine the concentration of the antibodies of each serum used before planning the experiment. The use of the anti-Dsg 1 / Dsg 3 scFv is a more standardisable in comparison to using patient serum because the scFv can be produced in large volumes at a certain concentration when the antibody specificity is known.

The injection of the scFv is performed intradermally in the HSOC model. This method mimics the physiological migration process of the antibodies from the small blood vessels which are located in the dermal layer of the skin. Intradermal injection

has also been described in previous studies using PV serum instead of the scFv (Ishii and Amagai 2012).

Ethically, the skin used for the HSOC is an ideal material as it consists of the 'leftovers' from elective plastic surgeries. However, when working with human tissue you are dependent on the elective surgeries to be performed in the clinics cooperating with your laboratory. I was working in the laboratory and performing the organ cultures from April to August and there was a noticeable summer break for surgeries. During the summer holidays and the warmer climate in general, the number of elective plastic surgeries performed decreases drastically. Wound infection rates are higher and the healing process in general is more difficult than during the colder months of the year. This means, it was not easy for me to receive the skin samples. A higher number of experiments would have been preferable for statistical reasons but was simply not practical at the time. Besides this and a few possible structural errors mentioned below, I find the HSOC to be a very good and reliable method for imitating the pathomechanisms of PV.

6.3 POSSIBLE SOURCES OF ERROR IN THE HUMAN SKIN ORGAN CULTURE MODEL

Working with human tissue can also pose certain difficulties that may lead to errors in the analysis. Firstly, it is not known how much the different origins of the skin used for the model affect the results. During my experiments, I used several different types of skin from various people (see **TABLE 1**). Both, the age of the skin donor and also the area of the body the skin was taken from, affect the composition and therefore the thickness of the skin. Nevertheless, I was able to find the split formation in all types of skin used suggesting that these differences do not interfere with the efficiency of the HSOC model.

Secondly, there could also be cutting artefacts caused by putting too much pressure on the scalpel when handling the samples after the incubation. I tried to eliminate this source of error by reducing the area measured in the semi-quantitative histomorphometry by 200 µm from each cutting edge. To prove the split formation

is definitely not caused by cutting the samples, our working group is cooperating with the Institute of Biomedical Optics at the University of Lübeck to see if the blisters can be seen in the intact samples from HSOCs using optical coherence tomography and also optical coherence microscopy.

When it comes to the evaluation of the HSOC, the informative value of the histomorphometry relies on the correct embedding of the skin sample. By flagging an edge opposite of the cutting edge, I attempted to ensure the correct embedding. However, in the dehydration process the skin sample shrinks and it becomes difficult to allocate the correct sides of the sample, even the one flagged edge. In one of my samples I could not find a split in the sample embedded in paraffin for HE staining due to wrong embedding. In the corresponding sample embedded in Tissue-Tek O.C.T., the split was visible proving that the lack of split formation in the paraffin sample must have been due to wrong embedding and not because the split did not form at this point of time. Especially when only having a low number of experiments, a mistake like this will change the results drastically. It should be discussed if marking the edge with a thread could maybe be a more precise method reducing such errors.
Besides this, I believe the semi-quantitative histomorphometry to be a very reliable method of evaluation because there is hardly any room for subjectiveness. The split formation is either clearly visible or it is not. The guidelines are very clear and there is no question of how and where to measure along the epidermis because the basal cell layer is distinctly visible.
In addition, the Institute of Biomedical Optics is working on a method to measure the size of the split formation with the intact skin samples through optical coherence microscopy. This method would reduce any possible errors of analysing the split formation manually and would also help to reduce cutting artefacts altogether.

Regarding the concentrations, volumes and also the choice of reagents used for the HSOC a few details should be discussed:
The 60 µg of Px4-3 were determined through studies from a previous medical student in our working group as the amount of scFv that will reliably cause a split formation. The limit of 50 µL maximum injection volume is justified by the future

attempt to create a mouse model using Px4-3 and the maximum volume to be injected into the ear of a mouse is 50 µL.
As a NC IVIg was used, which has a different size, weight and concentration than the scFv. The concentration of the IVIg used was 0.25 µg / µL in comparison to the scFv with a concentration of 2 µg / µL. Because we chose not to inject more than 50 µL at once into one skin section 60 µg of the Px4-3 scFv were diluted in 20 µL of PBS. Due to the much lower concentration of the IVIg we were not able to inject the same amount. We decided to keep the distribution of PBS to the scFv respectively the IVIg and injected 7.5 µg IVIg diluted in 20 µL PBS.
This could influence the results which is why I also performed an organ culture with a different scFv (BP scFv 3-14G) to ensure the specificity of Px4-3.
3-14G is a scFv that targets the NC16A domain of BP antigen 2 (BP180). It does not bind to BP antigen 1 (BP230). Similar to Px4-3, it is produced in *E. coli* and purified from *E. coli* supernatants by affinity chromatography (Hammers and Stanley 2014). The purification is performed with TALON beads which bind his-tagged proteins with higher specificity than nickel-charged resins.
The BP scFv was injected in the exact same concentration and volume as Px4-3 (60 µg in 30 µL) and diluted in 20 µL of PBS. It did not cause any split formation in the skin and also worked as a NC for the DIF staining for Px4-3.

6.4 FUTURE RELEVANCE OF THE HUMAN SKIN ORGAN CULTURE

Determining the point of time at which the split formation occurs within the HSOC model allows for more precise testing of possible treatment options. Several pathways and possible therapeutic approaches have been identified in our working group using both, cell cultures and the HSOC. The corresponding compounds will now be tested in the HSOC with emphasis on their effect after 5 to 7 h after injection of the scFv.

Furthermore, the knowledge is very helpful regarding a possible future mouse model. Currently available mouse models do not mimic the complete list of phenomena found in PV patients. There is a passive transfer model in which IgG is transferred into neonatal mice to investigate the pathogenicity of the autoantibodies

(Amagai, Nishikawa *et al.* 1998). The mice develop the typical skin lesions and the histological blister formation in the epidermis. However, the use of neonatal mice is very questionable regarding the not yet fully developed immune system of the mice and their still very thin and nearly hairless skin.

It could also be shown that injection of AK23, a monoclonal murine antibody against Dsg 3, leads to PV typical lesions in the mucous membranes of C57Bl/6J mice. The lesions appeared predominantly in the oral mucosa (Schulze, Galichet *et al.* 2012). Furthermore, the usage of ETA to cleave Dsg 1 is common in the passive disease models (Amagai, Matsuyoshi *et al.* 2000). ETA is an aggressive toxin and when looking at the split formation in the murine skin it cannot clearly be distinguished whether the split was caused by the PV antibodies or the ETA as it is an unphysiological factor.

Several active disease models are available to test therapeutic strategies. However, they are very complex to perform and some do not show all clinical signs of the disease what makes it difficult to classify therapeutic success. Because all available active models use immunodeficient mice, there is the question of how adequate the immune representation in these models really is.

The so-called humanised PV mouse model used major histocompatibility complex class II deficient mice that are engineered to express transgenic pemphigus associated HLA-DRB1*0402. Then, human recombinant Dsg 3 is injected into the mice causing production of anti-human Dsg 3 antibodies that induce split formation in human skin (Eming, Hennerici *et al.* 2014).

Another active model uses Dsg 3 knockout mice that are immunised with mouse recombinant Dsg 3. Then, their splenocytes are adoptively transferred into Rag-2$^{-/-}$ immunodeficient mice. The recipient mice express anti-Dsg 3 IgG and start to develop a PV phenotype (Amagai, Tsunoda *et al.* 2000). This model is used to assess anti-Dsg 3 mAbs (Tsunoda, Ota *et al.* 2003) to test possible treatment options regarding their efficiency to inhibit antibody production (Takae, Nishikawa *et al.* 2009) and to evaluate Dsg 3 reactive CD4+ clones (Takahashi, Amagai *et al.* 2008).

Developing a disease model for PV showing all signs of PV patients in the skin as well as showing the adequate reaction of immune cells and components is going to be a follow-up project of my work with the HSOC. We will use the anti-Dsg 1 / Dsg 3

scFv from the HSOC to induce blister formation in adult immunocompetent mice. The symptoms should include the effects of Dsg 1 and 3 targeting and will therefore be much closer to the physiological disease development and allow further analysis of possible future treatment options.

6.5 POSSIBLE SOURCES OF ERROR IN THE PROTEOME ANALYSIS

The proteome analysis is dependent on several steps in order to work smoothly. Firstly, the samples for proteome analysis must be frozen after they have been taken out of the incubator. Because I cut my samples before freezing one half for proteome analysis, there was a small period of time in between these steps. Ideally, this time should be reduced and the samples should be shock frozen directly when taken out of the incubator.
I then had to transport my samples to Copenhagen. For this, I used dry ice and isolated the package as well as possible. Nevertheless, this step is a possible source of error because the temperature of the samples cannot be controlled precisely.

Another possible source of error is the extraction of protein from the samples. There are many ways in which the protein can be extracted from the skin. I used two different methods and have found the Biorupter® sonication method to be more effective because I was able to process more tissue at once, meaning I had a more sufficient protein extraction. The PCT (Barocycler®) could only process 3 mg of skin at once meaning the protein extraction was approximately three times less. Therefore, the extraction process would have needed to be repeated at least three times for each experiment in order to receive the same amount of protein extracted using the Biorupter®. Another advantage of using the Biorupter® was that the piece of tissue collected from my sample was larger and therefore easier to cut. When cutting a 10 mg piece of skin from a 5 x 10 mm sample it is important to take the piece from the middle of the sample. Taking a 3 mg piece was much more difficult simply due to its size. The bigger the piece was the easier was the handling.
Literature research suggests that a different approach to sample preparation of full thickness human skin can also increase the number of identified proteins by

powdering the frozen tissue followed by further homogenisation using a glass homogeniser, sonication and filtration of interfering low molecular weight compounds (Bliss, Heywood *et al.* 2016).

The TAILS method requires very precise pipetting of small volumes. It is very important to stick to the protocol and not to change the order of each of the steps. Otherwise, the whole reaction will not work properly.
The HPG-ALD polymer used to perform the pull-out reaction can also cause errors. There are no clear guidelines how much polymer is necessary to perform the reaction. The polymer is very susceptible to disruptive factors such as the temperature and movement during the incubation time. It is very important to ensure the heating block is set on 0 rpm, otherwise the polymer will be destroyed and lose its function.

Lastly, the MS analysis of the TAILS sample must be run on the exact same settings and preferably at the same time to ensure comparable results. The settings for the *Proteome Discoverer* software are also crucial as the software normalises all values using the reference channel.

6.6 PROTEOME ANALYSIS: RELEVANCE AND CONSEQUENCES

Looking at the number of unique, quantifiably protein hits identified using both the preTAILS and the TAILS analysis, the TAILS method increased the proteome coverage by a few hundred proteins or a few thousand peptides for each experiment. This increases the relevance of the proteome analysis simply because of the quantity of proteins / peptides identified.
I compared the total amounts of protein hits to previous studies investigating the skin proteome. I found one study where skin biopsy samples were analysed using gel electrophoresis (Ge) LC-MS / MS and the isobaric tagging strategy called isobaric tags for relative and absolute quantitation (iTRAQ) (Parkinson, Skipp *et al.* 2014). 159 proteins were identified in the GeLC-MS / MS and 616 proteins in the iTRAQ approaches. One hundred and fifty µg of protein was processed for each sample which is three times more than what I used in my TAILS experiments.

However, the number of identified proteins is also approximately 400 proteins for the preTAILS and 200 proteins for the TAILS analysis smaller than what I identified in my analyses. A different paper investigating the anatomy of the human skin using LC-MS / MS analysis identified between 155 and 174 proteins per sample using another completely different method of sample preparation (Mikesh, Aramadhaka *et al.* 2013).
In comparison to my literature research, my approach for proteomic analysis of the human skin proteome seems to provide a very large and efficient proteome coverage.

Many signalling pathways are associated with the phosphorylation of proteins. The *Proteome Discoverer 2.2* allows identification of the dynamic modification “phosphorylation” within the results from the TAILS data. However, in order to quantify the phosphorylation process over the course of time, separate analyses using specific methods of phosphoproteomics would be necessary.

The discovered proteins and peptides originated from six different organ cultures performed with skin from five different patients and overall four different body parts. This means the samples show a wide range of variability increasing the relevance of the results for the proteins that were found in all experiments.
In the next step, I determined the overlap of proteins / peptides between the different skin donors. The numbers of all unique and quantifiable protein hits were compared in between the 24 h and 11 h experiments for both the preTAILS and the TAILS analysis. This showed how many of the identified proteins / peptides overlap between the different skin donors and therefore acts as one indicator to how comparable the results from the experiments might be.
The overlaps between the different experiments ranged from approximately 20 % to just over 50 % (**FIG. 24**, **FIG. 25**). In general, the overlaps measured in the 11 h experiments were higher than in the 24 h experiments which can be explained by the fact that the 24 h experiments contained the NC sample and the 11 h samples did not. Besides, the range of time points is much larger in the 24 h experiments. The extent of the intersections suggests that similar proteins / peptides were found in all samples and that they are comparable to one another to a certain point.

But how relevant are the identified proteins and peptides in reality for the PV pathogenesis?

The composition of molecular functions of the proteins identified was very consistent throughout all experiments (see chapter ***8.3 COMPOSITION OF MOLECULAR FUNCTIONS***). The largest subgroups found were protein binding, organic cyclic compound binding and heterocyclic compound binding. Interestingly, exactly these groups contain the same skin proteins I selected via literature research beforehand that are known to be involved with the PV pathogenesis (see chapter ***8.5 SKIN PROTEINS INVOLVED IN PEMPHIGUS PATHOGENESIS***). Therefore, we believe that the proteome analyses of the samples from the HSOC are representable for the effects found in PV patients.

By clustering of all quantifiable protein hits, a group of proteins showing an upregulation between 5 and 7 h after injection was identified (**FIG. 27**). The accession numbers and names of these proteins are not shown in this dissertation and will be subject of further research.

However, the results from the MS analysis alone do not enable a direct conclusion to the pathomechanisms behind PV pathogenesis. Further studies of the identified proteins and pathways will be necessary to validate and ascertain the results from my study. The analysis shown here in my dissertation should be considered as an outline study with the aim to discover new targets for further investigations.

6.7 INSIGHTS INTO THE PEMPHIGUS VULGARIS PATHOGENESIS CONSIDERING THE GAINED RESULTS

The point of time between 5 and 7 h after injection of the scFv into the HSOC at which the split formation occurs can most likely not be translated completely to what happens in a PV patient but it will help to investigate the mechanisms behind the blistering more in detail. Above all, it will help to investigate the effect of treatments that interfere at certain protein levels or pathways. It is now known what the crucial point of time is at which a compound must have developed its potential in order to affect the split formation in the HSOC. This information will especially be interesting when looking at the effect of locally applied compounds. We would expect a longer

time to onset of effect than if the same compound is injected intradermally because of the time needed to penetrate the *stratum corneum* which functions as a tight barrier of the skin.

The proteome analyses identified clusters of proteins that show an isolated upregulation during the period at which split formation first occurs (5–7 h). Furthermore, the clustering showed that the 5 and 7 h samples as well as the 6 h sample differed the most from all other samples. This suggests that the split formation during this time is caused by up- or downregulation of these proteins or proteases in comparison to the other points of time where the changes in abundance do not occur in the same way.

According to my findings in the proteome analysis, I can confirm the participation of the selected skin proteins (see chapter ***8.5 SKIN PROTEINS INVOLVED IN PEMPHIGUS PATHOGENESIS***) in the pathomechanisms behind the split formation.

The two main target structures of the PV antibodies and also the scFv used in the HSOC model are Dsg 1 and 3. Dsg 1 was identified in the preTAILS analysis of all quantifiable protein hits but did not show any significant in- or decrease over the course of 24 h. For Dsg 3 on the other hand, the highest abundance was identified in both experiments after approximately 6 h and declined from there. The decreasing amount of Dsg 3 over time would mean that it is cleaved in some way during the process of the split formation. This effect could be explained by the Dsg depletion theory which states that Dsg is clustered, internalised and prevented from being integrated into the desmosome (Mao, Choi *et al.* 2009) which would mean a decrease in appearance.
The behaviour of Dsg 3, however, was not confirmed in the other experiments which might be due to the separate measurements on the MS.

For kallikrein 7 the highest abundances were measured around 6 h throughout all proteome analyses meaning at the time of the split formation. Kallikrein 7 and other subtypes of the kallikrein family have been described as desquamation related proteins that destabilise the Dsg 1 structure (Borgono, Michael *et al.* 2007).

Kallikrein has also previously been described to be elevated in patients with PF (Rosatelli, Roselino *et al.* 2005) which would coincide with the abundances measured in the proteome analyses of my samples.

In our working group, Imke Burmester screened several compounds on their effect to reduce epidermal split formation first in different cell culture set-ups and then in the HSOC (the paper is currently being reviewed). Five substances were identified to reduce the epidermal split formation significantly: BIRB 796, GW441756, Selumetinib, A66 and Vandetanib. The target structures of these compounds were on the list with selected skin proteins involved in pemphigus pathogenesis (see chapter ***8.5 SKIN PROTEINS INVOLVED IN PEMPHIGUS PATHOGENESIS***) and some were also identified in the proteome analyses:
The tyrosine receptor kinase A (inhibited by GW441756) and phosphatidylinositol 3-kinase (inhibited by A66) were not identified in all six experiments and they did not show a significant behaviour over the course of time in comparison to the NC.
MEK (MAPK/ERK kinase) 1 / 2 which can be inhibited with Selumetinib were identified in the preTAILS analysis of the second 11 h experiment and showed an upregulation between 5 and 7 h. However, this effect could not be confirmed in the other experiments.
EGFR kinase was elevated between 5 and 12 h throughout all preTAILS analyses. The EGFR can be inhibited by Vandetanib which was tested in the HSOC. EGFR activation causes tyrosine phosphorylation of PG which then leads a decreasing connection of DP to the desmosome. This reduces the adhesive strength of the desmosomes (Yin, Getsios *et al.* 2005). Conveniently, PG is downregulated around the time of the split formation in most preTAILS analyses which supports the theory.

6.8 OUTLOOK

Currently, our working group is testing several substances in the HSOC which have proven to impact the split formation in cell culture models and also in the HSOC model on their ability to reduce blistering when applicated locally.
In the future, we will work to establish a new mouse model using the anti-Dsg 1 / Dsg 3 scFv to investigate the pathogenesis and possible treatment options for PV further.

In the next step of the proteome analysis, a bioinformatic expert needs to evaluate the concluded data from my proteome analysis because of its quantity and specific requirements. Unfortunately, the complete analysis of such data is beyond my personal knowledge and not within my area of expertise. The annotated peptides and their position in the master protein will be evaluated to identify the corresponding proteases. Moreover, the upregulated proteins that were identified in the cluster analyses from all quantifiable protein hits of the preTAILS analysis will be subject of further research as they might play a significant role in PV pathogenesis.
The proteome analysis will also provide new targets for substances that might reduce the split formation which will then be tested in the HSOC.
Additionally, a separate analysis of samples from the HSOC using phosphoproteomics should be considered to investigate the behaviour of the proteins associated with signalling pathways in more detail.

Lastly, it would also be very interesting to look into comparing the proteome of samples from the HSOC with samples from PV patients directly to investigate the ability of the scFv to mimic the disease on this level.

7 LITERATURE

Ahmad, Z. A., S. K. Yeap, A. M. Ali, W. Y. Ho, N. B. Alitheen and M. Hamid (2012). "scFv antibody: principles and clinical application." Clin Dev Immunol **2012**: 980250.

Alpsoy, E., A. Akman-Karakas and S. Uzun (2015). "Geographic variations in epidemiology of two autoimmune bullous diseases: pemphigus and bullous pemphigoid." Arch Dermatol Res **307**(4): 291-298.

Amagai, M. (1999). "Autoimmunity against desmosomal cadherins in pemphigus." J Dermatol Sci **20**(2): 92-102.

Amagai, M., P. J. Koch, T. Nishikawa and J. R. Stanley (1996). "Pemphigus vulgaris antigen (desmoglein 3) is localized in the lower epidermis, the site of blister formation in patients." J Invest Dermatol **106**(2): 351-355.

Amagai, M., N. Matsuyoshi, Z. H. Wang, C. Andl and J. R. Stanley (2000). "Toxin in bullous impetigo and staphylococcal scalded-skin syndrome targets desmoglein 1." Nat Med **6**(11): 1275-1277.

Amagai, M., T. Nishikawa, H. C. Nousari, G. J. Anhalt and T. Hashimoto (1998). "Antibodies against desmoglein 3 (pemphigus vulgaris antigen) are present in sera from patients with paraneoplastic pemphigus and cause acantholysis in vivo in neonatal mice." J Clin Invest **102**(4): 775-782.

Amagai, M., K. Tsunoda, H. Suzuki, K. Nishifuji, S. Koyasu and T. Nishikawa (2000). "Use of autoantigen-knockout mice in developing an active autoimmune disease model for pemphigus." J Clin Invest **105**(5): 625-631.

Amagai, M., K. Tsunoda, D. Zillikens, T. Nagai and T. Nishikawa (1999). "The clinical phenotype of pemphigus is defined by the anti-desmoglein autoantibody profile." J Am Acad Dermatol **40**(2 Pt 1): 167-170.

Anhalt, G. J., R. S. Labib, J. J. Voorhees, T. F. Beals and L. A. Diaz (1982). "Induction of pemphigus in neonatal mice by passive transfer of IgG from patients with the disease." N Engl J Med **306**(20): 1189-1196.

Aoyama, Y., M. K. Owada and Y. Kitajima (1999). "A pathogenic autoantibody, pemphigus vulgaris-IgG, induces phosphorylation of desmoglein 3, and its dissociation from plakoglobin in cultured keratinocytes." Eur J Immunol **29**(7): 2233-2240.

Barbas, C. F., D. R. Burton, J. K. Scott and G. J. Silverman (2001). "Phage display: a laboratory manual." Cold Spring Harbor Laboratory Press. Cold Spring Harbor, New York.

Bektas, M., P. S. Jolly, P. Berkowitz, M. Amagai and D. S. Rubenstein (2013). "A pathophysiologic role for epidermal growth factor receptor in pemphigus acantholysis." J Biol Chem **288**(13): 9447-9456.

Berkowitz, P., L. A. Diaz, R. P. Hall and D. S. Rubenstein (2008). "Induction of p38MAPK and HSP27 phosphorylation in pemphigus patient skin." J Invest Dermatol **128**(3): 738-740.

Bertram, F., E. B. Brocker, D. Zillikens and E. Schmidt (2009). "Prospective analysis of the incidence of autoimmune bullous disorders in Lower Franconia, Germany." J Dtsch Dermatol Ges **7**(5): 434-440.

Bliss, E., W. E. Heywood, M. Benatti, N. J. Sebire and K. Mills (2016). "An optimised method for the proteomic profiling of full thickness human skin." Biol Proced Online **18**: 15.

Blonder, J., A. Terunuma, T. P. Conrads, K. C. Chan, C. Yee, D. A. Lucas, C. F. Schaefer, L. R. Yu, H. J. Issaq, T. D. Veenstra and J. C. Vogel (2004). "A proteomic characterization of the plasma membrane of human epidermis by high-throughput mass spectrometry." J Invest Dermatol **123**(4): 691-699.

Boggon, T. J., J. Murray, S. Chappuis-Flament, E. Wong, B. M. Gumbiner and L. Shapiro (2002). "C-cadherin ectodomain structure and implications for cell adhesion mechanisms." Science **296**(5571): 1308-1313.

Borgono, C. A., I. P. Michael, N. Komatsu, A. Jayakumar, R. Kapadia, G. L. Clayman, G. Sotiropoulou and E. P. Diamandis (2007). "A potential role for multiple tissue kallikrein serine proteases in epidermal desquamation." J Biol Chem **282**(6): 3640-3652.

Burmester, I. A. K., S. Emtenani, J. G. Johns, R. J. Ludwig, C. M. Hammers and J. E. Hundt (2019). "Translational use of a standardized full human skin organ culture model in autoimmune blistering diseases." Curr Protoc Pharmacol **85**(1): e56.

Chen, J., Q. Zheng, C. M. Hammers, C. T. Ellebrecht, E. M. Mukherjee, H. Y. Tang, C. Lin, H. Yuan, M. Pan, J. Langenhan, L. Komorowski, D. L. Siegel, A. S. Payne and J. R. Stanley (2017). "Proteomic analysis of pemphigus autoantibodies Indicates a larger, more diverse, and more dynamic repertoire than determined by b cell genetics." Cell Rep **18**(1): 237-247.

Cipolla, G. A., J. K. Park, R. M. Lavker and M. L. Petzl-Erler (2017). "Crosstalk between signaling pathways in pemphigus: a role for endoplasmic reticulum stress in p38 mitogen-activated protein kinase activation?" Front Immunol **8**: 1022.

Di Zenzo, G., G. Di Lullo, D. Corti, V. Calabresi, A. Sinistro, F. Vanzetta, B. Didona, G. Cianchini, M. Hertl, R. Eming, M. Amagai, B. Ohyama, T. Hashimoto, J. Sloostra, F. Sallusto, G. Zambruno and A. Lanzavecchia (2012). "Pemphigus autoantibodies generated through somatic mutations target the desmoglein-3 cis-interface." J Clin Invest **122**(10): 3781-3790.

Didona, D., R. Maglie, R. Eming and M. Hertl (2019). "Pemphigus: current and future therapeutic strategies." Front Immunol **10**: 1418.

Doucet, A., O. Kleifeld, J. N. Kizhakkedathu and C. M. Overall (2011). "Identification of proteolytic products and natural protein n-termini by terminal amine isotopic labeling of substrates (TAILS)." Methods Mol Biol **753**: 273-287.

Eming, R., T. Hennerici, J. Backlund, C. Feliciani, K. C. Visconti, S. Willenborg, J. Wohde, R. Holmdahl, G. Sonderstrup and M. Hertl (2014). "Pathogenic IgG antibodies against desmoglein 3 in pemphigus vulgaris are regulated by HLA-DRB1*04:02-restricted T cells." J Immunol **193**(9): 4391-4399.

Evangelista F., D. A. Culton, L.A. Diaz (2015). "Desmosomal proteins as autoantigens in pemphigus." In: Murrell D. (eds) Blistering Diseases. Springer, Berlin, Heidelberg: 55-56.

Fenner, J. and R. A. F. Clark (2016). "Anatomy, physiology, histology, and immunohistochemistry of human skin." In: Skin Tissue Engineering and Regenerative Medicine, Amsterdam, Elsevier: 1-17.

Garrod, D. and M. Chidgey (2008). "Desmosome structure, composition and function." Biochim Biophys Acta **1778**(3): 572-587.

Hammers, C. M., J. Chen, C. Lin, S. Kacir, D. L. Siegel, A. S. Payne and J. R. Stanley (2015). "Persistence of anti-desmoglein 3 IgG(+) b-cell clones in pemphigus patients over years." J Invest Dermatol **135**(3): 742-749.

Hammers, C. M. and J. R. Stanley (2014). "Antibody phage display: technique and applications." J Invest Dermatol **134**(2): 1-5.

Hammers, C. M. and J. R. Stanley (2016). "Mechanisms of disease: pemphigus and bullous pemphigoid." Annu Rev Pathol **11**: 175-197.

Hammers, C. M., H. Y. Tang, J. Chen, S. Emtenani, Q. Zheng and J. R. Stanley (2018). "Research techniques made simple: mass spectrometry for analysis of proteins in dermatological research." J Invest Dermatol **138**(6): 1236-1242.

Harrison, O. J., J. Brasch, G. Lasso, P. S. Katsamba, G. Ahlsen, B. Honig and L. Shapiro (2016). "Structural basis of adhesive binding by desmocollins and desmogleins." Proc Natl Acad Sci U S A **113**(26): 7160-7165.

Hertl, M., H. Jedlickova, S. Karpati, B. Marinovic, S. Uzun, S. Yayli, D. Mimouni, L. Borradori, C. Feliciani, D. Ioannides, P. Joly, C. Kowalewski, G. Zambruno, D. Zillikens and M. F. Jonkman (2015). "Pemphigus. S2 guideline for diagnosis and treatment--guided by the european dermatology forum (EDF) in cooperation with the european academy of dermatology and venereology (EADV)." J Eur Acad Dermatol Venereol **29**(3): 405-414.

Heupel, W. M., D. Zillikens, D. Drenckhahn and J. Waschke (2008). "Pemphigus vulgaris IgG directly inhibit desmoglein 3-mediated transinteraction." J Immunol **181**(3): 1825-1834.

Hiroyasu, S., C. T. Turner, K. C. Richardson and D. J. Granville (2019). "Proteases in pemphigoid diseases." Front Immunol **10**: 1454.

Ishii, K. and M. Amagai (2012). "In vitro pathogenicity assay for anti-desmoglein autoantibodies in pemphigus." In: Molecular Dermatology. Humana Press, New York**:** 219-225.

Ishii, K. and K. J. Green (2001). "Cadherin function: breaking the barrier." Curr Biol **11**(14): R569-572.

Ishii, K., C. Lin, D. L. Siegel and J. R. Stanley (2008). "Isolation of pathogenic monoclonal anti-desmoglein 1 human antibodies by phage display of pemphigus foliaceus autoantibodies." J Invest Dermatol **128**(4): 939-948.

Jennings, J. M., D. K. Tucker, M. D. Kottke, M. Saito, E. Delva, Y. Hanakawa, M. Amagai and A. P. Kowalczyk (2011). "Desmosome disassembly in response to pemphigus vulgaris IgG occurs in distinct phases and can be reversed by expression of exogenous Dsg3." J Invest Dermatol **131**(3): 706-718.

Kamiya, K., Y. Aoyama, Y. Shirafuji, T. Hamada, S. Morizane, K. Fujii and K. Iwatsuki (2013). "A higher correlation of the antibody activities against the calcium-dependent epitopes of desmoglein 3 quantified by ethylenediaminetetraacetic acid-treated enzyme-linked immunosorbent assay with clinical disease activities of pemphigus vulgaris." J Dermatol Sci **70**(3): 190-195.

Kasperkiewicz, M., C. T. Ellebrecht, H. Takahashi, J. Yamagami, D. Zillikens, A. S. Payne and M. Amagai (2017). "Pemphigus." Nat Rev Dis Primers **3**: 17026.

Kleifeld, O., A. Doucet, U. auf dem Keller, A. Prudova, O. Schilling, R. K. Kainthan, A. E. Starr, L. J. Foster, J. N. Kizhakkedathu and C. M. Overall (2010). "Isotopic labeling of terminal amines in complex samples identifies protein N-termini and protease cleavage products." Nat Biotechnol **28**(3): 281-288.

Madzharova E., F. Sabino, U. auf dem Keller (2019). "Exploring extracellular matrix degradomes by TMT-TAILS N-terminomics." In: Sagi I., Afratis N. (eds) Collagen. Methods in Molecular Biology. vol 1944. Humana Press, New York: 115-126.

Mahmoud, A., I. D. Miziara, K. C. Costa, C. G. Santi, C. W. Maruta and V. Aoki (2012). "Laryngeal involvement in pemphigus vulgaris: a proposed classification." J Laryngol Otol **126**(10): 1041-1044.

Mahoney, M. G., Z. Wang, K. Rothenberger, P. J. Koch, M. Amagai and J. R. Stanley (1999). "Explanations for the clinical and microscopic localization of lesions in pemphigus foliaceus and vulgaris." J Clin Invest **103**(4): 461-468.

Mao, X., E. J. Choi and A. S. Payne (2009). "Disruption of desmosome assembly by monovalent human pemphigus vulgaris monoclonal antibodies." J Invest Dermatol **129**(4): 908-918.

Metsalu, T. and J. Vilo (2015). "ClustVis: a web tool for visualizing clustering of multivariate data using principal component analysis and heatmap." Nucleic Acids Res **43**(W1): W566-570.

Michailidou, E. Z., M. A. Belazi, A. K. Markopoulos, M. I. Tsatsos, O. N. Mourellou and D. Z. Antoniades (2007). "Epidemiologic survey of pemphigus vulgaris with oral manifestations in northern Greece: retrospective study of 129 patients." Int J Dermatol **46**(4): 356-361.

Mikesh, L. M., L. R. Aramadhaka, C. Moskaluk, P. Zigrino, C. Mauch and J. W. Fox (2013). "Proteomic anatomy of human skin." J Proteomics **84**: 190-200.

Nose, A., K. Tsuji and M. Takeichi (1990). "Localization of specificity determining sites in cadherin cell adhesion molecules." Cell **61**(1): 147-155.

Oktarina, D. A., G. van der Wier, G. F. Diercks, M. F. Jonkman and H. H. Pas (2011). "IgG-induced clustering of desmogleins 1 and 3 in skin of patients with pemphigus fits with the desmoglein nonassembly depletion hypothesis." Br J Dermatol **165**(3): 552-562.

OpenStax, C. (2013). "Layers of the skin." In: Anatomy and physiology, Rice University, Houston. Last access: 13.05.2020.

Pan, M., X. Liu and J. Zheng (2011). "The pathogenic role of autoantibodies in pemphigus vulgaris." Clin Exp Dermatol **36**(7): 703-707.

Parkinson, E., P. Skipp, M. Aleksic, A. Garrow, T. Dadd, M. Hughes, G. Clough and C. D. O'Connor (2014). "Proteomic analysis of the human skin proteome after in vivo treatment with sodium dodecyl sulphate." PLoS One **9**(5): e97772.

Payne, A. S., K. Ishii, S. Kacir, C. Lin, H. Li, Y. Hanakawa, K. Tsunoda, M. Amagai, J. R. Stanley and D. L. Siegel (2005). "Genetic and functional characterization of human pemphigus vulgaris monoclonal autoantibodies isolated by phage display." J Clin Invest **115**(4): 888-899.

Pretel, M., A. Espana, M. Marquina, B. Pelacho, J. M. Lopez-Picazo and M. J. Lopez-Zabalza (2009). "An imbalance in Akt/mTOR is involved in the apoptotic and acantholytic processes in a mouse model of pemphigus vulgaris." Exp Dermatol **18**(9): 771-780.

Rosatelli, T. B., A. M. Roselino, R. Dellalibera-Joviliano, M. L. Reis and E. A. Donadi (2005). "Increased activity of plasma and tissue kallikreins, plasma kininase II and salivary kallikrein in pemphigus foliaceus (fogo selvagem)." Br J Dermatol **152**(4): 650-657.

Ruocco, V., E. Ruocco, A. Lo Schiavo, G. Brunetti, L. P. Guerrera and R. Wolf (2013). "Pemphigus: etiology, pathogenesis, and inducing or triggering factors: facts and controversies." Clin Dermatol **31**(4): 374-381.

Saito, M., S. N. Stahley, C. Y. Caughman, X. Mao, D. K. Tucker, A. S. Payne, M. Amagai and A. P. Kowalczyk (2012). "Signaling dependent and independent mechanisms in pemphigus vulgaris blister formation." PLoS One **7**(12): e50696.

Sajda, T. and A. A. Sinha (2018). "Autoantibody signaling in pemphigus vulgaris: development of an integrated Model." Front Immunol **9**: 692.

Sarkany, I., K. Grice and G. A. Caron (1965). "Organ culture of adult human skin." Br J Dermatol **77**: 65-76.

Schlage P., F. E. Egli, U. auf dem Keller (2017). "Time-resolved analysis of matrix metalloproteinase substrates in complex samples." In: Galea C. (eds) Matrix Metalloproteases. Methods in Molecular Biology. vol 1579. Humana Press, New York: 185-198.

Schmidt, E., M. Kasperkiewicz and P. Joly (2019). "Pemphigus." Lancet **394**(10201): 882-894.

Schulze, K., A. Galichet, B. S. Sayar, A. Scothern, D. Howald, H. Zymann, M. Siffert, D. Zenhausern, R. Bolli, P. J. Koch, D. Garrod, M. M. Suter and E. J. Muller (2012). "An adult passive transfer mouse model to study desmoglein 3 signaling in pemphigus vulgaris." J Invest Dermatol **132**(2): 346-355.

Shah, A. A., K. Seiffert-Sinha, D. Sirois, V. P. Werth, B. Rengarajan, W. Zrnchik, K. Attwood and A. A. Sinha (2015). "Development of a disease registry for autoimmune bullous diseases: initial analysis of the pemphigus vulgaris subset." Acta Derm Venereol **95**(1): 86-90.

Sharma, P., X. Mao and A. S. Payne (2007). "Beyond steric hindrance: the role of adhesion signaling pathways in the pathogenesis of pemphigus." J Dermatol Sci **48**(1): 1-14.

Sinha, A. A. (2011). "The genetics of pemphigus." Dermatol Clin **29**(3): 381-391.

Spindler, V., F. Vielmuth, E. Schmidt, D. S. Rubenstein and J. Waschke (2010). "Protective endogenous cyclic adenosine 5'-monophosphate signaling triggered by pemphigus autoantibodies." J Immunol **185**(11): 6831-6838.

Sterry, W. and V. A. Czaika (2018). "Anatomische, physiologische und immunologische Grundlagen der Haut." In: Kurzlehrbuch Dermatologie, Thieme, Stuttgart, New York: 3-6.

Takae, Y., T. Nishikawa and M. Amagai (2009). "Pemphigus mouse model as a tool to evaluate various immunosuppressive therapies." Exp Dermatol **18**(3): 252-260.

Takahashi, H., M. Amagai, T. Nishikawa, Y. Fujii, Y. Kawakami and M. Kuwana (2008). "Novel system evaluating in vivo pathogenicity of desmoglein 3-reactive t cell clones using murine pemphigus vulgaris." J Immunol **181**(2): 1526-1535.

Tsunoda, K., T. Ota, M. Aoki, T. Yamada, T. Nagai, T. Nakagawa, S. Koyasu, T. Nishikawa and M. Amagai (2003). "Induction of pemphigus phenotype by a mouse monoclonal antibody against the amino-terminal adhesive interface of desmoglein 3." J Immunol **170**(4): 2170-2178.

Van der Wier, G., H. H. Pas, D. Kramer, G. F. H. Diercks and M. F. Jonkman (2014). "Smaller desmosomes are seen in the skin of pemphigus patients with anti-desmoglein 1 antibodies but not in patients with anti-desmoglein 3 antibodies." J Invest Dermatol **134**(8): 2287-2290.

Williamson, L., N. A. Raess, R. Caldelari, A. Zakher, A. de Bruin, H. Posthaus, R. Bolli, T. Hunziker, M. M. Suter and E. J. Muller (2006). "Pemphigus vulgaris identifies plakoglobin as key suppressor of c-myc in the skin." EMBO J **25**(14): 3298-3309.

Yin, T., S. Getsios, R. Caldelari, L. M. Godsel, A. P. Kowalczyk, E. J. Muller and K. J. Green (2005). "Mechanisms of plakoglobin-dependent adhesion: desmosome-specific functions in assembly and regulation by epidermal growth factor receptor." J Biol Chem **280**(48): 40355-40363.

Zhou, L., X. Zhang, R. Paus and Z. Lu (2018). "The renaissance of human skin organ culture: A critical reappraisal." Differentiation **104**: 22-35.

8 APPENDICES

8.1 ETHICS APPROVAL

UNIVERSITÄT ZU LÜBECK

Universität zu Lübeck · Ratzeburger Allee 160 · 23538 Lübeck

Herrn
PD Dr. med. Tobias Fischer
Klinik für Dermatologie und Venerologie

im Hause

Ethik-Kommission
Vorsitzender:
Herr Prof. Dr. med. Dr. phil. H. Raspe
Stellv. Vorsitzender:
Herr Prof. Dr. med. F. Gieseler
Universität zu Lübeck
Ratzeburger Allee 160
23538 Lübeck

Sachbearbeitung: Frau Janine Erdmann
Tel.: +49 451 500 4639
Fax: +49 451 500 3026
janine.erdmann@medizin.uni-luebeck.de

Aktenzeichen: 06-109
Datum: 15. März 2012

In-vitro-Untersuchung der Biologie des humanen Haarfollikels in bezug auf Wachstumseigenschaften, Apoptose, Wachstumsregulation, Pigmentierung und Immunprivileg im Haarorgankulturmodell
Hier: Amendment 2 –Ihr Schreiben vom 13. März 2012

Sehr geehrter Herr Dr. Fischer,

das Amendment bezüglich der Nutzung von Haut aus anderen behaarten Arealen mit den folgenden Unterlagen habe ich zustimmend zur Kenntnis genommen:

- Aufklärung und Einwilligung sowie
- Studienprotokoll.

Es bedarf keiner weiteren Begutachtung durch die Kommission.

Bitte beachten Sie folgenden Hinweis: Die Haarproben können nur vernichtet werden, wenn diese in pseudonymisierter Form vorliegen.

Die ärztliche und juristische Verantwortung des Leiters der klinischen Prüfung und der an der Prüfung teilnehmenden Ärzte bleibt entsprechend der Beratungsfunktion der Ethikkommission durch unsere Stellungnahme unberührt.

Mit freundlichem Gruß und besten Wünschen
für den weiteren Verlauf Ihrer Forschung bin ich
Ihr

Prof. Dr. med. Dr. phil. H. Raspe
Vorsitzender

8.2 LC-MS PARAMETERS FOR TAILS ANALYSIS

Liquid chromatography:

- Easy-nLC1000
- Solvent A (Water with 0.1 % Formic acid)
- Solvent B (80 % Acetonitrile, 0.1 % Formic acid)
- Trap column (2 cm x 75 µm, Acclaim®PepMap100 column, packed with 3 µm, C18 beads)
- Analytical column (50 cm x 75 µm, PepMap™RSLC column, packed with 2 µm C18 beads)
- Flow rate 250 nL / min
- Gradient: from 6 % to 60 % solvent B in 125 min (from 6 % to 23 % in 85 min; from 23 % to 38 % in 30 min; from 38 % to 60 % in 10 min; followed by wash steps from 60 % to 95 % in 5 min and removing the rest of the dirt at 95 % solvent B for 10 min)

Mass spectrometry:

- DDA mode for 140 min
- MS1 resolution at 70.000
- AGC target set to 3e6
- Maximum injection time (IT) set to 20 ms
- Scan range 300 to 1750 m / z (mass-to-charge ratio)
- Selecting top 10 for MS2 analysis
- MS2 resolution set to 17.500
- AGC target 1e6
- Maximum IT 60 ms
- Isolation window of 1.6 m / z
- Normalised collision energy at 28

8.3 COMPOSITION OF MOLECULAR FUNCTIONS

The classification according to molecular functions of the proteins identified in the preTAILS samples for each of the six time course experiments:

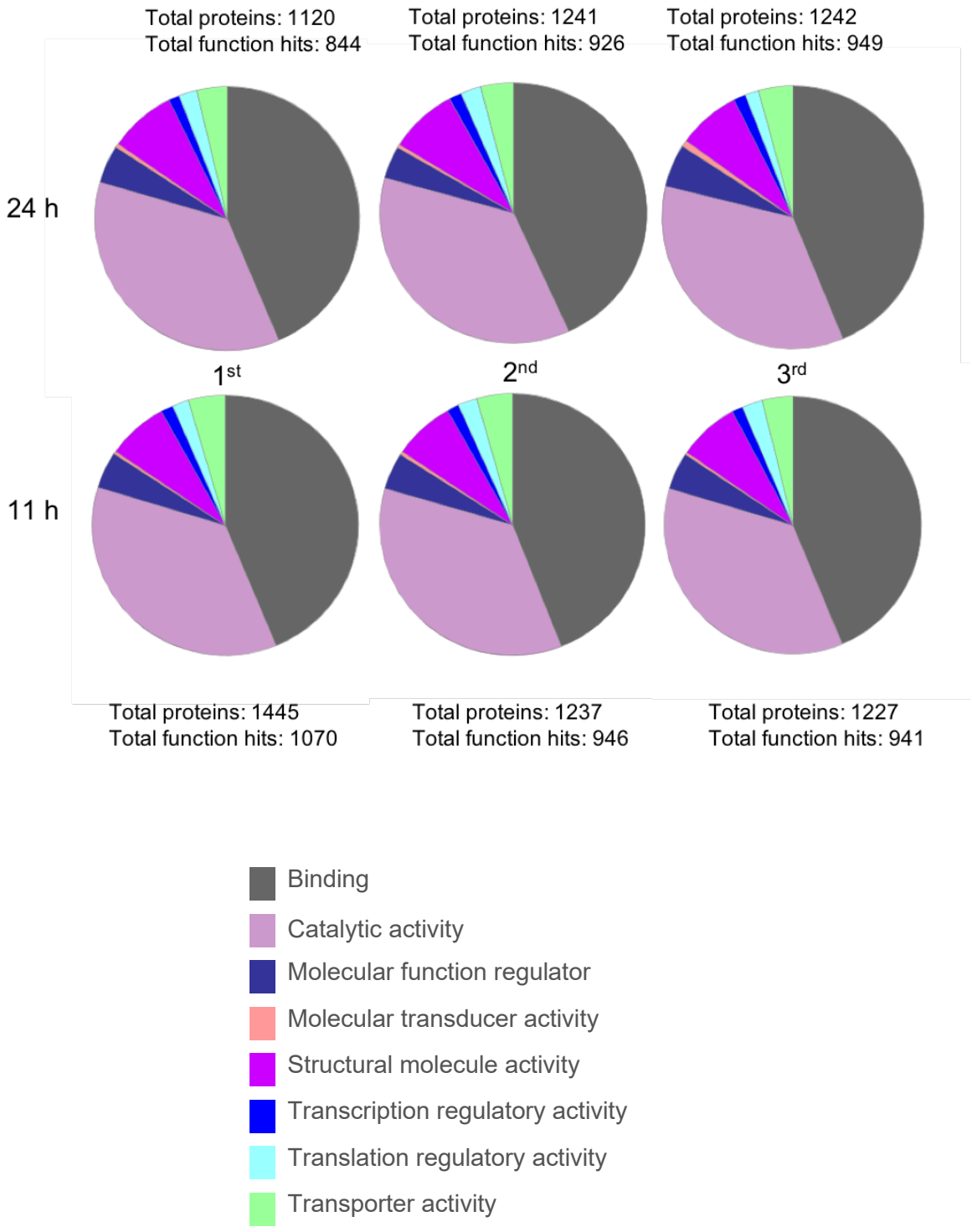

8.4 FURTHER PROTEIN CLUSTER ANALYSIS RESULTS

1st 24 h experiment:

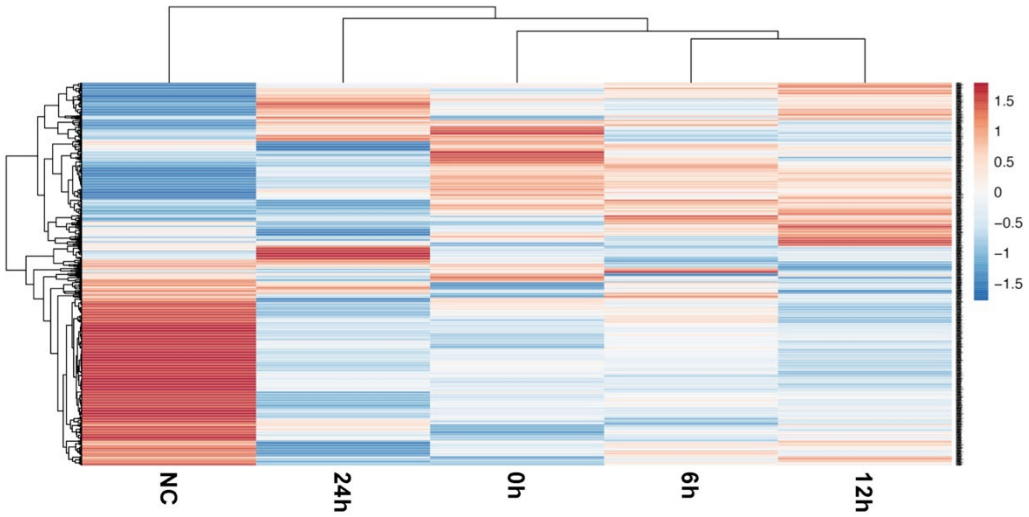

2nd 24 h experiment:

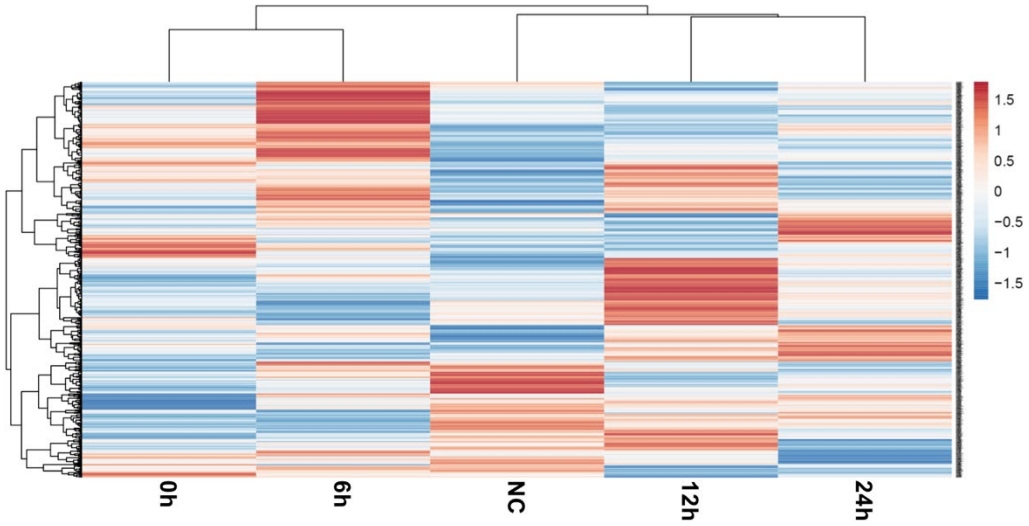

3rd 24 h experiment:

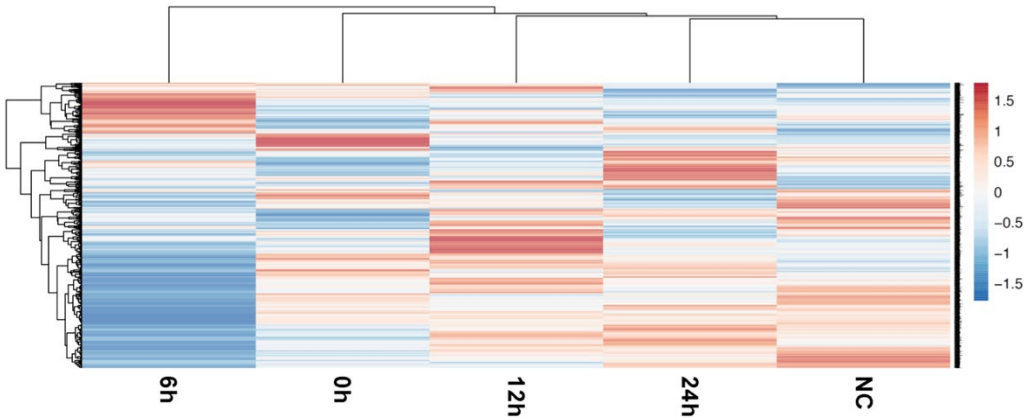

1st 11 h experiment:

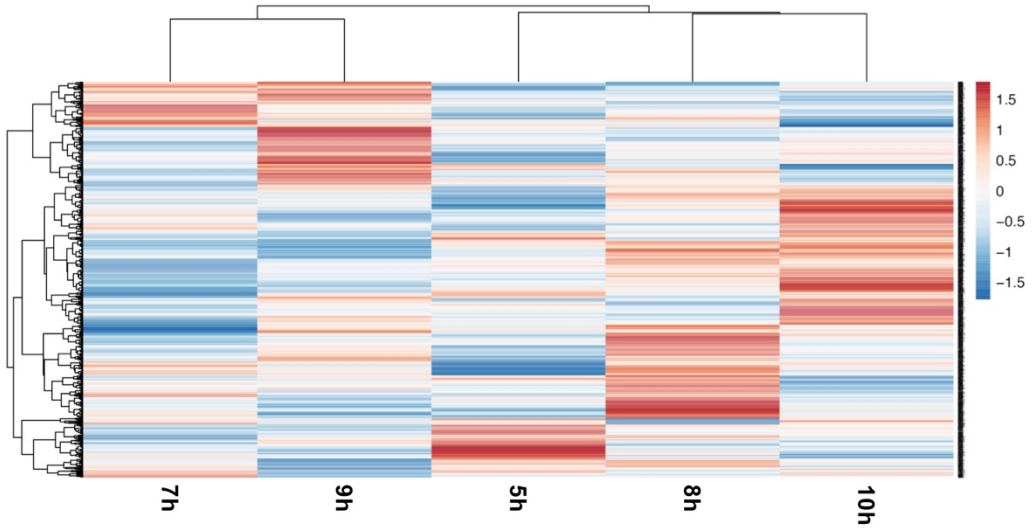

3rd 11 h experiment:

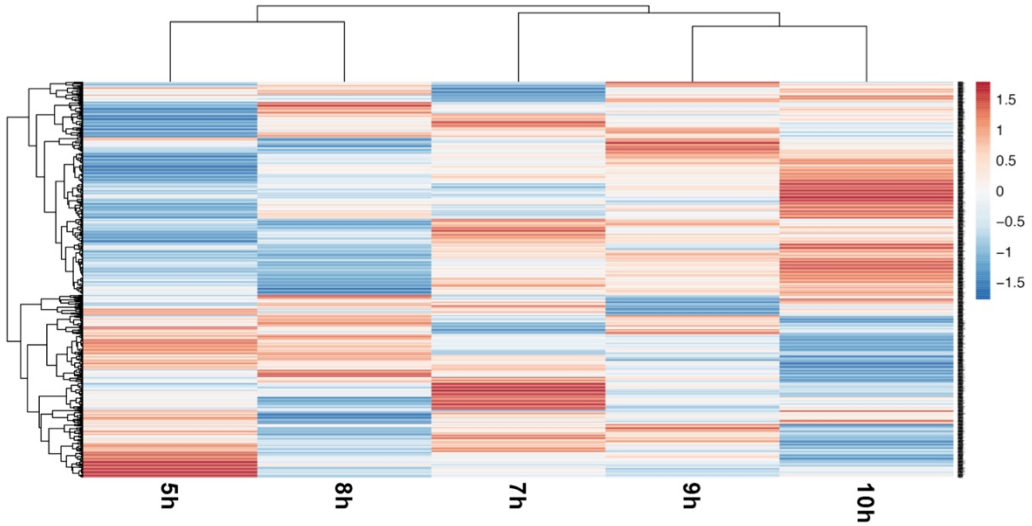

8.5 SKIN PROTEINS INVOLVED IN PEMPHIGUS PATHOGENESIS

- 14-3-3 proteins
- C-Jun N-terminal kinase
- C-myc
- cAMP
- Caspase
- Catalase
- Catenin
- Cluster of differentiation type 1a and 207
- Collagen type XVII Alpha 1
- Corneodesmosin
- Cytosolic phospholipases A2
- DP
- Dsc
- Dsg
- EGFRK
- Envoplakin
- Extracellular signal-regulated kinases 1/2
- Filaggrin
- HSP
- Janus kinases
- Kallikrein
- Keratin
- Kip-related proteins
- Loricrin
- MAPK
- MEK 1/2
- mTOR
- p38 MAPK
- PDK 1
- Peroxiredoxin
- PG
- Phosphatidylinositol 3-kinases
- PKC
- PLC
- Raf proteins
- Ras proteins
- Rho GTPases
- Secreted Ly-6/uPAR-related proteins
- Superoxide dismutase
- Thioredoxin
- Tumor protein 73
- Tyrosine receptor kinase Src
- Tyrosine receptor kinase A

8.6 SKIN PROTEINS IDENTIFIED

For all following tables (chapter 8.6, 8.7 and 8.8.):
Titles *0h, 6h, 12h, 24h, NC* and *5h, 7h, 8h, 9h, 10h* show the abundance measured at the defined points of time.

1st 24 h experiment:

Accession	0h	6h	12h	24h	NC
P61604	1	0.93215613	0.85873606	0.87081784	0.93773234
P31946	0.9658444	0.943074	0.90227704	0.88140417	1
P62258-1	1	0.96299722	0.93246994	0.9213691	0.8880666
Q04917	0.87540984	0.84016393	1	0.79508197	0.59672131
P61981	0.83187391	0.86952715	1	0.94308231	0.941331
P31947-1	0.69820555	0.7862969	0.78058728	0.74877651	1
P27348	0.97899543	0.96073059	0.92785388	1	0.8913242
P63104-1	0.7907585	0.97297297	0.84045336	0.93984307	1
P10809	0.75757576	0.71632997	0.74158249	0.80639731	1
O95433	0.76377953	0.96771654	1	0.81496063	0.68661417
P17612	0.93143976	0.89520078	0.85210578	0.85504407	1
P10644	1	0.8870674	0.77322404	0.75865209	0.76593807
P13861	0.85602775	0.89679098	0.88291414	0.82567216	1
P31944	0.53135536	0.63519892	0.55225893	0.51719488	1
P04040	0.9289012	0.89196676	0.8199446	0.86241921	1
P35221	0.94576594	0.99524263	0.92483349	0.77259753	1
P35221	0.94576594	0.99524263	0.92483349	0.77259753	1
O60716-1	0.85152057	0.87477639	0.86046512	0.88908766	1
O60716-1	0.85152057	0.87477639	0.86046512	0.88908766	1
Q6YHK3-1	0.95131579	1	0.86315789	0.64013158	0.87565789
P16070	0.5520111	0.64632455	0.61373093	0.5887656	1
O43866	0.98692308	1	0.94	0.77153846	0.60538462
Q8N5K1	0.65454545	0.79242424	0.71287879	0.55757576	1
Q9UMD9-1	0.72258065	0.74596774	0.93709677	1	0.78225806
Q08554-1	0.86565836	0.88879004	0.89234875	0.73309609	1
Q14574-1	0.6320969	0.76457229	0.7002271	0.54882665	1
Q02413	0.72208835	0.89236948	0.83614458	0.5935743	1
Q14126	0.68610224	0.69488818	0.70447284	0.6341853	1
P15924-1	0.57751397	0.64455307	0.61103352	0.56703911	1
Q12805	0.7489301	0.73252496	1	0.76890157	0.36947218
Q92817	0.75198098	0.78526149	0.71156894	0.6251981	1
P08294	0.91491154	0.82224094	1	0.78264532	0.67986521
P34932	0.75862069	0.86287089	0.61828388	0.66880513	1
P04792	0.67797948	0.76243094	0.84846093	0.89739542	1
P07900	0.75059571	0.77124702	0.7807784	0.70691025	1
P08238	0.81122864	0.71928397	0.71440195	0.60374288	1
P54652	0.68609169	0.81041181	0.73193473	0.73892774	1
Q16543	0.97795414	0.91269841	0.94620811	0.90035273	1
Q14155-1	0.77447142	0.75097886	0.65465936	0.78543461	1
P15924-2	0.6484318	0.78118162	0.79868709	0.50255288	1
P14923	0.81607143	0.94285714	0.90982143	0.70714286	1
Q9Y337	0.60435435	0.56081081	0.53678679	0.68543544	1
P49862	0.36054743	0.44690892	0.261916	0.32043417	1
P13645	0.58031838	0.69971056	0.61287988	0.61794501	1
P02533	0.66808511	0.84680851	0.81531915	0.85617021	1
P19012	0.64073777	0.81154771	0.69927827	0.71050521	1

P08779	0.62002946	0.66789396	0.64653903	0.9712813	1
Q04695	0.15881287	0.1746715	0.1690077	1	0.43112823
P05783	0.79699248	0.68045113	0.68796992	0.74962406	1
P08727	1	0.52057613	0.44958848	0.375	0.30864198
Q9C075	0.75411061	0.59043348	0.46860987	0.63153961	1
Q7Z3Y9	0.97121084	0.71803556	1	0.65707028	0.72904318
Q7Z3Y7	0.77806452	0.71419355	0.74580645	0.6316129	1
P35527	0.57441419	0.59151362	1	0.75300823	0.65547815
Q9NSB4	0.49391304	0.60347826	0.51246377	1	0.75188406
Q9NSB2	1	0.84414832	0.79432213	0.92699884	0.69351101
P04264	0.68382944	0.8004827	0.72083669	0.7232502	1
Q7Z794	0.78969957	0.84549356	0.68497854	0.68154506	1
P35908	0.47720365	0.60547112	0.45896657	0.37568389	1
P13647	0.60910518	0.76373626	0.72370487	0.81475667	1
P02538	0.19602494	0.22837101	0.22408418	0.39711613	1
P04259	0.2991988	0.20630946	0.25237857	1	0.16574862
P08729	1	0.36688051	0.29671211	0.24418605	0.19246191
Q3SY84	0.84811238	0.8595259	1	0.77172959	0.84460053
Q86Y46	0.63545151	0.9180602	0.65050167	0.81939799	1
O95678	0.3915547	1	0.29126679	0.36132438	0.27639155
Q8N1N4	0.5581246	0.63455363	0.46885035	0.43673732	1
Q5XKE5	0.17315504	0.18432634	0.19109682	1	0.16875423
P05787	1	0.34740133	0.31457601	0.17624072	0.18053927
Q6KB66	0.45224057	0.50648585	0.41391509	0.55601415	1
P28482	0.98	1	0.99263158	0.97578947	0.96736842
O15264	1	0.17175573	0.21246819	0.68999152	0.12637829
Q6ZN16-1	0.88065448	0.86333013	0.99230029	1	0.73243503
P08571	0.88343558	0.71165644	1	0.60276074	0.35889571
Q9NUJ1	0.58473896	0.69558233	1	0.89718876	0.90040161
Q06830	0.96875	1	0.9157197	0.96969697	0.80871212
P32119	1	0.88808007	0.95086442	0.85532302	0.84531392
P30044-1	1	0.82713348	0.77169949	0.87746171	0.80816922
P30041	1	0.90792453	0.94867925	0.73509434	0.56981132
Q00169	0.78537736	0.68081761	0.78537736	1	0.74842767
P48739	0.90079717	0.92205492	0.75642161	0.75819309	1
Q13492-1	0.89473684	0.95644283	1	0.83938294	0.67150635
P14555	0.65125241	0.8371869	0.86223507	0.89595376	1
Q13283	0.74660272	0.81454836	0.78657074	0.67226219	1
P46940	0.7485807	0.77777778	0.80291971	0.67721006	1
Q15404-1	1	0.71964018	0.60944528	0.88155922	0.52998501
P63000-1	0.86012163	0.92615117	0.92701998	1	0.7410947
P60763	0.95670275	1	0.95253955	0.86677769	0.72439634
P61026	0.65945513	0.76602564	0.67067308	0.53205128	1
P62491-1	0.91108987	0.98470363	0.99426386	0.8126195	1
P61106	0.95660203	1	0.98984303	0.80978763	0.84579871
P62820	0.9729225	0.92343604	1	0.77030812	0.89822596
P57735	0.75621492	0.90697674	1	0.74097835	0.9478749
P61019-1	0.83277592	0.94314381	1	0.72157191	0.86538462
Q15286	1	0.86145069	0.84515077	0.68459658	0.81010595
P20339	1	0.94633274	0.92754919	0.6842576	0.82289803
P61020	1	0.89123377	0.93506494	0.72970779	0.6387987
P51148	1	0.94777397	0.91010274	0.78938356	0.72517123
P51149	0.94479638	0.94751131	1	0.84343891	0.82352941
P11233	0.79441624	0.78510998	0.77918782	0.73519459	1
P62834	1	0.75238923	0.79582971	0.84708949	0.82536924
P61224-1	0.85586392	0.76991943	0.84064458	0.76186213	1
P10114	0.83856089	0.90867159	1	0.65590406	0.46402214
P04626-1	0.93505155	0.80206186	0.86597938	0.85876289	1
P52565-1	1	0.9935305	0.9676525	0.88170055	0.77171904

P52566	0.99125874	1	0.95367133	0.83216783	0.67482517
Q13464	1	0.81109325	0.88263666	0.84083601	0.93729904
P84095	0.92273535	0.90319716	1	0.84191829	0.94493783
Q14247-1	0.65922747	0.51845494	0.727897	0.7416309	1
P00441	1	0.96293312	0.7727639	0.90572119	0.78968574
P04179	0.68814433	0.78178694	0.72938144	0.8814433	1
Q8NBS9-1	0.69699431	0.80666125	0.71811535	0.84240455	1
P30048	0.93567753	0.80617496	0.81560892	1	0.82590051
O43396	1	0.90998043	0.99021526	0.74363992	0.80626223
Q9H3N1	0.79090029	0.97386254	0.98354308	0.9428848	1
P54577	0.93625498	0.9312749	1	0.78286853	0.91733068
Q06124	0.99261993	0.77398524	0.65498155	0.89852399	1
P29350-1	1	0.91418248	0.76242096	0.61517615	0.68473351

2nd 24 h experiment:

Accession	0h	6h	12h	24h	NC
P35221	0.80072137	0.78449053	1	0.79891794	0.95130748
Q9NSA3	0.8360515	0.88669528	1	0.88412017	0.98969957
O60716-1	0.86203787	0.84039675	1	0.92155095	0.87826871
P35222	1	0.64431725	0.62796402	0.99345871	0.75967078
Q9NUJ1	0.88962892	0.95528069	1	0.83063749	0.86203616
P10644	0.91751622	0.87395737	0.93512512	0.96848934	1
P17612	0.97316637	1	0.79516995	0.90876565	0.83810376
P13861	0.97647059	1	0.85	0.82156863	0.79803922
P31944	0.79184367	0.83007647	1	0.82158029	0.73661852
P04040	0.92592593	0.87918871	1	0.89241623	0.78835979
P08571	0.7517301	0.79152249	0.60899654	0.65397924	1
Q6YHK3-1	0.86355786	1	0.99740933	0.53022453	0.62867012
Q9Y5K6	0.85860656	0.89446721	0.90778689	0.95184426	0.976
P16070	0.81922761	0.79129006	1	0.96466721	0.81018899
O43866	0.66833751	1	0.6984127	0.83542189	0.85045948
Q9UMD9-1	0.77080063	0.67268446	1	0.78728414	0.71036107
Q14574-1	0.77806122	0.73129252	0.97704082	0.73809524	1
Q02413	0.74529915	0.72991453	0.91196581	0.72478632	1
P32926	0.66404406	0.76239182	0.95987411	1	0.64988198
Q08554-2	0.86582278	0.81012658	0.88016878	0.65485232	1
P15924-1	0.61265103	0.46695096	1	0.73205402	0.76901208
P15924-2	0.54706601	0.43643032	1	0.58618582	0.66625917
Q9H6S3	0.914969	0.88131089	1	0.88485385	0.82728078
Q92817	0.74546952	0.63920923	0.98682043	0.78500824	1
P0DMV8	0.8277972	0.81031469	1	0.89423077	0.8277972
P34932	0.87296137	0.7751073	1	0.83175966	0.98712446
O95757	0.84201537	1	0.66865927	0.82322801	0.90606319
P11142-1	0.86346516	0.9472693	1	0.92184557	0.92561205
Q92598	0.89961014	0.92202729	1	0.84990253	0.90935673
P04792	0.69030155	0.75305623	1	0.79299104	0.91361043
P07900	0.9271028	1	0.95327103	0.93084112	0.86635514
P08238	0.83304647	1	0.87091222	0.99225473	0.82013769
P54652	0.75504829	0.73485514	0.976295	0.90430202	1
Q15323	0.40240412	1	0.46823125	0.50143102	0.44819691
P13645	0.84176633	0.94296228	1	0.82060718	0.92456302
P02533	0.67634253	0.68650218	0.67053701	0.60159652	1
P19012	0.82735043	0.83846154	1	0.77777778	0.78547009
P08779	0.46918768	0.79761905	0.67366947	1	0.53501401
Q04695	0.205256	1	0.24558224	0.38740372	0.3497961
P05783	0.57237237	0.62762763	0.32732733	1	0.48648649
P08727	0.80865225	0.94758735	0.52412646	1	0.82778702

Q9C075	0.90205224	1	0.91791045	0.99533582	0.9113806
Q7Z3Z0	0.99101527	0.9083558	0.62713387	1	0.9901168
Q7Z3Y7	0.8296837	0.97485807	0.9432279	1	0.91321979
P35527	0.38864055	1	0.22850381	0.50223508	0.50433868
Q14533	0.25	1	0.23544521	0.24443493	0.25385274
P78386	0.21509434	1	0.21467505	0.2327044	0.22138365
P04264	0.77345133	0.84867257	0.97522124	0.74867257	1
Q7Z794	0.70244672	0.74112076	0.8026835	0.66298343	1
P35908	1	0.99450549	0.90659341	0.82692308	0.84162063
P13647	0.85040071	0.88423865	0.92520036	0.7586821	1
P02538	0.71374622	0.76283988	1	0.99018127	0.36555891
P04259	0.18513389	1	0.20590951	0.41135734	0.36472761
P08729	0.93430657	0.96441606	0.55018248	1	0.8540146
Q3SY84	0.18576907	1	0.37452066	0.16659565	0.1887516
Q86Y46	0.64849921	1	0.81516588	0.62085308	0.664297
O95678	0.15096066	1	0.22232388	0.4231473	0.26120769
Q8N1N4	0.91280654	0.90463215	1	0.83651226	0.83742053
Q5XKE5	0.3467033	1	0.35824176	0.36593407	0.49175824
P05787	0.70592764	0.87682833	0.46882217	1	0.80754426
Q6KB66	0.73412362	0.95512278	1	0.76121931	0.82980525
P49862	0.8065915	0.87424111	1	0.81266262	0.65134432
P03952	0.90630798	0.99814471	0.58719852	0.78293135	1
P36507	0.99823944	1	0.87676056	0.88028169	0.89348592
P28482	0.98895497	0.88870008	0.92608326	0.82158029	1
P53778	1	0.98414097	0.88898678	0.95594714	0.99373321
O15264	1	0.97943925	0.7635514	0.82616822	0.69847328
P27361-1	0.92542373	0.91864407	0.82118644	0.79915254	1
Q06830	0.86762075	0.84525939	0.93291592	0.91413238	1
P32119	0.99456029	1	0.90933817	0.90843155	0.87398005
Q13162	0.88208955	1	0.70149254	0.71716418	0.79776119
P30044-1	0.8269962	0.89353612	0.93441065	0.92870722	1
P30041	1	0.96335583	0.93442623	0.94214079	0.962
P14555	0.45158053	0.4164576	0.45609634	1	0.32463623
Q8IV08	1	0.79933665	0.81177446	0.86318408	0.70509126
Q9NTJ5	0.89862205	1	0.93700787	0.93503937	0.92519685
P14923	0.91887125	0.7345679	1	0.87654321	0.91534392
Q9UNF0	0.83214286	1	0.99821429	0.78214286	0.85535714
Q9UN86	0.7444898	1	0.70693878	0.78122449	0.76
P46940	0.99904215	0.98754789	0.98659004	0.98850575	1
Q15404-1	0.81750466	1	0.79795158	0.87430168	0.95344507
P63000-1	0.90503324	0.99430199	0.95631529	1	0.86894587
P15153	0.94540943	1	0.77088503	0.78825476	0.70471464
P61026	0.8913676	0.82929195	1	0.87196896	0.95150339
Q15907	0.95939566	1	0.96600567	0.86496695	0.85741265
P61106	0.96070727	1	0.9891945	0.90373281	0.98330059
P62820	0.96903097	1	0.85214785	0.91208791	0.99200799
P57735	0.65288612	1	0.85803432	0.61466459	0.68876755
Q15286	0.84851301	1	0.92100372	0.71282528	0.91171004
Q14964	0.70822731	1	0.88804071	0.86513995	0.89143342
P20338	0.95591182	0.86873747	0.98597194	0.85270541	0.998
P20339	1	0.8905694	0.91370107	0.91459075	0.99319066
P61020	0.96676442	0.83479961	0.92473118	0.94623656	1
P20340-1	0.91607685	0.93023256	1	0.92719919	0.924
P51149	1	0.99520154	0.96449136	0.99328215	0.88717454
Q96AH8	0.98779496	0.89096827	1	0.83482506	0.84947111
P61006	1	0.95557656	0.86011342	0.78544423	0.79426311
Q92930	0.43831338	0.59239979	0.39406559	0.56480999	1
P11234	0.99287169	0.98370672	1	0.94297352	0.912
P62834	0.84809028	0.95746528	0.81597222	0.87760417	1

P61224-1	0.7654424	1	0.71786311	0.80634391	0.83222037
P10114	0.82612383	0.91772689	0.90924512	0.8235793	1
P52565-1	0.91899711	0.97299904	1	0.96624879	0.94985535
P52566	0.82991986	0.75422974	0.85307213	0.94211932	1
Q07960	0.7410947	0.81407472	1	0.68027802	0.89574283
P08134	0.984	1	0.92977778	0.85333333	0.95288889
P84095	0.96161228	0.97600768	1	0.93953935	0.99136276
P61586	0.99905033	1	0.87559354	0.94966762	0.90693257
Q14155-1	0.78706897	0.7387931	1	0.84310345	0.86637931
Q8IXI1	0.88681319	1	0.98791209	0.88681319	0.812
Q14247-1	0.87172538	0.83288166	1	0.86630533	0.86178862
P08294	0.7923588	0.85215947	0.73172757	1	0.80730897
P00441	0.77331052	0.73053892	0.93755346	0.94952951	1
P10599-1	0.8297491	0.89247312	0.90322581	1	0.98924731
Q9BRA2	0.75139888	0.76818545	0.85851319	0.88888889	1
Q8NBS9-1	0.99801784	0.96134787	0.96927651	1	0.99405352
P30048	0.97028862	0.83022071	0.72665535	1	0.6910017
O43396	0.82774674	0.90875233	1	0.86405959	0.9320298
Q9H3N1	0.75901495	1	0.97361478	0.92700088	0.78891821
Q9H1E5	0.58823529	1	0.78405573	0.69040248	0.70897833
P31946	0.93813481	0.90304709	1	0.8578024	0.87996307
P62258-1	0.93409742	0.94746896	1	0.94555874	0.91881566
Q04917	0.83050847	0.93577163	1	0.89206066	0.82158787
P61981	0.94559099	0.96716698	0.99155722	1	0.82270169
P31947-1	0.80706076	0.75123153	1	0.84318555	0.73316913
P27348	0.90051458	1	0.88593482	0.84305317	0.83619211
P63104-1	1	0.95966229	0.96529081	0.81988743	0.82798834

3rd 24 h experiment:

Accession	0h	6h	12h	24h	NC
Q9NSA3	0.79152731	0.8483835	0.90301003	0.87625418	1
Q9NUJ1	0.87967644	0.97472194	1	0.6653185	0.93528817
P17275	0.53377877	1	0.77802524	0.56792873	0.62657758
P17612	1	0.81464738	0.83725136	0.93761302	0.83725136
P10644	0.57210626	0.68500949	1	0.93548387	0.9316888
P13861	0.80650542	0.87989992	1	0.91993328	0.84737281
P31944	1	0.86771508	0.91581869	0.88436633	0.99814986
P04040	1	0.9400369	0.90867159	0.97140221	0.97140221
Q6YHK3	1	0.82721576	0.95255148	0.95792301	0.91136974
P48509	0.80325444	1	0.75147929	0.78476331	0.71523669
P16070	0.95585413	0.83397313	0.99520154	0.94241843	1
P21926	0.91595033	0.96848138	0.91977077	1	0.78987584
P48960	0.65687053	0.9833201	0.68069897	1	0.94837172
Q15517	0.91057692	0.86730769	1	0.74230769	0.85673077
P08571	0.72829132	1	0.81512605	0.66876751	0.80042017
Q9BUL8	1	0.72800646	0.91848265	0.68684423	0.88861985
Q9UMD9	0.89307625	0.77475898	1	0.99211218	0.85363716
Q08554	1	0.99321048	0.9970902	0.85160039	0.98836081
Q14574	1	0.87242026	0.9315197	0.84709193	0.97842402
P15924	0.92527675	0.83118081	0.94464945	0.88560886	1
P15924-2	0.82158399	0.85465622	1	0.78764143	0.79982594
Q9H6S3-3	0.87251356	1	0.98191682	0.80470163	0.85443038
Q92817	0.95845137	0.86591124	0.96978281	0.90745987	1
P20930	0.92542677	1	0.86612758	0.76370171	0.90386343
Q5D862	0.87234043	1	0.88159112	0.71415356	0.90656799
P0DMV9	0.9826087	0.9294686	0.98067633	0.97487923	1
P34932	0.90718039	0.83362522	0.92031524	0.85464098	1

P11142	0.942607	0.88229572	0.98832685	0.97568093	1
P04792	0.97708524	0.84234647	0.90742438	0.91659028	1
P08238	0.92518939	0.76420455	1	0.93844697	0.98106061
P54652	0.91284816	0.67115903	0.97304582	0.86612758	1
Q16543	0.93406593	0.96062271	0.93772894	1	0.86538462
P07900-2	0.96142992	0.80620884	0.95954845	0.96801505	1
P61604	0.90256864	0.81842338	0.83613818	1	0.9574845
P10809	0.85941893	0.74414246	0.94283037	0.96719775	1
P11021	0.92396535	0.9518768	0.96727623	0.92781521	1
P14625	0.8442623	0.79508197	0.94262295	0.93897996	1
P49862	0.75520833	1	0.84895833	0.71701389	0.875
P05787-2	0.64546226	0.7591179	0.65648855	1	0.956743
Q6KB66-3	0.92234848	1	0.89299242	0.8125	0.91666667
P13645	0.9441903	1	0.915828	0.90759378	0.84537969
Q99456	0.79192547	1	0.66873706	0.89648033	0.70600414
P02533	0.87249545	0.79508197	0.98087432	1	0.94626594
P19012	0.92555147	0.75459559	1	0.96783088	0.92830882
P08779	0.64206349	0.78015873	0.73174603	1	0.8047619
Q04695	0.78710645	0.70464768	0.68290855	1	0.75562219
P05783	0.72966102	0.82711864	0.90254237	1	0.93474576
P08727	0.51652625	0.6448477	0.51717434	1	0.67077122
Q9C075	0.66281588	1	0.66425993	0.65198556	0.65415162
Q7Z3Y7	0.96440678	0.85338983	0.96610169	0.89576271	1
P35527	0.66298812	0.54584041	0.83701188	0.53989813	1
P04264	0.93796296	1	0.88888889	0.95555556	0.86018519
Q7Z794	0.96621005	1	0.7826484	0.83378995	0.87305936
P35908	0.84826325	1	0.87842779	0.79798903	0.94149909
P13647	0.89502262	0.79457014	0.96199095	1	0.92126697
P02538	0.3630094	0.47962382	0.54294671	1	0.77554859
P04259	0.39315068	0.68219178	0.58561644	1	0.7630137
P08729	0.65566392	0.90022506	0.74043511	1	0.73218305
Q86Y46	0.64924886	0.64924886	1	0.54082299	0.42586545
O95678	0.62126477	0.83321751	0.68450313	1	0.56845031
Q8N1N4	0.95290859	1	0.96768236	0.95290859	0.91597415
Q9HA64	1	0.67211774	0.76287817	0.94930499	0.88879804
O43504	0.60237781	0.80647292	0.79128137	0.8011889	1
P28482	0.84645287	0.696793	0.92225462	1	0.88046647
P27361	0.92064923	0.83769161	0.9386835	0.8638413	1
Q9NSA3	0.79152731	0.8483835	0.90301003	0.87625418	1
P35222	1	0.91532258	0.76290323	0.69435484	0.93145161
O60716-3	0.95193214	0.90103676	0.93496701	0.96512724	1
P35221-2	0.9554731	0.85157699	1	0.90166976	0.94248609
Q06830	1	0.82406563	0.9325433	0.96080219	0.92889699
P32119	0.99808429	0.84386973	0.97605364	1	0.93582375
P30044	1	0.72441743	0.95947315	0.9189463	0.87639311
P30041	1	0.7036036	0.88558559	0.96576577	0.87207207
P14923	1	0.89115646	0.95043732	0.88532556	0.99028183
Q13464	0.8202995	0.79700499	0.80199667	1	0.78785358
P08134	0.88985507	0.83961353	0.89178744	1	0.83188406
P84095	0.96736174	0.80417044	1	0.79147779	0.88032638
P52565	0.91131222	0.77556561	0.92126697	1	0.89502262
P52566	0.92837466	1	0.90174472	0.83562902	0.92194674
Q07960	0.94341373	0.69109462	0.8729128	0.87105751	1
Q14155	0.79356769	0.65220643	0.71802543	1	0.93492895
P55000	0.76996805	0.76517572	0.79632588	0.80750799	1
Q14247	0.94791667	0.87405303	0.91193182	0.94412879	1
P08294	0.85035842	1	0.96146953	0.84139785	0.87007168
P04179	0.50782845	0.56841389	0.65350579	1	0.65078285
P00441	0.92534562	0.77235023	1	0.85990783	0.8359447

Q9BRA2	0.4972752	1	0.8119891	0.5633515	0.87874659
Q8NBS9	0.86478873	0.89859155	0.84413146	0.96995305	1
P10599	0.97189922	0.96511628	1	0.97286822	0.88081395
P30048	0.80960549	0.73670669	0.86277873	1	0.89365352
O43396	0.92775665	0.97718631	1	0.878327	0.89258555
P31946-2	0.94232476	0.80922804	1	0.91215617	0.9609583
P62258	0.90892696	0.73850316	0.89630298	1	0.96302976
Q04917	0.96199783	0.82301846	0.95331162	0.93268187	1
P61981	0.8985782	0.92037915	0.94691943	1	0.97725118
P27348	0.93976971	0.7918512	1	0.94331267	0.95925598
P63104	0.95970009	0.76757263	0.93533271	1	0.99906279
Q02413	0.94485981	0.88971963	1	0.86542056	0.95327103
P32926	0.83217478	1	0.83813307	0.84011917	0.74975174
Q9UMD9	0.89307625	0.77475898	1	0.99211218	0.85363716
Q13283	0.92530756	0.82161687	1	0.85588752	0.83831283
P46940	0.99217221	0.8776908	0.97260274	0.98630137	1
Q15404	0.67583835	1	0.82803095	0.74634566	0.80137575
P10301	0.92289157	0.96787149	0.93574297	1	0.82168675
P61026	1	0.67108534	0.96603148	0.85501243	0.95691798
P62491	0.92732291	0.88776449	1	0.89972401	0.91444342
Q15907	0.90667887	0.90667887	1	0.87191217	0.82891125
P61106	1	0.88183594	0.9921875	0.87695313	0.93652344
P62820	0.99429658	0.88688213	1	0.98954373	0.99714829
P57735	0.75	1	0.875	0.70659722	0.85243056
P61019	0.7587477	0.84254144	1	0.85635359	0.95948435
P20339	0.98859316	0.81273764	0.93441065	1	0.91539924
P61020	0.87658802	0.80943739	1	0.82940109	0.88475499
P51149	0.80411449	0.91502683	1	0.93381038	0.8255814
P11233	0.95391705	0.84700461	1	0.96036866	0.94746544
P62834	0.68077601	0.84303351	1	0.55731922	0.64550265
P61224	0.94542091	0.87789084	1	0.96484736	0.97039778

1st 11 h experiment:

Accession	5h	7h	8h	9h	10h
P31946	0.90489381	0.78762696	1	0.85041551	0.95198523
P62258-1	1	0.84782609	0.9905482	0.87712665	0.95652174
Q04917	0.82608696	0.88714154	1	0.84921369	0.84736355
P61981	0.9481268	0.92122959	0.97790586	0.94428434	1
P31947-1	1	0.75838349	0.91315563	0.78503869	0.90885641
P27348	1	0.62379182	0.78438662	0.59776952	0.72118959
P63104-1	1	0.8845815	0.97092511	0.75682819	0.94713656
P10809	1	0.94165814	0.99385875	0.98669396	0.99078813
O95433	0.77787307	1	0.89279588	0.89279588	0.88936535
O60271	0.70163934	0.83852459	0.97540984	1	0.84344262
P17612	0.86708861	1	0.90415913	0.77938517	0.84629295
P10644	0.97761953	0.93896236	1	1	0.93489318
P13861	0.83527132	0.86918605	1	0.85077519	0.88953488
P29466-1	0.89559877	0.9877175	1	0.98567042	0.97134084
P31944	0.70631068	0.82443366	0.89158576	0.63106796	1
P04040	0.64504373	0.72376093	0.7048105	1	0.75874636
P35221	1	0.83473389	0.91596639	0.83846872	0.9589169
Q6YHK3-1	1	0.63369176	0.79641577	0.55483871	0.68817204
P48509	0.86298259	1	0.87358062	0.80999243	0.88796366
P16070	0.8186864	0.87049029	0.86679001	0.9426457	1
Q9UMD9-1	0.936721	1	0.87344199	0.8801534	0.85522531
Q08554-1	0.76902417	0.89435989	0.89973142	0.8343778	1
Q14574-1	1	0.84220355	0.90009337	0.83099907	1

Q02413	0.8733945	0.88165138	0.91651376	0.81284404	1
Q14126	1	0.8849481	0.85121107	0.82266436	0.89532872
P32926	1	0.79689018	0.89407191	0.81146744	0.90087464
P15924-1	0.98767773	0.82274882	1	0.90236967	1
P36507	0.90377358	0.79811321	0.89339623	1	0.84245283
Q92817	0.80371353	0.82847038	0.88859416	0.86648983	1
Q9H6S3	0.8085456	0.8093673	0.83237469	0.87181594	1
P08294	0.89752348	0.96157131	0.80785653	1	0.83689155
P0DMV8	1	0.80503145	0.89128482	0.80413297	0.96316262
P34932	0.93021033	0.96940727	1	0.97418738	0.94072658
P11142-1	0.97363465	0.83992467	1	0.94444444	0.92372881
P04792	1	0.5323654	0.44343618	0.51966122	0.68481549
P07900	1	0.87165282	0.95937211	0.8744229	0.96768236
P08238	0.94299065	0.86261682	0.9728972	0.88598131	1
P54652	1	0.63490854	0.67301829	0.66996951	0.73704268
Q16543	0.90681622	0.80069025	1	0.82312338	0.89042278
Q14155-1	0.96472518	0.82854799	1	0.79819524	0.96062346
O60716-3	0.91300191	0.91300191	0.95219885	0.95506692	1
P15924-2	0.86643234	0.78822496	1	0.76713533	0.8602812
P14923	0.97021661	0.82942238	0.91606498	0.79693141	1
O43240	0.69975981	0.73658927	0.82866293	0.82546037	1
Q9P0G3	1	0.77229437	0.76796537	0.93939394	0.69350649
P49862	0.83245614	0.82807018	0.72280702	0.84473684	1
Q15323	0.72330548	0.84401114	1	0.89972145	0.82636955
P13645	0.73428799	0.77645187	0.73587908	0.69530628	1
P13646	0.84094755	0.85532995	0.8714044	0.71742809	1
P02533	1	0.74654752	0.77010561	0.70917953	0.82778229
P19012	0.84802687	0.7884131	0.868178	0.74895046	1
P08779	1	0.23425197	0.25905512	0.22795276	0.23543307
Q04695	1	0.51971748	0.56032961	0.48440259	0.43790465
P05783	1	0.66113875	0.43559978	0.44444444	0.28247651
P08727	1	0.84632353	0.62720588	0.71617647	0.49264706
Q9C075	0.91024479	1	0.83499547	0.82774252	0.96192203
Q7Z3Z0	0.98632813	0.84277344	1	0.93652344	0.94335938
Q7Z3Y8	0.91464435	0.90292887	0.88368201	0.558159	1
Q7Z3Y7	0.79831933	0.93417367	0.86064426	0.64985994	1
Q14533	0.48257969	0.73832468	1	0.61675315	0.64862861
Q9NSB4	0.82999354	0.64899806	0.53458306	0.48480931	1
P78386	0.5065407	0.83430233	1	0.60755814	0.70348837
P04264	0.75946372	0.7318612	0.74921136	0.68138801	1
Q7Z794	0.9116321	0.96753832	0.82777277	0.70243463	1
P35908	0.43145442	0.86221294	0.63395964	0.53653445	1
P13647	1	0.77777778	0.80892256	0.72979798	0.88299663
P02538	1	0.35039925	0.44903711	0.32315641	0.34288398
P04259	1	0.17477049	0.20061204	0.14892894	0.15572934
P08729	1	0.83345561	0.62068966	0.69112252	0.4409391
Q3SY84	0.88184932	0.87328767	0.89811644	0.55222603	1
Q86Y46	0.85770492	0.53704918	0.48131148	0.65180328	1
Q7RTS7	1	0.70729927	0.74014599	0.58540146	0.75036496
O95678	1	0.66205943	0.70628887	0.53282654	0.6406358
Q8N1N4	0.62086093	0.88741722	0.87417219	0.6986755	1
Q5XKE5	0.94283122	0.84119782	1	0.9137931	0.71415608
P05787	1	0.76861702	0.55784574	0.59906915	0.4268617
P28482	0.9895288	0.9434555	0.99162304	1	0.87015707
P27361-1	0.88265746	0.80500431	1	0.84210526	0.88869715
P08571	0.69672131	0.97131148	0.98114754	1	0.7704918
Q9NUJ1	0.95279912	0.88913282	0.90010977	0.86278814	1
Q06830	0.95238095	1	0.98214286	0.99107143	0.98313492
P32119	0.82049111	0.76629975	0.84250635	1	0.77646063

P30044-1	0.81506276	0.80502092	1	0.7874477	0.8334728
P30041	0.75642088	0.84424192	1	0.78210439	0.8036454
P27986	0.98662846	0.85195798	0.93791786	0.96179561	1
P14555	1	0.49329446	0.49970845	0.58542274	0.47230321
P03952	0.80544106	0.76586974	1	0.65869744	0.6422094
Q05655	0.71354616	0.79378775	1	0.99741156	0.90595341
Q9UN86	0.84818182	0.92636364	0.89454545	1	0.93454545
P46940	1	0.87618147	0.95935728	0.91398866	0.97353497
Q15404-1	0.61226054	0.73409962	0.78390805	1	0.87049808
P63000-1	0.80298013	0.8236755	1	0.77235099	0.86092715
P60763	0.91269841	0.80511464	1	0.83156966	0.9664903
Q5VZM2	0.82466871	0.73802243	0.96024465	0.83893986	1
P10301	0.9556213	1	0.86982249	0.97140039	0.8678501
P61026	0.79706601	0.75224124	0.85574572	0.79543602	1
P62491-1	0.83583407	0.72197705	0.87908208	0.81465137	1
Q15907	0.84286804	0.81845919	1	0.74141876	0.78794813
P61106	0.97240723	0.89628925	1	0.92673644	0.97526166
P62820	0.85897436	0.82417582	0.90750916	0.80860806	1
P57735	0.76153177	0.897302	0.82332463	0.85465622	1
O00194	0.8788501	0.84291581	0.8449692	1	0.99897331
P61019-1	0.8308887	0.84555651	0.92752373	0.78429681	1
Q15286	0.90369733	0.80739467	0.96904557	0.81427343	1
Q14964	0.95188679	0.9745283	0.95754717	1	0.89811321
P20339	0.83536091	0.80940795	0.90673155	0.80129765	1
P61020	0.92509363	0.86610487	0.95599251	0.8829588	1
P51148	0.9697286	0.87995825	0.96868476	0.93319415	1
P20340-1	0.88986784	0.84669604	0.86784141	0.89955947	1
P51149	0.79218107	0.89197531	1	0.95884774	0.9063786
Q96AH8	0.77197802	0.98351648	1	0.77747253	0.81501832
P11233	0.73894189	0.72679965	0.89505637	0.8065915	1
P62834	0.88309179	0.8705314	0.94492754	1	0.83768116
P61224-1	0.82961641	0.73684211	0.94826048	0.90900981	1
P10114	0.78775168	0.87080537	1	0.7114094	0.68540268
P52565-1	0.79742489	0.83175966	1	0.79227468	0.79570815
P52566	0.85428051	0.85245902	0.99453552	1	0.84699454
Q07960	0.82118056	0.75347222	0.88541667	0.81857639	1
Q12774-1	1	0.51202263	0.50565771	0.59123055	0.7397454
P08134	0.89181818	0.90545455	1	0.96090909	0.92090909
P84095	0.85980479	0.79236912	0.96805679	0.86779059	1
Q14247-1	0.98522167	0.88965517	0.95073892	0.91330049	1
P00441	0.75416667	1	0.85916667	0.8475	0.73916667
P04179	0.87828371	0.78371278	0.83712785	1	0.83712785
P10599-1	0.82798574	0.96969697	1	0.95008913	0.9144385
Q9BRA2	1	0.83705357	0.97209821	0.89732143	0.8984375
Q8NBS9-1	0.84649512	0.77905945	0.7826087	1	0.8296362
P30048	1	0.84827586	0.92315271	0.96551724	0.96650246
O43396	0.96231884	0.94299517	0.9942029	1	0.94492754
Q9H3N1	0.87671233	0.86130137	0.96660959	0.82791096	1
Q99757	0.92307692	0.71547729	0.83688601	1	0.74235403
P61586	0.87635379	0.8700361	1	0.88267148	0.94223827

2nd 11 h experiment:

Accession	5h	7h	8h	9h	10h
P31946	0.99533582	0.98973881	1	0.87779851	0.8619403
P62258-1	0.99816514	0.95688073	1	0.91192661	0.85963303
Q04917	0.81467545	0.87300094	1	0.85888993	0.86735654
P61981	0.95789474	0.92440191	1	0.93971292	0.96746411

P31947-1	0.98502203	1	0.90220264	0.80969163	0.74008811
P27348	0.96872038	0.92606635	1	0.91374408	0.85687204
P63104-1	0.92625899	1	0.89388489	0.88129496	0.72571942
Q9NSA3	0.87829246	1	0.81743869	0.89464124	0.79291553
P17612	0.87697161	0.96319664	0.95268139	1	0.94637224
P10644	0.83931777	1	0.88509874	0.81149013	0.86804309
P13861	0.94444444	0.92416226	0.90035273	1	0.84303351
P31944	0.97127937	1	0.80069626	0.84769365	0.71192341
P04040	0.96575342	0.96183953	0.90508806	1	0.90900196
P35221	1	0.99722992	0.92059095	0.87165282	0.80424746
P35222	0.92910053	0.83915344	0.98730159	0.92169312	1
Q6YHK3-1	0.88490409	0.87906589	1	0.90408674	0.83319433
Q9Y5K6	0.88641975	1	0.94814815	0.80411523	0.83374486
P16070	0.96934866	0.96168582	1	0.93103448	0.97126437
P08962	0.82513661	0.96018735	1	0.91569087	0.84933646
Q9UMD9-1	0.95475113	1	0.83167421	0.79547511	0.96470588
Q08554-1	0.97050938	1	0.87935657	0.90169794	0.7077748
Q14574-1	0.95655877	1	0.84241908	0.7572402	0.72487223
Q02413	0.97001764	1	0.86155203	0.8324515	0.74955908
P32926	1	0.9017199	0.93447993	0.85257985	0.86158886
P15924-1	0.89590444	1	0.83447099	0.82935154	0.73208191
Q02750	1	0.83856502	0.9103139	0.89686099	0.78176383
P36507	0.87426655	0.92791282	1	0.72590109	0.80050293
Q92817	0.97045245	1	0.83010157	0.92705448	0.80055402
Q9H6S3	0.94054054	1	0.95405405	0.77567568	0.76756757
P0DMV8	0.99814471	1	0.90166976	0.90816327	0.87662338
P34932	0.83827493	0.93530997	1	0.91554358	0.93980234
P11142-1	1	0.98571429	0.94285714	0.93904762	0.91904762
P04792	0.93738657	1	0.86479129	0.99637024	0.97368421
P07900	1	0.95288889	0.94311111	0.88	0.792
P08238	1	0.91479401	0.91947566	0.95973783	0.87640449
P54652	0.92061955	1	0.93417231	0.86060019	0.96418199
Q16543	0.97265625	0.95703125	1	0.86914063	0.83984375
Q14155-1	0.91489362	1	0.90336879	0.73847518	0.79078014
O60716-3	0.93912265	1	0.90689346	0.85496867	0.78961504
P15924-2	0.94605809	1	0.97095436	0.81493776	0.66141079
P14923	1	0.99125364	0.94752187	0.94169096	0.85714286
P49862	0.83644068	1	0.69915254	0.86610169	0.64745763
P13645	0.975	0.98888889	0.81851852	1	0.75462963
P13646	0.94399351	0.81899351	0.80844156	0.84496753	1
P02533	1	0.97549482	0.82280867	0.89915174	0.97172479
P19012	1	0.93176074	0.74473463	0.73967987	0.86604886
P08779	1	0.72916667	0.67227564	0.78926282	0.72916667
Q04695	1	0.53904874	0.50616559	0.4997064	0.40810335
P05783	0.56527778	0.68055556	0.65555556	1	0.75486111
P08727	0.45133292	0.47303162	0.55114693	1	0.70055797
Q9C075	0.95404412	0.96691176	0.80882353	1	0.77849265
Q2M2I5	0.55738935	0.73293323	0.66091523	1	0.89722431
Q7Z3Y8	1	0.78914591	0.91281139	0.86120996	0.68683274
Q9NSB4	1	0.86298422	0.5286944	0.68723099	0.52941176
P04264	1	0.96576577	0.7972973	0.93423423	0.73963964
Q7Z794	0.97113594	1	0.84823091	0.99348231	0.74767225
P35908	0.87758621	1	0.78534483	0.92758621	0.66810345
P13647	1	0.98403756	0.79624413	0.92676056	0.97183099
P02538	1	0.60912698	0.6712963	0.61111111	0.58134921
P04259	1	0.3973064	0.44107744	0.93198653	0.7037037
P08729	0.28826816	0.4396648	0.4972067	1	0.59217877
Q86Y46	0.90693591	1	0.91395961	0.76207199	0.86918349
O95678	0.46649649	0.76068922	0.43203574	1	0.66879387

Q8N1N4	1	0.98314108	0.79148181	0.94232476	0.67790594
P05787	0.40096911	0.48455482	0.54875833	1	0.65475469
Q6KB66	0.91	1	0.92090909	0.93090909	0.70909091
P28482	0.87329079	1	0.92980857	0.86690975	0.66362808
P27361-1	0.99731903	1	0.89008043	0.86148347	0.8847185
Q9NUJ1	1	0.76854599	0.89020772	0.97032641	0.66864491
Q06830	0.97433547	0.95142071	1	0.91292392	0.91750687
P32119	0.97086466	1	0.96428571	0.99530075	0.94642857
P30044-1	0.97788018	0.959447	1	0.98064516	0.94930876
P30041	0.98888889	0.95811966	1	0.77863248	0.83589744
P14555	0.96871945	0.771261	0.7771261	0.85239492	1
Q9UNF0	0.9490085	0.90840415	0.90462701	1	0.94428706
Q05655	0.80203046	0.83350254	1	0.74416244	0.81827411
Q13283	0.72764228	0.8	1	0.94878049	0.85691057
Q9UN86	0.70746528	0.79861111	1	0.99392361	0.90277778
P46940	0.96691871	0.97920605	1	0.92344045	0.85916824
P63000-1	0.86612576	1	0.9959432	0.90466531	0.87626775
P15153	0.86032389	1	0.87550607	0.97469636	0.81275304
P60763	0.85446985	0.78482328	0.98128898	0.77754678	1
P10301	0.86865149	0.82311734	0.87302977	0.97810858	1
P61026	1	0.94043624	0.84983221	0.77684564	0.68624161
Q15907	0.99272066	0.95541401	1	0.92629663	0.81073703
P61106	0.95921986	0.84485816	1	0.92730496	0.96187943
P62820	0.98777046	0.86453434	1	0.87300094	0.95108184
P57735	0.88117953	1	0.86816999	0.90026019	0.79444926
P61019-1	0.91543756	0.99115044	0.95476893	1	1
Q15286	0.93756004	0.93275696	1	0.81748319	0.80307397
P20339	0.95009785	1	0.89334638	0.98630137	0.9109589
P61020	0.94686411	0.98432056	1	0.92682927	0.83797909
P20340-1	1	0.97481343	0.97294776	0.89458955	0.9636194
P51149	0.86756757	0.78018018	0.99459459	1	0.92522523
P11233	1	0.98269896	0.81228374	0.88581315	0.75865052
P11234	0.97050691	0.86912442	1	0.80645161	0.84516129
P62834	0.93613445	0.9210084	1	0.83445378	0.86218487
P61224-1	0.98287345	0.98192198	1	0.8943863	0.92673644
P10114	0.92577488	0.91924959	1	0.862969	0.95106036
P52565-1	0.96209913	0.97667638	1	0.91933916	0.94752187
P52566	0.78937894	0.85148515	1	0.90819082	0.98649865
P08134	0.88785047	0.95514019	1	0.90841121	0.92990654
P84095	0.94894027	1	0.98554913	0.89884393	0.94894027
Q14247-1	1	0.98869144	0.82552504	0.78917609	0.72132472
P00441	0.99520614	0.90795781	0.76126558	0.87823586	1
P04179	0.6403832	0.57037583	0.64922623	0.78408254	1
P10599-1	0.81844946	0.96957802	1	0.89892051	0.74779195
Q8NBS9-1	0.8466604	0.86265287	0.90780809	0.90968956	1
P30048	0.84894837	0.93881453	0.99235182	1	0.96845124
O43396	0.94834711	0.88429752	0.98966942	0.93078512	1
Q9H3N1	0.98781631	1	0.94095595	0.78350515	0.8284911
P61586	1	0.8575152	0.87402259	0.8662033	0.8575152

3rd 11 h experiment:

Accession	5h	7h	8h	9h	10h
P61604	0.90714286	0.89464286	1	0.95267857	0.90714286
P31946	0.97750703	1	0.89971884	0.94095595	0.99812559
P62258-1	0.9620133	1	0.90693257	0.94207028	0.94207028
Q04917	0.93975904	0.82429719	1	0.85742972	0.84236948
P61981	0.91021968	1	0.95033429	0.95033429	0.87774594

P31947-1	0.82851817	0.92823858	0.92730662	0.96458527	1
P27348	0.93093923	1	0.86279926	0.89779006	0.88121547
P63104-1	0.82846715	1	0.90054745	0.95529197	0.94708029
P10809	0.925	0.95961538	0.90096154	1	0.90576923
Q9NSA3	0.9055912	0.98166819	0.87076077	0.89367553	1
P17612	0.93458781	0.97759857	0.89695341	1	0.90143369
P10644	0.90472378	1	0.85348279	0.84307446	0.84867894
P13861	0.95068206	0.8772298	0.95278069	1	0.98426023
P31944	0.77065026	0.8427065	0.89630931	0.86467487	1
P04040	0.9587242	0.91744841	0.75234522	0.92401501	1
P35221	0.84176633	0.90800368	0.89328427	0.95676173	1
P35222	0.81240064	0.82352941	0.70349762	0.89189189	1
O60716-1	0.78736655	0.91103203	0.85587189	0.91014235	1
Q6YHK3-1	0.60635481	1	0.85348632	0.83230362	0.85525154
P48509	0.79528986	1	0.76902174	0.86594203	0.91666667
Q9Y5K6	0.9375	0.90719697	1	0.98390152	0.95833333
P16070	0.78467153	0.92062044	0.89233577	0.97262774	1
O43866	1	0.89561587	0.89039666	0.79645094	0.92901879
Q9UMD9-1	0.69784768	0.93625828	0.69453642	0.92880795	1
Q08554-1	0.86621094	0.89355469	0.9609375	0.91210938	1
Q14574-1	0.71236333	0.81497056	0.76534903	0.87047939	1
Q02413	0.71195185	0.8288908	0.83920894	0.81513328	1
P32926	0.72253788	1	0.7282197	0.83143939	0.9905303
P15924-1	0.65199336	0.73671096	0.84800664	0.81644518	1
Q02750	1	0.82871126	0.83768352	0.78384992	0.87928222
P45985	0.82425308	1	0.93585237	0.96133568	0.90509666
Q92817	0.73761946	0.78627281	0.87141616	0.86707211	1
Q9H6S3	0.8867083	1	0.90811775	0.90276539	0.93933988
P08294	0.93611111	0.89074074	1	0.98425926	0.83611111
P0DMV8	0.85701021	0.93871866	0.86072423	0.96750232	1
P34932	0.80225989	0.9180791	0.80225989	1	0.826742
P11142-1	0.98956357	1	0.88519924	0.971537	0.9345351
Q92598	0.937046	0.97740113	0.84422922	1	0.91202583
Q12931	0.82446809	1	0.75443262	0.86258865	0.81294326
P04792	0.84416741	0.81745325	0.89047195	0.91184328	1
P07900	0.89895138	1	0.83031459	0.96949476	0.97807436
P08238	0.81136951	0.86993971	0.79586563	1	0.90611542
P54652	0.78691589	0.95607477	0.86261682	0.89252336	1
Q16543	0.92753623	0.9468599	0.96328502	1	0.95652174
Q14CN4-2	0.71361059	0.89319471	0.8289225	0.75141777	1
P15924-2	0.65087282	0.80881131	0.879468	0.82294264	1
P15924-3	0.85512367	0.93109541	0.93109541	0.83480565	1
P14923	0.83539486	0.8943863	0.93529971	0.93529971	1
Q9Y337	0.60261652	0.62959935	0.84546198	1	0.92722813
P49862	0.68321513	0.70291568	0.75965327	0.89519307	1
Q15323	0.79104478	0.94496269	1	0.86567164	0.87966418
P13645	0.73994638	0.84450402	0.94101877	0.87310098	1
P02533	0.6907489	0.95066079	0.77797357	0.8722467	1
P19012	0.79555556	0.95644444	0.75644444	1	0.96622222
P08779	0.82263242	1	0.6918138	0.8434992	0.67014446
Q04695	0.73874927	1	0.29982466	0.73056692	0.27001753
P08727	0.72657343	1	0.67832168	0.65104895	0.52587413
Q9C075	0.83256244	0.69842738	0.99074931	0.93246994	1
P35527	0.67930205	0.59747292	0.66666667	0.64079422	1
Q9NSB4	0.63239645	1	0.83727811	0.80843195	0.7714497
P04264	0.71748493	0.80706288	0.89922481	0.82256675	1
Q7Z794	0.76567944	0.7369338	0.81881533	0.89547038	1
P35908	0.69087838	0.79898649	0.83023649	0.86064189	1
P13647	0.7191601	0.92650919	0.80664917	0.90813648	1

P02538	0.75111111	1	0.77777778	0.91555556	0.93688889
P04259	0.85767557	1	0.34679925	0.68116843	0.20758235
P08729	0.64412568	1	0.73702186	0.55806011	0.57308743
Q3SY84	0.68121911	0.82537068	0.84678748	0.7660626	1
Q86Y46	0.63996828	1	0.78112609	0.89770024	0.93973037
Q7RTS7	0.58935993	0.75810474	0.69160432	0.80631754	1
O95678	0.41185334	1	0.38221999	0.60622803	0.34203918
Q8N1N4	0.72671353	0.80667838	0.8629174	0.8831283	1
Q5XKE5	1	0.59686775	0.26798144	0.92923434	0.23027842
P05787	0.64091471	1	0.51359703	0.50556242	0.35290482
Q6KB66	0.73285841	0.83882458	0.81923419	0.85930543	1
Q8IXI1	0.84246575	1	0.96771037	0.89138943	0.96868885
P28482	0.79759863	0.88421955	0.81732419	1	0.87993139
O15264	0.91239515	0.80615098	0.90493942	0.89095993	1
P08571	0.9989418	1	0.82751323	0.88677249	0.78624339
Q06830	0.96877956	0.8987701	0.92526017	1	0.93093661
P32119	1	0.9163034	0.80209241	0.90671316	0.85353095
P30044-1	0.98098098	0.98298298	1	0.91891892	0.92292292
P30041	1	0.88555347	0.96341463	0.91463415	0.8564728
P14555	0.99034749	0.996139	0.97393822	1	0.83880309
P03952	0.82064298	0.88494078	0.84094755	1	0.67174281
Q05655	0.93218807	0.89240506	0.83815552	0.84719711	1
Q13283	1	0.97544204	0.92632613	0.96070727	0.90569745
P46940	0.93054234	1	0.92197907	0.96955281	0.94957184
Q15404-1	1	0.96600567	0.86968839	0.94995279	0.78470255
P63000-1	0.96038647	1	0.94202899	0.9236715	0.96135266
P61026	0.77958834	0.88936535	0.76415094	0.89279588	1
P62491-1	0.72202487	0.89431616	0.97690941	0.84991119	1
Q15907	0.84124629	0.88946588	1	0.68991098	0.65875371
P61106	0.84964413	0.88434164	1	0.86209964	0.79893238
Q9NP72	0.94731707	0.85463415	1	0.99512195	0.89365854
P62820	1	0.99191919	1	0.87777778	0.9020202
P57735	0.85349233	0.8637138	0.95741056	0.78364566	1
P61019-1	0.93047619	0.85904762	0.82952381	1	0.94380952
P51148	0.91130435	0.90869565	0.95391304	0.81826087	1
P20340-1	0.83440073	0.98536139	0.83257091	0.98719122	1
P51149	0.85079929	0.86056838	0.91385435	0.90142096	1
P11233	0.80451128	0.95958647	0.83552632	0.95394737	1
P62834	1	0.980322	0.80500894	0.80143113	0.88908766
P61224-1	0.92713327	1	0.8590604	0.83700863	0.92042186
P52565-1	1	0.92534562	0.91705069	0.91059908	0.85714286
P52566	1	0.86510009	0.91906005	0.82158399	0.77719756
P84095	0.95821462	0.97435897	0.9002849	0.9031339	1
Q14247-1	0.79121864	0.87365591	0.85304659	0.97132616	1
P00441	1	0.89299242	0.87026515	0.89867424	0.84564394
P04179	0.93830571	0.95764273	0.95764273	0.88581952	1
P10599-1	0.86297376	1	0.99902818	0.94655005	0.83965015
Q8NBS9-1	0.93171997	1	0.86689715	0.99135696	0.92134831
P30048	1	0.86488812	0.85800344	0.69018933	0.85283993
O43396	0.91850431	1	0.95877277	0.93480345	0.96260786
Q9H3N1	0.69704861	0.88368056	0.81684028	0.8125	1
Q9H1E5	0.86811201	1	0.67570009	0.85275519	0.99186992
Q99757	0.96601942	0.92718447	0.96019417	0.99902913	1
P61586	1	0.93253235	0.81700555	0.85027726	0.92421442

8.7 CLUSTERED PEPTIDE HITS AT 6 HOURS

Annotated Sequence	Master Protein Accessions	0h	6h	12h	24h
[F].AVAPNQNLKEQGLR.[D]	P12110; P12110-2	0.37854564	1	0.27694687	0.31253225
[P].GADGVAGPKGPAGER.[G]	P02452	0.45144805	1	0.5224304	0.37932992
[G].APGAPGPVGPAGKSGDR.[G]	P02452	0.510303	1	0.5781818	0.40363637
[L].GIAGITGAR.[G]	P02461	0.4721734	1	0.55946106	0.48154658
[F].SDQVEVFSPPGSDR.[A]	P12110; P12110-2	0.571987	1	0.504886	0.5296417
[P].GpGPAGAR.[G]	P08123	0.56105196	1	0.60300565	0.5159674
[S].PGEQGPSGASGPAGPR.[G]	P02452	0.49535808	1	0.53249335	0.3388594
[K].PGANGLSGER.[G]	P02461	0.5065693	1	0.5459854	0.40656933
[G].PQGPPGPSGEEGKR.[G]	P08123	0.61533195	1	0.5509925	0.42505133
[P].AGPPGPIGNVGAPGAKGAR.[G]	P02452	0.5308057	1	0.5842925	0.41029114
[V].GPAGAVGPR.[G]	P08123	0.5291391	1	0.6543046	0.5801324
[V].AGPKGPAGER.[G]	P02452	0.546814	1	0.6105332	0.46098828
[P].GAPGPLGIAGITGAR.[G]	P02461	0.51812786	1	0.55636126	0.5326302
[S].VPGPMGPSGPR.[G]	P02452	0.64241594	1	0.6334935	0.568291
[K].TEESPASDEAGEKEAKSD.[-]	P05114	0.5847348	1	0.66882277	0.5931436
[K].ELPEKMPKTLQELR.[A]	P07585	0.6361186	1	0.5808625	0.5754717
[G].AQGPPGPAGPAGER.[G]	P02452	0.5231939	1	0.6463878	0.5756654
[F].LLALEPELEAR.[L]	P04843	0.715981	1	0.7523734	0.6613924
[F].GGGGDAGSKGPMVSAQESQAQAILQQAR.[L]	P20908	0.5947368	1	0.61729324	0.6255639
[Y].GGGNYGPGGSGGSGGYGGR.[S]	P22626	0.7880851	1	0.77446806	0.7557447
[S].TGGISVPGPMGPSGPR.[G]	P02452	0.7660142	1	0.8211744	0.76067615
[P].GPSGEPGKQGPSGASGER.[G]	P02452	0.37696335	1	0.42460734	0.31099477
[P].SGEPGKQGPSGASGER.[G]	P02452	0.40699708	1	0.46297377	0.34402332
[P].GAPGPVGPAGKSGDR.[G]	P02452	0.40816328	1	0.4699248	0.33727175
[S].GEPGKQGPSGASGER.[G]	P02452	0.38598442	1	0.48498333	0.33870968
[P].AGKEGGKGPR.[G]	P02452	0.42543858	1	0.48135966	0.37171054
[D].AGPKGADGSPGKDGVR.[G]	P02452	0.4271739	1	0.43913043	0.33695653
[P].AGKDGEAGAQGPPGPAGPAGER.[G]	P02452	0.4813992	1	0.530261	0.38200998
[A].GPKGADGSPGKDGVR.[G]	P02452	0.42767653	1	0.46298406	0.36161733
[P].GPVGAAGATGAR.[G]	P08123	0.42544842	1	0.5100897	0.37724215
[P].VGPAGAVGPR.[G]	P08123	0.52103746	1	0.5458213	0.42247838
[P].GENGSPGPMGPR.[G]	P02458	0.36863425	1	0.43113425	0.359375
[A].VGAKGEAGPQGPR.[G]	P02452	0.45346197	1	0.52099884	0.38706017
[P].GPSGEEGKR.[G]	P08123	0.44025522	1	0.5150812	0.3799304
[Q].GPPGPSGEEGKR.[G]	P08123	0.40473506	1	0.4785795	0.3664036

[P].GKQGPSGASGER.[G]	P02452	0.42947248	1	0.4896789	0.3772936
[A].GAAGPAGPAGPR.[G]	P08123	0.43004587	1	0.5149082 5	0.4008027 6
[P].GPAGAPGDKGESGPSGPAGPTGAR.[G]	P02452	0.38087606	1	0.5133547	0.3301282
[P].VGPAGKSGDR.[G]	P02461; P02452	0.42653278	1	0.4587738	0.352537
[P].GGPGADGVPGKDGPR.[G]	P02461	0.4320442	1	0.4723757	0.3734806 8
[P].GPQGVKGESGKPGANGLSGER.[G]	P02461	0.40984544	1	0.4476245	0.3875214 8
[P].GPAGPAGER.[G]	P02458; P02452	0.4530783	1	0.5062761 3	0.3945009
[P].QGPPGPSGEEGKR.[G]	P08123	0.44412443	1	0.5178571 3	0.3634792 6
[Q].GPSGASGPAGPR.[G]	P02452	0.40404624	1	0.4601156	0.3791907 4
[K].SSSSGSVGESSSKGPR.[Y]	P13645	0.61036587	1	0.6993902 3	0.5829268
[AQ].GPPGPAGPAGER.[G]	P02458; P02452	0.4675615	1	0.5380313 4	0.3898210 2
[E].QGPSGASGPAGPR.[G]	P02452	0.42914286	1	0.4851428 6	0.3982857 2
[P].SGPSGLPGER.[G]	P08123	0.46585834	1	0.5724314	0.3848117 3
[P].GPQGVKGER.[G]	P02461	0.40625	1	0.4571759 4	0.3842592 5
[P].GLPGPSGEPGKQGPSGASGER.[G]	P02452	0.45397007	1	0.4810126 7	0.3406214
[E].AGAAGPAGPAGPR.[G]	P08123	0.44566473	1	0.5427745 6	0.3953757 3
[A].DGVAGPKGPAGER.[G]	P02452	0.44528964	1	0.4868344	0.3803393 8
[P].AGAAGQPGAKGER.[G]	P08123	0.42629716	1	0.5053066	0.3520047
[P].GENGTPGQTGAR.[G]	P08123	0.3862982	1	0.4870466 3	0.3258491 8
[P].GSAGPQGPPGPSGEEGKR.[G]	P08123	0.42464954	1	0.5239486	0.317757
[K].GADGSPGKDGVR.[G]	P02452	0.44306785	1	0.5073746 4	0.3651917 3
[P].GPVGPAGKSGDR.[G]	P02461; P02452	0.46356502	1	0.4837443 8	0.389574
[P].GPIGNVGAPGAKGAR.[G]	P02452	0.42962185	1	0.4579832	0.3188025 4
[D].KGETGEQGDR.[G]	P02452	0.4864182	1	0.5072647	0.4219835 7
[P].GPQGIAGQR.[G]	P02458; P02452	0.414267	1	0.5301047	0.4345549 6
[P].GPKGEIGAVGNAGPAGPAGPR.[G]	P08123	0.459225	1	0.5529207 6	0.4626952
[P].KGADGSPGKDGVR.[G]	P02452	0.49776536	1	0.5139665	0.3977653 7
[P].AGAPGDKGESGPSGPAGPTGAR.[G]	P02452	0.3722416	1	0.4709639 8	0.3118467
[P].GAPGAPGPVGPAGKSGDR.[G]	P02452	0.49617067	1	0.5153172 6	0.3588621 3
[V].GVQGPPGPAGEEGKR.[G]	P02452	0.43373495	1	0.5228916	0.3879518 2
[R].ADSSGHSQVGQGQSEGPR.[T]	P20930	0.5751015	1	0.5426252	0.4391069
[P].GESGAAGPTGPIGSR.[G]	P08123	0.5006188	1	0.615099	0.4783415 8
[S].GPSGPAGPTGAR.[G]	P02452	0.4764151	1	0.5807783	0.4398585
[P].AGPSGPAGKDGR.[T]	P08123	0.44376048	1	0.4941242 3	0.4141018 4
[P].GEKGPAGER.[G]	P02461	0.46534654	1	0.4907178 3	0.3842821 7
[H].PGPPGPVGPAGKSGDR.[G]	P02461	0.5172181	1	0.4854827 8	0.403106
[P].VGPAGKHGNR.[G]	P08123	0.49179253	1	0.5633617 6	0.4326986
[P].GAVGAKGEAGPQGPR.[G]	P02452	0.46182495	1	0.5021726	0.4407200 5

[P].GPQGVKGESGKPGANGLSGER.[G]	P02461	0.39838803	1	0.4876223 5	0.421991 94
[R].GDAGPKGADGSPGKDGVR.[G]	P02452	0.45650753	1	0.5408764	0.409417 93
[V].GPAGKSGDR.[G]	P02461; P02452	0.47583178	1	0.5486503	0.383553 06
[E].SGAAGPTGPIGSR.[G]	P08123	0.46530074	1	0.5816259 4	0.423000 66
[N].VGAPGAKGAR.[G]	P02452	0.43927357	1	0.4682179 4	0.362088 53
[P].GLAGPPGESGR.[E]	P02452	0.4106825	1	0.5044510 4	0.426112 77
[P].GKNGDKGHAGLAGAR.[G]	P08123	0.51331717	1	0.527845	0.452179 16
[P].GKNGDKGHAGLAGAR.[G]	P08123	0.44697905	1	0.540074	0.427866 82
[E].SGPSGPAGPTGAR.[G]	P02452	0.45773324	1	0.5729493	0.421415 15
[K].GEAGPQGPR.[G]	P02452	0.4163722	1	0.4911660 9	0.412838 64
[G].ESGPSGPAGPTGAR.[G]	P02452	0.4657271	1	0.5759129	0.449071 1
[P].PGSPGEQGPSGASGPAGPR.[G]	P02452	0.42108625	1	0.4357827 6	0.253035 16
[S].AGPQGPPGPSGEEGKR.[G]	P08123	0.48152786	1	0.5848466	0.409517 85
[V].QGPPGPAGEEGKR.[G]	P02452	0.5281955	1	0.5814536	0.421679 2
[A].GKDGEAGAQGPPGPAGPAGER.[G]	P02452	0.5248619	1	0.577655	0.427869 86
[G].PVGPAGAVGPR.[G]	P08123	0.5413314	1	0.5508413	0.424286 75
[G].AVGAKGEAGPQGPR.[G]	P02452	0.5013038	1	0.5397653	0.405475 88
[P].GPLGIAGITGAR.[G]	P02461	0.35033393	1	0.4183363 6	0.431086 84
[P].VGVQGPPGPAGEEGKR.[G]	P02452	0.53590506	1	0.5750742	0.430860 52
[G].ADGSPGKDGVR.[G]	P02452	0.4838497	1	0.5767963	0.404746 2
[P].KGEIGAVGNAGPAGPAGPR.[G]	P08123	0.48174706	1	0.5880052 4	0.449804 43
[PA].PGPVGPAGKSGDR.[G]	P02461; P02452	0.5284128	1	0.5741345	0.422599 6
[P].GPPGPVGPAGKSGDR.[G]	P02461	0.43404996	1	0.4572922 6	0.349796 62
[A].VGPAGKDGEAGAQGPPGPAGPAGER.[G]	P02452	0.45363408	1	0.5770677	0.405388 47
[P].AGEVGKPGER.[G]	P08123	0.521603	1	0.5860989	0.410770 2
[G].SAGPQGPPGPSGEEGKR.[G]	P08123	0.40646365	1	0.5506525 6	0.371037 9
[P].AGEKGSPGADGPAGAPGTPGPQGIAGQR.[G]	P02452	0.4955357	1	0.5529337	0.423469 4
[G].EAGAAGPAGPAGPR.[G]	P08123	0.5299934	1	0.6196440 5	0.469347 4
[P].GAPGAPGAPGPVGPAGKSGDR.[G]	P02452	0.49638397	1	0.5588428 4	0.414858 64
[I].GAVGNAGPAGPAGPR.[G]	P08123	0.51750475	1	0.6168046	0.493952 9
[L].KELPEKMPKTLQELR.[A]	P07585	0.7026022	1	0.6047088	0.629491 9
[E].PGGPGADGVPGKDGPR.[G]	P02461	0.50659263	1	0.4913254 7	0.367106 17
[G].PSGASGPAGPR.[G]	P02452	0.52294856	1	0.5938804	0.422114 04
[P].SGPAGEVGKPGER.[G]	P08123	0.50417244	1	0.6063977 5	0.479137 7
[A].PGTPGPQGIAGQR.[G]	P02452	0.49456915	1	0.5582911	0.404779 14
[D].KGESGPSGPAGPTGAR.[G]	P02452	0.48766604	1	0.5970904	0.463630 62
[H].GPVGPAGKHGNR.[G]	P08123	0.5366667	1	0.6213333 6	0.494

[G].AAGPAGPAGPR.[G]	P08123	0.5348226	1	0.607753	0.43955323
[F].SLPQTPQTDNPSEGR.[G]	Q9Y2D5-4	0.58494335	1	0.6302465	0.48301134
[G].EQGPSGASGPAGPR.[G]	P02452	0.44825396	1	0.567619	0.4393651
[P].GTPGPQGIAGQR.[G]	P02452	0.54765016	1	0.54699737	0.53067887
[P].GPPGAVGPAGKDGEAGAQGPPGPAGPAGER.[G]	P02452	0.5153538	1	0.53271025	0.493992
[P].LGIAGITGAR.[G]	P02461	0.599361	1	0.52779555	0.49009585
[P].GPQGLAGQR.[G]	P02458; P02452	0.4718706	1	0.55977494	0.47679326
[G].PVGPAGKSGDR.[G]	P02461; P02452	0.59665555	1	0.5324415	0.45351171
[T].GPSGPVGPAGAVGPR.[G]	P08123	0.51449764	1	0.59069455	0.52798384
[V].GNAGPAGPAGPR.[G]	P08123	0.59059477	1	0.6023513	0.5816044
[E].GPDSKLHHGHDPR.[G]	P48634	0.54545456	1	0.5568182	0.46122995
[P].GPAGPAGPPGPIGNVGAPGAKGAR.[G]	P02452	0.48600975	1	0.57177615	0.40997568
[A].GPTGPIGSR.[G]	P08123	0.4764706	1	0.5588235	0.4620915
[A].AGPTGPIGSR.[G]	P08123	0.60181	1	0.68649	0.5546219
[E].AGAQGPPGPAGPAGER.[G]	P02452	0.5556328	1	0.61821973	0.527121
[P].SGPVGPAGAVGPR.[G]	P08123	0.58536583	1	0.6675958	0.5337979
[G].PAGPSGPAGKDGR.[T]	P08123	0.56332844	1	0.59204715	0.48453608
[H].GSYGSGSSSGGYR.[G]	P04264	0.80876493	1	0.787251	0.7824701
[A].PGPLGIAGITGAR.[G]	P02461	0.56875837	1	0.5834446	0.4753004
[G].PAGKDGEAGAQGPPGPAGPAGER.[G]	P02452	0.5837527	1	0.58087707	0.47160316
[P].AGPAGPPGPIGNVGAPGAKGAR.[G]	P02452	0.512	1	0.544	0.45666668
[K].DGEAGAQGPPGPAGPAGER.[G]	P02452	0.5157401	1	0.5994642	0.47689217
[P].GAVGAPGPAGATGDR.[G]	P08123	0.45422536	1	0.53943664	0.39295775
[E].TGPSGPVGPAGAVGPR.[G]	P08123	0.62085307	1	0.6838186	0.57075155
[K].PGANGLSGER.[G]	P02461	0.64540625	1	0.6651481	0.53682613
[F].QEDPQTKEEVASLR.[A]	O60437	0.71812594	1	0.6236559	0.6298003
[A].PGDKGESGPSGPAGPTGAR.[G]	P02452	0.5569343	1	0.5627737	0.4503649
[K].QSESSHGWTGPSTGVR.[Q]	P20930	0.7653936	1	0.6679657	0.6196415
[E].NSDTQSVSGHGKAGLR.[Q]	P20930	0.8001567	1	0.62460816	0.5815047
[L].QAALDDEEAGGRPAMEPGNGSLDLGGDSAGR.[S]	Q00839	0.78908	1	0.68661183	0.6813762
[L].LDGSINFR.[R]	P12111; P12111-4	0.48123884	1	0.33591422	0.3621203
[F].QDDVDLEDQPR.[G]	Q3YEC7-2	0.66926676	1	0.7176287	0.6341653
[R].GFPGLPGPSGEPGKQGPSGASGER.[G]	P02452	0.62824786	1	0.6528981	0.5516322
[W].AAQTTDGKLPEVTKDVER.[T]	P50454	0.69930553	1	0.6125	0.55625
[P].GENGAPGQMGPR.[G]	P02452	0.57661927	1	0.657188	0.5742496
[R].NIDSEEVGKIASNSATAFR.[V]	P12111; P12111-4	0.5674505	1	0.5482673	0.5235148
[P].TGDPGKNGDKGHAGLAGAR.[G]	P08123	0.58254546	1	0.6021818	0.5316336
[P].GTPGPQGIAGQR.[G]	P02452	0.5839368	1	0.6879526	0.5753784

[Y].DMENPPADEYFGR.[C]	Q93052	0.5573204	1	0.6781768	0.57596684
[YR].VLQKER.[EA]	P46821	0.6355014	1	0.5670731 7	0.56639564
[L].SESVQVEKGDTEQEIQR.[L]	O60437	0.68240345	1	0.6008584	0.64663804
[K].VGLEHLR.[V]	P12111; P12111-4	0.5294486	1	0.3822055 2	0.39097744
[V].SVSTSHTTISGGGSR.[G]	P04264	0.70250607	1	0.7227163	0.67259496
[P].DSTEIDQDTINR.[I]	P12110; P12110-2	0.60413474	1	0.7143951	0.6646248
[F].ESDLAAHQDR.[V]	P12814-3; O43707	0.6433409	1	0.6802107	0.61173815
[R].KLVILEGELER.[SA]	P67936; P07951	0.7742681	1	0.7966102	0.71879816
[F].DVVEGEKGAEAANVTGPDGVPVEGSR.[Y]	P16989-2	0.70942026	1	0.6028985 4	0.54565215
[P].GENGSPGPMGPR.[G]	P02458	0.5976231	1	0.6443124	0.5050934
[F].AGLDLNSSDNQSGGSTASKGR.[Y]	O00571	0.6082725	1	0.6926196	0.6561233
[Y].DSQQTNDYMQPEEDWDR.[D]	P12814-3	0.7416608	1	0.7239176 6	0.715401
[P].EFTVHER.[H]	Q5D862	0.7676856	1	0.8061135 4	0.7659389
[K].GVGLGPGPMGLMGPR.[G]	P08123	0.72226655	1	0.8076616	0.7366321
[P].PGAPGPLGIAGITGAR.[G]	P02461	0.6583541	1	0.7439734	0.6550291
[G].VKGESGKPGANGLSGER.[G]	P02461	0.5919344	1	0.6739576 5	0.6356801
[T].GGISVPGPMGPSGPR.[G]	P02452	0.6424196	1	0.7327718	0.6171516
[G].PIGNVGAPGAKGAR.[G]	P02452	0.619462	1	0.5917721 4	0.49208862
[C].KNVQDAIADAEQR.[G]	P35908	0.7016129	1	0.7564516	0.7387097
[KR].AQYEEIAQR.[S]	P35908; P04259; P02538	0.66584563	1	0.7019704 6	0.6839080 5
[S].TGGISVPGPMGPSGPR.[G]	P02452	0.7055118	1	0.7692913 4	0.6732283
[R].SSGGGSSGSSSGSSIAQGGSAGSFKPGTGY.[S]	Q15517	0.74640286	1	0.7805755	0.7041366 7
[T].GGISVPGPMGPSGPR.[G]	P02452	0.79637265	1	0.8252267	0.7584501 5
[Y].GDDEDSLSSAYIQR.[V]	O14773	0.7639123	1	0.7301855	0.7032040 4
[L].QPLNVKVDPEIQNVKAQER.[E]	P35908	0.8599656	1	0.8694158	0.8634020 7
[F].SDAGLTFTSSSGQQTAQR.[A]	P01024	0.86040384	1	0.7734855 4	0.7743634 6
[Y].QGAGGPGPGGFGAQGPKGGSGSGPTIEEVD.[-]	P0DMV9	0.6490272	1	0.7439688 4	0.6941634 4
[E].LSQMQTHVSDTSVVLSMDNNR.[N]	P13647	0.88383836	1	0.8838383 6	0.8424242
[L].VNADGEEVAMR.[T]	Q03252	0.73934424	1	0.6696721 3	0.6803279
[P].GAVGPAGKDGEAGAQGPPGPAGPAGER.[G]	P02452	0.43769634	1	0.5109948	0.3350785 4
[P].GPAGATGDR.[G]	P08123	0.3874459	1	0.530303	0.3701298 8
[R].GGSGGGGSISGGGYGSGGGSGGR.[Y]	P35908	0.6904762	1	0.5699404 5	0.4635416 6
[Y].TLLAPTNEAFEKIPSETLNR.[I]	Q15582	0.82145715	1	0.7125701	0.6236989 5
[G].PSGEPGKQGPSGASGER.[G]	P02452	0.5496783	1	0.5296640 4	0.3502501 8
[F].DDAVEER.[V]	Q09028	0.76888216	1	0.6722054 5	0.5838368 5
[Y].EESGLLETDEATLDTR.[K]	Q9NT62	0.76180255	1	0.7317596 7	0.6194563 5
[K].VSPGAFTPLVKLER.[L]	P07585	0.7302682	1	0.7279693 5	0.6183908

[E].ASLAETEGR.[Y]	P13645	0.85028476	1	0.7648495	0.6590724
[GRH].GLLSGNEKVTMQNLNDR.[L]	Q7Z3Y7; P13645; Q7Z3Y8	0.89272386	1	0.8572761 4	0.790111 96
[SG].DTSVVLSMDNNR.[NCSY]	P04259; P02538; O95678; Q8N1N4; P13647	0.778481	1	0.8101266	0.722310 1
[PT].PGPQGIAGQR.[G]	P02458; P02452	0.5603799	1	0.5848033	0.389416 55
[P].IGNVGAPGAKGAR.[G]	P02452	0.51540786	1	0.5812689	0.388519 64
[R].PGPIGPAGAR.[G]	P08123	0.546864	1	0.5912614 5	0.387596 9
[H].AETSSGGQAASSQEQARSSPGER.[H]	P20930	0.6268797	1	0.625	0.453947 37
[V].PGPPGAVGPAGKDGEAGAQGPPGPAGPAGER.[G]	P02452	0.5601604	1	0.5641711 4	0.355614 96
[G].PAGEEGKR.[G]	P02458; P02452	0.5484341	1	0.5965040 3	0.408594 3
[Q].GSSVSQDSDSQGHSEDSER.[W]	P20930	0.704398	1	0.7368421	0.608507 6
[G].PIGPAGAR.[G]	P08123	0.61923075	1	0.6538461 4	0.486923 07
[V].GTAGPSGPSGLPGER.[G]	P08123	0.50271904	1	0.6338368 7	0.465256 8
[G].PVGVQGPPGPAGEEGKR.[G]	P02452	0.61048156	1	0.6126062	0.424929 17
[P].GPVGVQGPPGPAGEEGKR.[G]	P02452	0.5386534	1	0.6471321 6	0.480049 88
[G].PMGPSGPR.[G]	P02452	0.6622976	1	0.6569005	0.485736 3
[G].NAGPAGPAGPR.[G]	P08123	0.6018786	1	0.6979769	0.554913 3
[L].ENTVEER.[L]	Q07065	0.81661445	1	0.7750783 6	0.652037 6
[V].PGPMGPSGPR.[G]	P02452	0.6580997	1	0.6721183 7	0.501557 65
[Y].IEKIQPSGGTNINEALLR.[A]	P19823	0.78003246	1	0.799513	0.6875
[M].VEVGADDDEGGAER.[G]	Q6NZI2	0.75615215	1	0.7404921 7	0.585384 1
[L].IDELLER.[D]	Q7Z6Z7	0.92874694	1	0.8976249	0.829647 84
[D].GEAGAQGPPGPAGPAGER.[G]	P02452	0.7202426	1	0.7429871	0.602729 3
[G].APGPLGIAGITGAR.[G]	P02461	0.7531915	1	0.8246808 6	0.741276 6
[AP].PGPAGEEGKR.[G]	P02458; P02452	0.59512526	1	0.5870006 7	0.350710 9
[G].PSGPAGPTGAR.[G]	P02452	0.5485232	1	0.6104079	0.409282 7
[P].PGAVGPAGKDGEAGAQGPPGPAGPAGER.[G]	P02452	0.5666907	1	0.5775054	0.328767 12
[T].GPVGPVGAR.[G]	P02452	0.65228426	1	0.6821066	0.504441 6
[P].PGPAGPAGER.[G]	P02458; P02452	0.63826716	1	0.6353791	0.398555 96
[G].ESGAAGPTGPIGSR.[G]	P08123	0.47575757	1	0.6272727	0.431515 16
[R].EDSAPVATAAAAGQVQQQQQR.[R]	Q8TAE6	0.5	1	0.6341463 3	0.447832
[PT].PGPQGLAGQR.[G]	P02458; P02452	0.57543105	1	0.6630747 3	0.489942 52
[L].SEAGSTAGAAETR.[G]	O75781	0.7664747	1	0.5060780 6	0.506717 86
[P].PGAPGAPGAPGPVGPAGKSGDR.[G]	P02452	0.42935905	1	0.5223983 5	0.276361 14
[S].PGENGSPGPMGPR.[G]	P02458	0.6046348	1	0.630618	0.430477 53
[Q].QEAVEGGCSHLGQSYADR.[D]	P02461	0.7488076	1	0.7241653	0.536565 96
[P].PGPIGNVGAPGAKGAR.[G]	P02452	0.5692908	1	0.6187378	0.392973 33
[R].GVPGPPGAVGPAGKDGEAGAQGPPGPAGPAGER.[G]	P02452	0.4590723	1	0.5661664 6	0.306957 72

[G].PPGPSGEEGKR.[G]	P08123	0.5737452	1	0.6725868	0.4772201
[K].GEIGAVGNAGPAGPAGPR.[G]	P08123	0.6180867	1	0.6875934	0.5231689
[R].GDKGETGEQGDR.[G]	P02452	0.6001415	1	0.6871903	0.5194621
[G].AAGPTGPIGSR.[G]	P08123	0.5888502	1	0.6787456	0.4996515
[IL].YQVSTHEQSESAHGR.[TA]	P20930	0.5662739	1	0.6745213	0.4985276
[I].GPEVPDDR.[D]	P07585; P07585-3	0.8073947	1	0.8022356	0.6689595
[K].SEDGVEGDLGETQSR.[T]	Q09666	0.6963623	1	0.7535263	0.6028211
[K].STGGISVPGPMGPSGPR.[G]	P02452	0.68683004	1	0.7756508	0.6454823
[L].LFSDGNSQGATPAAIEKAVQEAQR.[A]	P12109	0.6227273	1	0.744697	0.6174242
[L].SSETEVALAR.[D]	P27816	0.8575949	1	0.6969936	0.6859174
[L].SDETLPAPEFSPEPESGR.[A]	P04217	0.81698775	1	0.8353765	0.7241681
[L].LDLQNNDISELR.[K]	P21810	0.7631379	1	0.8362528	0.7380057
[S].GAAGPTGPIGSR.[G]	P08123	0.48919085	1	0.6312538	0.4033354
[P].PGPSGEEGKR.[G]	P08123	0.5528811	1	0.6177972	0.3406272
[P].GENGAPGQMGPR.[G]	P02452	0.48388988	1	0.6367897	0.4159343
[P].GPKGPTGDPGKNGDKGHAGLAGAR.[G]	P08123	0.5975232	1	0.6702786	0.4226006
[Q].QQEVISPDTTER.[N]	P12110; P12110-2	0.6248	1	0.692	0.4768
[P].GDLGAPGPSGAR.[G]	P02452	0.56038964	1	0.675974	0.4746753
[D].GQVINETSQHHDDLE.[-]	P08670	0.81673306	1	0.7729084	0.5043825
[G].VGLGPGPMGLMGPR.[G]	P08123	0.6254392	1	0.7252283	0.5179199
[I].SVPGPMGPSGPR.[G]	P02452	0.6020408	1	0.7386185	0.588697
[V].SQDSDSEAYPEDSER.[R]	P20930	0.7813195	1	0.8220904	0.6775389
[K].STGGISVPGPMGPSGPR.[G]	P02452	0.70494294	1	0.7939163	0.6448669
[M].QTHVSDTSVVLSMDNNR.[N]	P13647	0.73434705	1	0.8211091	0.7093023
[I].GAVGNAGPAGPAGPR.[G]	P08123	0.67674226	1	0.7951301	0.6725440
[G].KDGEAGAQGPPGPAGPAGER.[G]	P02452	0.35961872	1	0.6130849	0.4129116
[R].HSASQDGQDTIR.[G]	P20930	0.7009494	1	0.7681962	0.5688291
[G].PSGPSGLPGER.[G]	P08123	0.6053435	1	0.7259542	0.5022907
[L].SSTTDDEAPR.[L]	O00515	0.5866013	1	0.7549019	0.6192805
[P].GDVGPQGPR.[G]	P20908	0.6791886	1	0.7888805	0.6401202
[N].QGSSVSQDSDSQGHSEDSER.[W]	P20930	0.7619849	1	0.8116064	0.6375104
[G].ISVPGPMGPSGPR.[G]	P02452	0.7355555	1	0.8014815	0.6377778
[S].KVSPGAFTPLVKLER.[L]	P07585	0.8533698	1	0.8907103	0.7832423
[R].GEAGAAGPAGPAGPR.[G]	P08123	0.6798144	1	0.7942769	0.6627997
[K].GIMEEDEACGR.[Q]	P14923	0.7330435	1	0.8434782	0.7530435
[F].PGLPGPSGEPGKQGPSGASGER.[G]	P02452	0.54497004	1	0.6648900	0.3277814
[P].GAAGTPGLQGMPGER.[G]	P02461	0.5042017	1	0.7037815	0.4887955
[P].VLQPLPSPGVGGKR.[D]	P12111; P12111-4	0.84759575	1	0.8891606	0.7832111

[Y].GVEEEPAELPEGTSLTVDNKR.[F]	Q00577	0.80117387	1	0.5619956	0.556859 85
[G].VGLGPGPMGLMGPR.[G]	P08123	0.7208238	1	0.8283753	0.694126 6
[P].GEQGPSGASGPAGPR.[G]	P02452	0.6560196	1	0.8067158	0.673218 67
[G].PPGPAGPAGER.[G]	P02458; P02452	0.5821221	1	0.7318314	0.478924 42
[P].GVVGAVGTAGPSGPSGLPGER.[G]	P08123	0.643906	1	0.8024963	0.648311 3
[P].GFPGAVGAKGEAGPQGPR.[G]	P02452	0.62528735	1	0.7593869 6	0.526436 8
[E].SGKPGANGLSGER.[G]	P02461	0.6110283	1	0.7637854	0.552161
[L].EDDAKDNQQKANEVEQMIR.[D]	Q14204	0.5377907	1	0.7281977	0.507994 2
[P].GLIGEQGISGPR.[G]	P12111; P12111-4	0.7135843	1	0.8428805 5	0.709492 6
[T].ELHLDGNKISR.[V]	P07585; P07585-3	0.71031743	1	0.8436508	0.717460 33
[T].AGPSGPSGLPGER.[G]	P08123	0.5430029	1	0.7390671	0.518950 46
[V].GAVGTAGPSGPSGLPGER.[G]	P08123	0.5949367	1	0.7967651 5	0.625879 05
[C].IDNSGVYTNEYGGR.[E]	Q02413	0.8479485	1	0.8994368 3	0.781174 6
[F].DQDIYGR.[E]	P50454	0.6519461	1	0.7919162	0.558383 2
[I].SVPGPMGPSGPR.[G]	P02452	0.79568964	1	0.8620689 5	0.686206 9
[Y].YDVMSDEEIER.[I]	O15460	0.6995633	1	0.8445415	0.677729 25
[W].GDSLEETGAATGSR.[R]	Q8IVF2	0.6294487	1	0.8108862 6	0.607815 74
[S].SQFSSGSQSSR.[D]	P02533	0.6743295	1	0.8482758 4	0.694252 85
[G].GISVPGPMGPSGPR.[G]	P02452	0.6738609	1	0.8657074 6	0.705036
[R].QLEEAEEEAQR.[A]	P35579	0.7375215	1	0.8760757 4	0.712564 5
[H].AEAQGDEGDGEEGLQR.[T]	Q8IVF2	0.58226836	1	0.8290735	0.599840 3
[Q].AVQGQSEGSR.[R]	P20930	0.80316204	1	0.8434782 6	0.601581 04
[P].LNVKVDPEIQNVKAQER.[E]	P35908	0.81439084	1	0.9035159 3	0.769419 43
[C].SQTPGGGNTNFGR.[G]	P05997	0.6310452	1	0.8369735	0.622464 9
[F].QINQDEEEEEDED.[-]	P35268	0.7415459	1	0.8510467	0.623188 4
[S].GGGFGGGGFGGGR.[F]	P35908	0.82752764	1	0.9116397 5	0.763806 3
[I].DGRPGPIGPAGAR.[G]	P08123	0.7846154	1	0.8704454	0.643724 7
[L].ADEIANSSGKGALALEEKR.[R]	P35579	0.6699322	1	0.4634514	0.593820 63
[Y].DEKSTGGISVPGPMGPSGPR.[G]	P02452	0.77598155	1	0.6143187	0.688991 55
[Y].LEIDEVTTDSFR.[V]	Q05707	0.757329	1	0.5708469	0.649022
[G].GDGGLLSGNEKVTMQNLNDR.[L]	P13645	0.90142024	1	0.8345864 4	0.860484 54
[Y].VGDEAQSKR.[G]	P63267; P60709; P62736; P68133; P63261	0.6897759	1	0.5259104	0.604341 75
[L].EEAEKAADESER.[G]	P09493-5; P09493-7; P67936; P06753-2; P07951	0.5913371	1	0.4149403 6	0.519146 26
[L].HDAMHETLCPGVTDAAKACNLDVILGFDGSR.[D]	P12111; P12111-4	0.7113821	1	0.5020325	0.560298 1
[K].ISNIPDEYFKR.[F]	P51884	0.7471182	1	0.5994236 5	0.648414 97
[F].GLDEEDEDEDEDEEEEEGGKGEKR.[K]	Q92688	0.7254902	1	0.5408497	0.589052 26
[K].SVPKEISPDTTLLDLQNNDISELR.[K]	P21810	0.8216927	1	0.7337715 6	0.763352 5
[R].ETDPLGKPR.[F]	Q7Z7G0	0.7623574	1	0.5982256	0.625475

8.8 CLUSTERED PEPTIDE HITS AT 5-7 HOURS

Annotated Sequence	Master Protein Accessions	5h	7h	8h	9h	10h
[Q].EMIGSVEEQLAQLR.[C]	P02533	1	0.993614	0.54917	0.475734	0.568966
[K].DAEEWFFTKTEELNR.[E]	P02533	1	0.781633	0.559864	0.519048	0.622449
[L].VQSGKSEISELR.[R]	P02533; Q04695	1	0.851461	0.358608	0.482909	0.504661
[E].VATNSELVQSGKSEISELR.[R]	P02533; Q04695	1	0.72973	0.420206	0.509009	0.509009
[L].DTKWTLLQEQGTKTVR.[Q]	P04259; P13647	1	0.876494	0.522709	0.596016	0.560159
[V].KAQYEEIANR.[S]	P13647	1	0.923025	0.404284	0.556225	0.585676
[T].EAESWYQTKYEELQQTAGR.[H]	P13647	1	0.880902	0.45666	0.606765	0.591966
[V].ATNSELVQSGKSEISELR.[R]	P02533; Q04695	1	0.866291	0.428571	0.571429	0.615764
[N].VEMNAAPGVDLTQLLNNMR.[S]	P13645	1	0.822546	0.49137	0.592772	0.433118
[L].EPLFEQYINNLR.[R]	P04259; P02538; P13647	1	0.684138	0.377931	0.54069	0.488276
[A].GGDGLLVGSEKVTMQNLNDR.[L]	P02533; P08779	0.911383	1	0.589337	0.70317	0.695965
[E].MDAAPGVDLSR.[I]	P02533; Q04695; P08779	1	0.912727	0.682909	0.610182	0.681455
[Y].SHGSQETDEEFDAR.[W]	P20674	1	0.909605	0.763519	0.730428	0.72155
[F].SSGSAGIINYQR.[R]	P04264	1	0.914821	0.759796	0.751278	0.725724
[E].PLFEQYINNLR.[R]	P04259; P02538; P13647	1	0.751719	0.530261	0.480055	0.515818
[P].VNSVFLPKDVALAR.[G]	P15924-1	1	0.878378	0.644381	0.608819	0.539118
[V].EMDAAPGVDLTR.[VL]	P19012; Q99456	1	0.841667	0.64697	0.613636	0.581061
[T].VDTSKLVFDGLR.[K]	P15924-1	1	0.968264	0.647668	0.617228	0.593264
[C].IAGVFVDATKER.[L]	Q15149-1; Q15149-2	1	0.96238	0.668947	0.648427	0.606019
[E].EANADLEVKIR.[D]	P02533; P13646; P08779	1	0.964418	0.602669	0.573758	0.619718
[CT].KEIDLVNR.[D]	Q03135	1	0.891509	0.688679	0.67217	0.658019
[Q].VGGDVNVEMDAAPGVDLSR.[I]	P02533	1	0.887395	0.665546	0.617647	0.692437
[H].VSDTSVVLSMDNNR.[N]	P13647	1	0.936348	0.742044	0.720268	0.701843
[L].EEANADLEVKIR.[D]	P02533; P13646; P08779	1	0.951405	0.671222	0.637054	0.726651
[D].PNTEENLTYLQLKER.[C]	P15924-1	1	0.831748	0.572787	0.580102	0.503292
[T].PLNLQIDPSIQR.[V]	P13647	1	0.719767	0.472093	0.484884	0.511047
[P].DPSLGAR.[S]	Q2TBC4-2	1	0.871881	0.522589	0.500337	0.551585
[R].NTKHEISEMNR.[M]	P13647	1	0.795625	0.544771	0.544087	0.552973
[R].TKYETELNLR.[M]	P02533	1	0.853755	0.561924	0.542161	0.600791
[L].QIDPSIQR.[V]	P13647	1	0.951529	0.57569	0.577927	0.603281
[R].MSVEADINGLR.[R]	P02533; P08727	1	0.960128	0.570175	0.567783	0.633971
[Q].LDSIVGER.[G]	P02538; P13647	1	0.90981	0.642405	0.644778	0.659019
[E].QEIATYR.[SRH]	P02533; P08727; P19012; P13646; Q04695; P08779	1	0.971591	0.619318	0.628247	0.706981

[F].GGGFAGGDGLLVGSEKVTMQNLNDR.[L]	P02533; P08779	1	0.952456	0.63233	0.627575	0.727417
[S].VEEQLAQLR.[C]	P02533; Q04695; P08779	1	0.884728	0.690162	0.708517	0.743759
[L].YNLGGSKR.[I]	P13647	1	0.815033	0.484314	0.54183	0.488889
[E].PLFEQYINNLR.[R]	P04259; P02538; P13647	1	0.837425	0.425348	0.46848	0.489715
[NS].VVLSMDNNR.[NCSY]	P04259; P02538; P13647	1	0.785808	0.437582	0.478975	0.497372
[V].LDELTLAR.[TA]	P02533; P08727; P19012; Q04695; P08779	1	0.814312	0.409007	0.47008	0.526835
[L].VEDFKNKYEDEINKR.[T]	P02538; P05787; P13647	1	0.71313	0.495955	0.567517	0.535781
[H].LIKEAGDAESR.[V]	P31947-1	1	0.919192	0.603175	0.649351	0.541847
[LM].ALDVEIATYR.[K]	P17661; P35908; P04259; P02538; P13647	1	0.979349	0.530663	0.590113	0.545682
[NQTH].EISEMNR.[AMN]	P08729; P05787; P13647	1	0.89397	0.565938	0.621604	0.572565
[P].LNLQIDPSIQR.[V]	P13647	1	0.83415	0.513646	0.563331	0.575227
[R].EVATNSELVQSGKSEISELR.[R]	P02533; Q04695	1	0.914991	0.466973	0.513498	0.594486
[S].QLSMKASLENSLEETKGR.[Y]	P02533; P08779	1	0.974396	0.480614	0.558888	0.595465
[L].VGSEKVTMQNLNDR.[L]	P02533; P08779	1	0.86386	0.522807	0.557193	0.618246
[ML].IGSVEEQLAQLR.[C]	P02533; Q04695; P08779	1	0.979527	0.481766	0.521433	0.641075
[T].KWTLLQEQGTKTVR.[Q]	P04259; P02538; P13647	1	0.901495	0.512908	0.592391	0.654891
[I].QEMIGSVEEQLAQLR.[C]	P02533	0.976962	1	0.624573	0.603242	0.674061
[V].EMDAAPGVDLSR.[I]	P02533; Q04695; P08779	1	0.946695	0.596304	0.627576	0.676617
[T].VDNANVLLQIDNAR.[L]	P02533	1	0.875387	0.630805	0.675697	0.678793
[V].SDDVFSSSR.[H]	P15924-1	1	0.907225	0.719212	0.764368	0.701149
[R].GSGGLGGACGGAGFGSR.[S]	P04259; P02538	1	0.710204	0.556463	0.603401	0.708844
[Q].SGKSEISELR.[R]	P02533; Q04695	1	0.974589	0.627055	0.674888	0.721226
[E].LVQSGKSEISELR.[R]	P02533; Q04695	1	0.94427	0.596546	0.655416	0.737049
[Q].VGGDVNVEMDAAPGVDLSR.[I]	P02533	0.973861	1	0.587752	0.597461	0.737864
[L].PKDVALAR.[G]	P15924-1	1	0.809458	0.440195	0.53338	0.406815
[T].KYETELNLR.[M]	P02533	1	0.920113	0.351275	0.448159	0.44136
[V].EDFKNKYEDEINKR.[T]	P02538; P05787; P13647	1	0.82097	0.30396	0.456776	0.460123
[KQ].ILLDVKTR.[L]	P02533; Q04695; P08779	1	0.947235	0.332486	0.479975	0.464717
[P].LFEQYINNLR.[R]	P04259; P02538; P13647	1	0.68341	0.403833	0.503635	0.468605
[I].AEVKAQYEEIANR.[S]	P13647	1	0.876777	0.36019	0.479265	0.475711
[K].EELAYLKKNHEEEMNALR.[G]	P02533; Q04695	1	0.957609	0.449618	0.551772	0.494788
[L].PVDIAYKR.[G]	P15924-1	1	0.782847	0.465328	0.543187	0.495742
[L].KEELAYLKKNHEEEMNALR.[G]	P02533; Q04695	1	0.947429	0.390526	0.518198	0.499711
[T].LLQEQGTKTVR.[Q]	P04259; P02538; P13647	1	0.877309	0.465699	0.550792	0.505277
[Q].TKYEELQQTAGR.[H]	P13647	1	0.888962	0.400788	0.513798	0.507227

[L].DSIVGER.[G]	P02538; P13647	1	0.830375	0.416831	0.531229	0.514135
[NQTH].EISEMNR.[AMN]	P08729; P05787; P13647	1	0.915989	0.460705	0.544715	0.514905
[D].FKNKYEDEINKR.[T]	P02538; P05787; P13647	1	0.774317	0.396694	0.525111	0.522568
[LF].KNKYEDEINKR.[T]	P04259; P02538; P05787; P13647	1	0.8349	0.446653	0.575878	0.527502
[E].VKAQYEEIANR.[S]	P13647	1	0.810828	0.420037	0.501556	0.528314
[T].KYEELQQTAGR.[H]	P13647	1	0.845388	0.405441	0.517585	0.532847
[R].KLLEGEECR.[MLI]	Q86Y46; P35908; P04259; P02538; P13647	0.962891	1	0.469401	0.566406	0.533854
[L].QKAKQDMAR.[L]	P13647	1	0.953802	0.437811	0.560768	0.534471
[R].VLDELTLAR.[TA]	P02533; P08727; P19012; Q04695; P08779	1	0.88	0.402759	0.486897	0.538621
[G].ELALKDAR.[AN]	P08729; P13647	1	0.902334	0.396192	0.52887	0.539926
[E].DFKNKYEDEINKR.[T]	P02538; P05787; P13647	1	0.798229	0.317521	0.483871	0.540164
[TDAN].AIADAEQR.[G]	Q86Y46; P35908; P04259; P02538; Q14CN4-1; P05787; P13647	1	0.916667	0.428091	0.58871	0.542339
[N].ADLEVKIR.[D]	P02533; P13646; P08779	1	0.8449 1	0.368862	0.535329	0.543713
[AS].LDVEIATYR.[KQR]	Q7Z794; P17661; P35908; P04259; P02538; P13647	1	0.961672	0.503136	0.629965	0.549826
[TSM].KTEELNR.[EY]	P02533; Q04695	1	0.936801	0.374589	0.5549 7	0.551679
[L].DVEIATYR.[KQR]	Q7Z794; P17661; P35908; P04259; P02538; P13647	0.951706	1	0.485512	0.573084	0.556986
[K].WTLLQEQGTKTVR.[Q]	P04259; P02538; P13647	1	0.831359	0.385366	0.521254	0.571429
[R].DQYEKMAEKNR.[K]	P02533; Q04695	1	0.866084	0.459243	0.565502	0.572052
[S].GKSEISELR.[R]	P02533; Q04695	1	0.801993	0.455814	0.568106	0.574751
[R].GELALKDAR.[AN]	P08729; P13647	1	0.878399	0.534743	0.622356	0.579305
[L].ENSLEETKGR.[Y]	P02533; P08779	1	0.974394	0.449461	0.553908	0.598383
[D].AAPGVDLSR.[I]	P02533; Q04695; P08779	1	0.981615	0.58753	0.694644	0.606715
[N].LQNAIADAEQR.[G]	P13647	1	0.818951	0.526227	0.641286	0.620981
[E].IDNVKKQCANLQNAIADAEQR.[G]	P13647	0.951648	1	0.586813	0.610256	0.630769
[L].DELTLAR.[TA]	P02533; P08727; P19012; Q04695; P08779	1	0.95578	0.595811	0.691234	0.633049
[V].GSEKVTMQNLNDR.[L]	P02533; P08779	1	0.875475	0.525437	0.625664	0.647684
[H].EEEMNALR.[G]	P02533; Q04695	0.978528	1	0.465491	0.642638	0.65184
[F].AGGDGLLVGSEKVTMQNLNDR.[L]	P02533; P08779	1	0.916067	0.592326	0.685851	0.652278
[N].LPISGHKHR.[K]	P20930	1	0.942649	0.501616	0.6979	0.659128

[Q].NAIADAEQR.[G]	P13647	1	0.894583	0.557833	0.690337	0.661054
[C].EMEQQNQEYKILLDVKTR.[L]	P02533; Q04695	1	0.929329	0.443816	0.568905	0.665018
[SG].DTSVVLSMDNNR.[NCSY]	P04259; P02538; P13647	1	0.89909	0.643399	0.73824	0.668437
[E].ELQQTAGR.[H]	P13647	1	0.860759	0.451973	0.675354	0.686523
[S].MKASLENSLEETKGR.[Y]	P02533; P08779	1	0.989729	0.477623	0.650037	0.705796
[VI].NVEMDAAPGVDLSR.[I]	P02533; Q04695; P08779	1	0.907121	0.595201	0.71904	0.72678
[A].LEEQLQQIR.[A]	P13645	1	0.871579	0.483509	0.630175	0.472982
[E].ANADLEVKIR.[D]	P02533; P13646; P08779	1	0.778238	0.413365	0.598462	0.525133
[W].YQTKYEELQQTAGR.[H]	P13647	1	0.894118	0.40346	0.584083	0.528028
[A].IADAEQR.[G]	Q86Y46; P35908; P04259; P02538; Q14CN4-1; P05787; P13647	1	0.865772	0.471812	0.632886	0.530872
[L].LVGSEKVTMQNLNDR.[L]	P02533; P08779	1	0.799599	0.356713	0.577822	0.537074
[KR].LLEGEECR.[MLI]	Q86Y46; P35908; P04259; P02538; P13647	0.912814	1	0.454425	0.551519	0.549538
[D].NNIEQISSYKSEITELR.[R]	P13645	0.938122	1	0.579659	0.635846	0.55192
[Q].LSMKASLENSLEETKGR.[Y]	P02533; P08779	0.93652	1	0.490596	0.61442	0.557994
[E].CQNTEYQQLLDIKIR.[L]	P13645	1	0.961868	0.506615	0.662257	0.566537
[E].EALQKAKQDMAR.[L]	P13647	1	0.965091	0.408	0.613091	0.568727
[I].SALEEQLQQIR.[A]	P13645	1	0.87331	0.515302	0.67331	0.570819
[M].EQQNQEYKILLDVKTR.[L]	P02533; Q04695	1	0.881124	0.516466	0.704418	0.636948
[L].LEGEDAHLSSSQFSSGSQSSR.[D]	P02533	1	0.940708	0.568142	0.743363	0.677876
[S].LENSLEETKGR.[Y]	P02533; P08779	1	0.962418	0.504085	0.728758	0.699346
[W].DLEKQIKQLR.[N]	P15924-1	1	0.962072	0.748381	0.827012	0.742831
[R].LENEIQTYR.[S]	P13645	0.938672	1	0.569986	0.661616	0.559163
[L].TATVDNANVLLQIDNAR.[L]	P02533	0.920814	1	0.57994	0.633484	0.573152
[V].EADINGLR.[RK]	P02533; Q7Z3Y7; P08727; Q2M2I5; P13645; P19012; Q99456; P13646; Q04695; Q7Z3Y8	1	0.918129	0.595656	0.773601	0.712615
[T].LEGELHDLR.[G]	P02545	0.958333	1	0.593364	0.799383	0.740741
[A].SYLDKVR.[A]	P02533; P08727; P13645; P19012; Q99456; Q04695; P08779	1	0.875619	0.40099	0.632426	0.490718
[L].LEGEECR.[MLI]	Q86Y46; P35908; P04259; P02538; P13647	1	0.943028	0.422789	0.715142	0.614693
[F].AGGDGLLVGSEKVTMQNLNDR.[L]	P02533; P08779	1	0.967449	0.485995	0.780469	0.707797

[P].PSLTELHLDGNKISR.[V]	P07585	1	0.63307	0.431489	0.689065	0.732543
[C].EWEEITITGSDGSTR.[V]	P15924-1	1	0.975155	0.706004	0.701863	0.644582
[C].TPAAQYVR.[I]	Q14574-1	1	0.943498	0.679567	0.654799	0.597523
[M].ASLSLAPVNIFKAGADEER.[A]	P78371-1	1	0.853116	0.676558	0.545252	0.631306
[K].IHFNPR.[F]	Q9H720	0.869268	1	0.528405	0.715264	0.744011
[R].QLSILVHPDKNQDDADR.[A]	O75937	0.946277	1	0.869934	0.738926	0.69934
[-].MFAKGKGSAVPSDGQAR.[E]	Q9BWW4	0.924448	1	0.820034	0.713073	0.636672
[R].VEEDIQQQKATGSEVSQR.[K]	P15924-1	0.935484	1	0.867281	0.778802	0.711521
[F].SSGSAGIINYQR.[R]	P04264	0.960938	1	0.827257	0.756076	0.741319
[M].AAAKVALTKR.[A]	Q9UJS0	0.940063	1	0.835174	0.69795	0.555994
[R].AEIDNVKKQCANLQNAIADAEQR.[G]	P13647	0.940356	1	0.845081	0.773819	0.683191
[K].IEVLEEELR.[L]	P15924-1	0.937223	1	0.786558	0.70384	0.546529
[S].SGGYGGLGGFGGGSFR.[G]	P13645	0.991228	1	0.846093	0.724083	0.574163
[G].GFSGGSFSR.[G]	P13645	0.968439	1	0.818937	0.768272	0.651993
[C].QEYSGTLR.[R]	Q02413	0.996721	1	0.768033	0.672131	0.513115
[R].YEVTSGGGGTSR.[M]	P15924-1	0.954887	1	0.77218	0.710526	0.582707
[G].GSSGGYGGLGGFGGGSFR.[G]	P13645	0.936762	1	0.782462	0.724283	0.611298
[-].MEGVEEKKKEVPAVPETLKKKR.[R]	P18124	0.977528	1	0.732584	0.642697	0.509363
[V].STGDVNVEMNAAPGVDLTQLLNNMR.[S]	P13645	1	0.997604	0.746805	0.63738	0.503195
[R].IIKGFECKPH.[S]	Q9UBX7-1	1	0.996013	0.665116	0.58804	0.488372
[G].IIEPSLR.[Q]	P62987	0.918398	1	0.75	0.680267	0.589763
[G].SSGGYGGLGGFGGGSFR.[G]	P13645	0.983788	1	0.880546	0.766212	0.639078
[F].GGSSGGYGGLGGFGGGSFR.[G]	P13645	0.921697	1	0.774062	0.71615	0.639478
[-].MEKQPQNSR.[R]	Q9H5K3	1	0.98041	0.803206	0.756901	0.710597
[S].EADSDKNATILELR.[S]	P15924-1	0.961125	1	0.709677	0.628619	0.594706
[Q].AQISALEEQLQQIR.[A]	P13645	0.840241	1	0.715901	0.504898	0.457423
[M].AAEADGPLKR.[L]	O75352	0.95791	1	0.797533	0.573295	0.55225
[-].MKHYEVEILDAKTR.[E]	Q9NZ01-1	0.977666	1	0.847983	0.653458	0.56196
[R].AAPAVQTKTKKTLAKPN.[I]	P55084	0.897632	1	0.805959	0.65699	0.629488
[R].QKEYKCGDLVF.[A]	P51858	0.993743	1	0.883212	0.754953	0.667362
[M].SSKTASTNNIAQAR.[R]	Q9UBI6	0.956835	1	0.884892	0.766587	0.692246
[Y].SKDNEGSWFR.[S]	Q9BPW8	1	0.996503	0.897727	0.777098	0.70542
[G].GGCFGGSSGGYGGLGGFGGGSFR.[G]	P13645	0.855022	1	0.750218	0.606987	0.575546
[R].AAPAVQTKTKKTL.[A]	P55084	0.976654	1	0.765759	0.619455	0.648249
[A].ETDVNVVMLQESQVCEKR.[A]	O14524-1	0.926202	1	0.773632	0.676617	0.674129
[R].KQLATKA.[A]	P84243; P68431	0.813096	1	0.62047	0.481246	0.440559
[-].MLMPKKNR.[I]	P46783	1	0.999198	0.757819	0.619086	0.568565

[M].PKCPKCNKEVYFAER.[V]	P50238	0.951627	1	0.730871	0.6253	0.702726
[Q].ISYDEVGER.[I]	P15924-1	1	0.987858	0.860364	0.772767	0.707719
[D].NNIEQISSYKSEITELR.[R]	P13645	1	0.926913	0.717111	0.651763	0.576956
[V].DNANVLLQIDNAR.[L]	P02533	1	0.984232	0.790871	0.762656	0.711203
[M].TKAGSKGGNLR.[D]	Q96AG4	1	0.993701	0.858268	0.674016	0.672441
[-].MMGHRPVLVLSQNTKR.[E]	P49368-1	0.99907	1	0.906047	0.768372	0.723721
[M].GKVKVGVNGFGR.[I]	P04406-1	0.950337	1	0.860269	0.722222	0.723906
[R].AHESVVKSEDFSLPAYMDR.[R]	P13073	0.974131	1	0.897332	0.773646	0.742118
[A].DITDGNSEHLKR.[E]	Q12907	1	0.957259	0.852616	0.674282	0.578482
[S].ISTSGGSFR.[N]	P13647	0.931818	1	0.783279	0.668019	0.730519
[S].AVAVGKPR.[A]	Q96HS1-1	1	0.977536	0.798502	0.617427	0.559564
[Y].AKDVKFGADAR.[A]	P10809	1	0.958816	0.743243	0.581725	0.535393
[M].PLAKDLLHPSPEEEKR.[K]	P42677	1	0.94632	0.738528	0.596537	0.596537
[M].VNLGLSR.[V]	Q96I45	1	0.948697	0.807003	0.699511	0.699511
[G].PSSTQPALPKAR.[A]	O75251	1	0.92486	0.733813	0.636291	0.652278
[G].GGGVSSLR.[I]	P13645	1	0.943336	0.826816	0.693536	0.573823
[A].LTPTHYLTKHDVER.[L]	P04844-1	1	0.898649	0.731757	0.597973	0.522297
[R].SEIESVKKQCANLETAIADAEQR.[G]	Q86Y46	1	0.94412	0.85575	0.703704	0.573749
[R].QTGKTSIAIDTIINQKR.[F]	P25705-1	1	0.913009	0.749216	0.666144	0.605016
[R].SLNESKIEIER.[L]	P15924-1	1	0.938362	0.869424	0.739659	0.639903
[A].TSVATKKTVQGPPTSDDIFER.[E]	P04181-1	1	0.9592	0.864	0.6872	0.6992
[M].TGYTPDEKLR.[L]	O95139	1	0.940141	0.847183	0.625352	0.602113
[D].GLLVGSEKVTMQNLNDR.[L]	P02533; P08779	0.895131	1	0.803745	0.668165	0.703371
[T].ATVDNANVLLQIDNAR.[L]	P02533	1	0.915323	0.744355	0.6	0.65
[D].AEEWFFTKTEELNR.[E]	P02533	1	0.918285	0.754045	0.610032	0.652104
[S].LLTPLNLQIDPSIQR.[V]	P13647	1	0.983378	0.675603	0.495979	0.639678
[F].SGDTTAPKKTSFGSLKDEDR.[I]	P49821	1	0.973098	0.838586	0.603382	0.62721
[R].QDAYDGKDYIALKEDLR.[S]	P01891	0.979447	1	0.826087	0.603162	0.652174
[R].SGGGGGGGGCGGGGGVSSLR.[I]	P13645	0.918161	1	0.825409	0.653157	0.663289
[M].ADGKAGDEKPEKSQR.[A]	Q8WW12	0.942882	1	0.840949	0.677504	0.728471
[R].TMQNTSDLDTAR.[C]	P14923	1	0.941901	0.883803	0.731514	0.669014
[-].MQSNKTFNLEKQNHTPR.[K]	Q15233	0.996091	1	0.882721	0.664582	0.624707
[Y].AAQTSPSPKAGAATGR.[I]	P06576	1	0.978741	0.918367	0.806122	0.743197
[N].QSLLQPLNVEIDPEIQKVKSR.[E]	P04264	0.923767	1	0.787743	NaN	0.438714
[G].LYFHIGETEKR.[C]	Q7Z7H5	0.992281	1	0.893654	0.703259	0.711835
[C].FGGSSGGYGGLGGFGGGSFR.[G]	P13645	0.985724	1	0.839565	0.530252	0.49898
[M].DNADSSPVVDKR.[E]	Q86UP2-1	1	0.962993	0.834704	0.590461	0.674342

[M].ATKGGTVKAASGFNAMEDAQTLR.[K]	P09525	1	0.984153	0.899083	0.697248	0.674729
[C].YSKSPSNKDAALLEAAR.[A]	Q9H078-1	1	0.978261	0.903986	0.711051	0.736413
[M].SGFLEGLR.[C]	O95807	1	0.976285	0.866403	0.662451	0.544664
[P].NTEENLTYLQLKER.[C]	P15924-1	1	0.889279	0.79877	0.641476	0.605448
[A].SANLGGVPSKR.[L]	P62341	1	0.908745	0.873004	0.712548	0.662357
[V].PVPPLPEYGGKVR.[Y]	P24539	1	0.8761	0.743399	0.57346	0.578876
[-].MKPILLQGHER.[S]	Q13347	1	0.943994	0.900974	0.676136	0.667208
[M].PGPTPSGTNVGSSGR.[S]	P60468	1	0.879593	0.853792	0.568413	0.588741
[M].APKGSSKQQSEEDLLLQDFSR.[N]	Q9UNL2	1	0.971831	0.866197	0.614789	0.497183
[D].TSVVLSMDNNR.[NCSY]	P04259; P02538; P13647	1	0.886918	0.740576	0.643016	0.659276
[M].AAVAATAAAKGNGGGGGR.[A]	Q6Y1H2	1	0.872175	0.815678	0.65113	0.579096
[M].SQAEFEKAAEEVR.[H]	P07108	1	0.891913	0.885692	0.703733	0.657854
[R].SATHLLR.[V]	Q5VT79	1	0.889291	0.752533	0.668596	0.568017
[L].SQMQTHVSDTSVVLSMDNNR.[N]	P13647	1	0.909247	0.821918	0.761986	0.713185
[K].QCANLQNAIADAEQR.[G]	P13647	1	0.888046	0.870019	0.693548	0.677419
[Q].MQTQISETNVILSMDNNR.[S]	P04264	1	0.83365	0.648289	0.459125	0.58365
[A].PEVLPKPR.[M]	P09669	1	0.87813	0.787145	0.614357	0.699499
[M].ASLPVLQKESVFQSGAHAYR.[I]	Q9Y3R4	1	0.94449	0.848384	0.77879	0.677713
[A].APDQDEIQR.[L]	P10619	1	0.940537	0.758521	0.687455	0.564902
[A].EIDNVKKQCANLQNAIADAEQR.[G]	P13647	1	0.863636	0.76025	0.657754	0.58467
[M].PMFIVNTNVPR.[A]	P14174	1	0.981326	0.912232	0.679739	0.715219
[Y].QAELSQMQTQISETNVILSMDNNR.[S]	P04264	1	0.8226	0.724787	0.454435	0.580802
[W].VSSAAQTEKGGR.[T]	Q92947-1	1	0.871674	0.796557	0.641628	0.64867
[C].GVGGYGSR.[S]	P13647	0.914207	1	0.776939	0.482498	0.595745
[D].AALHFNPR.[L]	P47929	0.915254	1	0.798821	0.704495	0.56448
[I].LQEAADVHAR.[Y]	P15924-1	1	0.941652	0.886894	0.821364	0.713645
[QR].GSSVSQDSDSEGHSEDSER.[WR]	P20930	0.524164	1	0.409542	0.465304	0.652416
[I].QEMIGSVEEQLAQLR.[C]	P02533	0.814078	1	0.58378	0.594491	0.648049
[S].CGIGGGIGGGSSR.[I]	P02533; P08779	0.785297	1	0.822891	0.685881	0.715957
[C].EMEQQNQEYKILLDVKTR.[L]	P02533; Q04695	0.710653	1	0.702405	0.528522	0.590378
[M].ADKMDMSLDDIIKLNR.[S]	Q86V81	0.822302	1	0.738849	0.623741	0.643885
[L].FVAPVGVASKR.[H]	O00515	0.714472	1	0.598435	0.434159	0.448501
[M].AEDMETKIKNYKTAPFDSR.[F]	P14854	0.860749	1	0.773616	0.70684	0.75
[R].QGSSVSQDSDSEAYPEDSER.[R]	P20930	0.54729	1	0.453287	0.243945	0.487889
[L].EQPLLGELTVTGVTPDSLR.[L]	P22105	0.540727	1	0.530075	0.450501	0.570802
[H].QGSSVSQDSDSER.[H]	P20930	0.721161	1	0.546218	0.509549	0.587471
[R].NQGSSVSQDSDSQGHSEDSERW.[S]	P20930	0.617072	1	0.439241	0.461766	0.649081

[R].ISSSKGSLGGGF.[S]	P13645	0.886442	1	0.690984	0.702684	0.67722
[R].VTSLGKDWHR.[P]	P50238	0.629963	1	0.563296	0.496629	0.685393
[M].ADKMDMSLDDIIKLNR.[S]	Q86V81	0.824636	1	0.774166	0.710864	0.690334
[R].QSVFPFESGKPF.[K]	P17931	0.593008	1	0.548813	0.651715	0.712401
[-].MNHSPLKTALAYECFQDQDNSTL.[A]	Q13835	0.811452	1	0.764025	0.743783	0.713707
[L].SEVQGWKQR.[M]	Q8IW75	0.706605	1	0.706605	0.623656	0.726575
[K].SISISVAR.[G]	P04264	0.851682	1	0.769113	0.747706	0.738532
[K].NVQDAIADAEQR.[G]	P35908	0.913043	1	0.725821	0.737356	0.73913
[Y].LKKNHEEEMNALR.[G]	P02533; Q04695	0.833742	1	0.523926	0.558896	0.510429
[DE].LEEALQKAKQDMAR.[L]	P13647	0.860883	1	0.581152	0.627524	0.57442
[R].YSSSKHY.[S]	P13645	0.745263	1	0.532632	0.647719	0.644211
[H].SLVGQGQSSGPR.[T]	P20930	0.733182	1	0.7044	0.727135	0.657596
[K].QSLDDAAKTIQDKNKEIER.[L]	P15924-1	0.737734	1	0.7876	0.810883	0.73595
[F].WVNPQFKIR.[L]	P07384	0.572062	1	0.713969	0.605322	0.692535
[R].QLEEAEEEAQR.[A]	P35579-1	0.562362	1	0.707749	0.693727	0.712177
[H].SQAVQGQSEGSR.[R]	P20930	0.89551	1	0.670204	0.653061	0.737959
[I].SISTSGGSFR.[N]	P13647	0.868421	1	0.688722	0.635338	0.740602
[M].SNPRSLEEEKYDMSGAR.[L]	P31944	0.836338	1	0.67129	0.646325	0.581831
[K].QLATKAAR.[K]	P84243; P68431	0.89945	1	0.711705	0.695994	0.6685
[R].KQLATKAAR.[K]	P84243; P68431	0.798784	1	0.545897	0.442553	0.447416
[R].LEQEIATYR.[SRH]	P02533; P08727; P19012; P13646; Q04695; P08779	0.883201	1	0.692141	0.68349	0.620043
[K].LAADAGTFLSR.[A]	Q9Y371	0.848921	1	0.746603	0.727418	0.665068
[R].KQLATKAAR.[K]	P84243; P68431	0.806433	1	0.492982	0.424561	0.363158
[M].TDGILGKAATMEIPIHGNGEAR.[Q]	P53365	0.813333	1	0.848627	0.774118	0.74902
[S].SLPEGIRPGTVLR.[I]	P47929	0.86672	1	0.833998	0.684757	0.748603
[N].LLCGEEQGSDAALHFNPR.[L]	P47929	0.768645	1	0.745053	0.601218	0.577626
[R].LLEGEDAHLSSSQFSSGSQSSR.[D]	P02533	0.791632	1	0.729707	0.623431	0.578243
[R].QATKDAGVIAGLNVLR.[I]	P0DMV8	0.809365	1	0.707358	0.676421	0.588629
[A].GPVLGLKECTR.[G]	P07602-1	0.847515	1	0.877001	0.779275	0.748104
[R].ISSSKGSLGGGFSSGGFSGGSF.[S]	P13645	0.835593	1	0.788983	0.725424	0.665254
[-].KVHGSLAR.[A]	P62861	0.861654	1	0.73985	0.609023	0.615789
[-].MDKVCAVFGGSR.[G]	Q8N4T8	0.953802	0.892204	1	0.447546	0.635226
[M].AQNLKDLAGR.[L]	Q99623	0.961762	1	0.955112	0.680798	0.712386
[M].AADISESSGADCKGDPR.[N]	O43583	0.9348	1	0.934014	0.653574	0.722702
[M].PGVTVKDVNQQEFVR.[A]	P39019	1	0.920418	0.909968	0.584405	0.730707
[M].VLESVAR.[I]	Q8N5K1	0.985207	1	0.907544	0.567308	0.586538

[G].VGGYGSR.[S]	P13647	0.830898	1	0.844816	0.434934	0.629784
[-].MKDSLVLLGR.[V]	O76071	0.962351	1	0.899908	0.598714	0.64371
[R].EITEKQIDDNR.[K]	P23229-1	0.929128	1	0.878505	0.485202	0.727414
[M].GKDYYQTLGLAR.[G]	P25685	0.879087	1	0.844106	0.584791	0.623574
[M].VDYYEVLGVQR.[H]	O75190	0.835059	1	0.892012	0.636834	0.68787
[R].QTATQLLKLAH.[K]	P62424	0.962963	1	0.953488	0.694229	0.729543
[M].APSVPAAEPEYPKGIR.[A]	P54819	0.958333	1	0.936667	0.721667	0.734167
[M].GQNDLMGTAEDFADQFLR.[V]	O15260-1	0.924754	1	0.892405	0.567511	0.747539
[R].QNISPDKIPW.[S]	Q14204	0.963546	1	0.921292	0.478873	0.593206
[R].QVVNFGPGPAKLPH.[S]	Q9Y617-1	0.949165	1	0.939302	0.617602	0.626707
[M].SKISEAVKR.[A]	P30838	1	0.989379	0.95098	0.620098	0.661765
[-].MDNSGKEAEAMALLAEAER.[K]	P54920	0.940625	1	0.942188	0.317969	0.707031
[R].QLVEAKLLDMR.[T]	Q03001-3	0.867226	1	0.867226	0.372467	0.557652
[T].MQKEEDTSGYR.[A]	P15924-1	0.916388	1	0.91806	0.621237	0.625418
[R].QQELKDVGHR.[D]	P35221	0.919968	1	0.91046	0.687005	0.694136
[D].GGNKHFLR.[N]	P40967-1	0.94	1	0.856154	0.499231	0.700769
[N].GAGGALFVHR.[D]	P19404	0.956823	1	0.89283	0.634541	0.709329
[E].QDPGLLQESSR.[L]	Q92817	0.94547	1	0.90604	0.67198	0.72651
[M].APKFPDSVEELR.[A]	Q15785	0.903912	1	0.903912	0.643707	0.730442
[M].VDREQLVQKAR.[L]	P61981	0.899153	1	0.898305	0.7	0.733898
[M].AHYKAADSKR.[E]	Q99417	0.916221	1	0.944742	0.724599	0.738859
[Y].TNEYGGR.[E]	Q02413	0.934646	1	0.912265	0.735004	0.747538
[M].SDFDSNPFADPDLNNPFKDPSVTQVTR.[N]	O15126-1	0.800403	1	0.841398	0.544355	0.584005
[R].QFTSSSSMKGSC.[G]	P02533; P08779	0.8393	1	0.874304	0.609387	0.643596
[-].MIEVVCNDR.[L]	Q9BZL1	0.838658	1	0.895367	0.64377	0.646965
[A].CGVGGYGSR.[S]	P13647	0.932813	1	0.8375	0.589063	0.669531
[M].SLSNKLTLDKLDVKGKR.[V]	P00558	0.897301	1	0.869565	0.678411	0.684408
[M].SSPPEGKLETKAGHPPAVKAGGMR.[I]	P51397	0.844411	1	0.885952	0.660121	0.703172
[A].TVDNANVLLQIDNAR.[L]	P02533	0.890411	1	0.814212	0.612158	0.722603
[R].QSVYEEKLKQFEER.[L]	Q14152	0.842663	1	0.908472	0.576399	0.580182
[R].QYDIDDAIAKNLIDR.[S]	Q15149-1; Q15149-2	0.830952	1	0.9	0.614286	0.630952
[R].QIILEKEETEELKR.[F]	P12956	0.892596	1	0.938975	0.555736	0.653377
[K].LDDGHLNNSLSSPVQADVYFPR.[L]	Q3ZCW2	0.872781	1	0.947732	0.61144	0.689349
[A].TPENYLFQGR.[Q]	P04440	0.940138	1	0.967767	0.621642	0.7099
[M].PAYFQRPENALKR.[A]	Q14152	1	0.984155	0.971831	0.585387	0.663732
[M].GVQGFQEFLEKR.[C]	Q9NX05-1	0.862445	1	0.946143	0.521834	0.590975
[R].QKDVKDGKYSQVLANGLDNKLR.[E]	P62269	0.966693	1	0.980967	0.60904	0.692308

[G].AEGPDEDSSNR.[E]	P13667	0.893117	1	0.965182	0.68502	0.71498
[L].LTPLNLQIDPSIQR.[V]	P13647	0.950249	0.99005	1	0.495854	0.684909
[-].MQPASAKWYDR.[R]	Q15185	0.987654	1	0.998354	0.609053	0.700412
[M].SAEVETSEGVDESEKKNSGALEKENQMR.[M]	P30519	0.84009	1	0.840841	0.66967	0.677177
[R].TTAENEFVML.[K]	P13647	0.868007	1	0.881993	0.694056	0.700175
[M].ATVTATTKVPEIR.[D]	Q9Y230	0.876442	1	0.855848	0.733114	0.743822
[G].EICGPGIDIR.[N]	P08069	0.828549	1	0.854067	0.686603	0.745614
[M].AANATTNPSQLLPLELVDKCIGSR.[I]	Q9Y4Y9	0.770207	1	0.784903	0.50501	0.513694
[-].MPPYTVVYFPVR.[G]	P09211	0.899753	1	0.996713	0.662284	0.720624
[-].MLGGLGKLAAEGLAHR.[T]	B3EWG6	0.784817	1	0.934462	0.432004	0.472966
[F].LTALAQDGVINEEALSVTELDR.[V]	Q8WUM4	0.844106	1	0.977186	0.557668	0.664766
[M].PDYLGADQR.[K]	P35998	0.915011	0.961369	1	0.626932	0.737307
[-].MMLGTEGGEGFVVKVR.[G]	P31943	0.906585	0.948698	1	0.534456	0.740429
[A].SSEAPPLINEDVKR.[T]	P04843	0.962069	1	0.987931	0.700862	0.716379
[D].SEESPAIEAIHLLR.[K]	P13716-1	0.835025	1	0.970389	0.637902	0.691201
[M].MLGTEGGEGFVVKVR.[G]	P31943	0.910201	0.982563	1	0.648649	0.707062
[R].APDPGFQER.[F]	Q9UHL4	0.941448	0.996918	1	0.654083	0.674114
[M].AKEEPQSISR.[D]	Q96B96	1	0.999147	0.998295	0.690537	0.702472
[S].FSWDNCDEGKDPAVIR.[S]	P17900	1	0.851899	0.735443	0.646203	0.491139
[Y].SKDNEGSWFR.[S]	Q9BPW8	1	0.884465	0.836066	0.751756	0.622951

9 ABSTRACT

Pemphigus vulgaris (PV) is an autoimmune skin blistering disease. Autoantibodies (IgG) form against desmoglein (Dsg) 1 and 3 and induce the separation of keratinocytes (acantholysis) leading to intraepidermal split formation of the skin and / or mucous membranes. The current treatment options are not considered satisfactory as they consist mostly of systemic corticosteroid application. To improve treatment options, the underlying pathogenesis causing the loss of cell adhesion needs to be fully understood. Therefore, comprehensive insights into anti-Dsg 1 / 3 induced signalling in the course of split formation are needed.

To address this, a human skin organ culture model was employed and intraepidermal split formation induced by injecting an anti-Dsg 1 / 3 single-chain variable fragment (scFv). We set up time course experiments using defined time points within a 24 hours (h) time frame. By performing immunofluorescence stainings, we could show the honeycomb-like binding pattern of the scFv and also the binding pattern of the main target structures of PV autoantibodies Dsg 1 and 3. Semi-quantitative histomorphometry of Haematoxylin and Eosin stained skin sections was performed. First blisters could be observed already 5 h after scFv injection while the first significant increase in split formation was reached after 7 h.

In the next step, a proteome analysis of the samples from the time course experiments was performed to identify proteins, peptides and proteases that might be involved in PV pathogenesis.

The peptides originating from the skin samples were distinguished from tryptic peptides using terminal amine isotopic labelling of substrates (TAILS). TAILS is a method of quantitative proteomics and its efficiency to increase the proteome coverage could be shown. Furthermore, the overlap of proteins and peptides between the different skin donors was measured suggesting a certain comparability between the samples. All unique, quantifiable protein hits were clustered to identify proteins showing an upregulation at 5–7 h after injection of the scFv and confirmed the role of previously described proteins that are suspected to be involved in the pathomechanisms of PV such as kallikrein and the epidermal growth factor.

The identified proteins and peptides could potentially act as target structures for future treatment options.

10 EXTENDED ABSTRACT IN GERMAN

Einleitung

Pemphigus vulgaris (PV) gehört zu den blasenbildenden Autoimmundermatosen und ist gekennzeichnet durch die Aufhebung der epithelialen Zelladhäsion (Akantholyse) sowie Bildung intraepidermaler Blasen an mukösen Geweben und Teilen des restlichen Integuments. Es findet eine pathologische Bildung zirkulierender Immunglobulin G (IgG) Antikörper (AK) statt, welche gegen strukturelle desmosomale Adhäsionsproteine epidermaler Keratinozyten gerichtet sind. Die Zielantigene des PV sind Desmoglein (Dsg) 1 und 3.

Klinisch führt PV zu schmerzhaften, erythematösen, oberflächlichen Läsionen an Haut und Schleimhäuten, wodurch eine massive Einschränkung der Lebensqualität bei PV Patienten vorliegt. Zusätzlich zu der Entwicklung der klinisch sichtbaren Erkrankung sind in der histologischen Untersuchung einer Läsion intraepitheliale Spaltbildung und in der direkten Immunfluoreszenz (DIF) ein Honigwaben-artiges, interzelluläres Fluoreszenzmuster der abgelagerten Auto-AK erkennbar.

Für die Therapie des PV stehen derzeit vor allem die Gabe von hochdosierten Kortikosteroiden, Immunapherese, die intravenöse Immunglobulin (IVIg) -Therapie sowie die Gabe von Rituximab, einem Anti-CD20 AK, zur Verfügung. Alle diese Therapieansätze beruhen auf einer generellen Immunsuppression. Aufgrund des großen Spektrums an unerwünschten Nebenwirkungen und einer mäßigen Remissionsrate besteht großer Bedarf für zielgerichtetere und nebenwirkungsärmere Therapieoptionen. Ohne immunsuppressive Therapie betrug die Letalität von PV beinahe 100 % und auch mit den heutigen Therapieoptionen liegt sie bei 5–10 %. Zur Verbesserung der Lebensqualität und der weiteren Senkung der Letalität ist die präzise Erforschung des Pathomechanismus und der Signalwege von PV erforderlich.

Ein Modell für PV ist die humane Hautorgankultur (engl. *human skin organ culture*, *HSOC*), welche ein Anti-Dsg 1 / Dsg 3 Einzelkettenfragment (engl. *single chain variable fragment*, *scFv*) nutzt, um die intraepidermale Blasenbildung in gesunder Haut hervorzurufen. Das *scFv* Px4-3 wurde durch *Antibody Phage Display* aus dem Serum von an PV erkrankten Patienten gewonnen und in *Escherichia coli* (*E. coli*) vermehrt.

Ziel meiner Arbeit ist es, in diesem *HSOC* Modell den exakten Zeitpunkt der intraepidermalen Spaltbildung durch Px4-3 zu bestimmen. Ein weiteres Ziel ist, aus den Proben der *HSOC* eine Proteomanalyse durchzuführen, um an der Pathogenese von PV beteiligte Proteine, Peptide und Proteasen als mögliche Zielstrukturen für neue Therapieoptionen zu identifizieren.

Methoden

Um den Zeitpunkt der intraepidermalen Blasenbildung zu bestimmen wurden Zeitreihenversuche in der *HSOC* etabliert, bei denen nach einer definierten Zeit die Inkubation der Hautproben abgeschlossen und die Probe auf eine Blasenbildung hin mithilfe einer Hämatoxylin-Eosin (HE) Färbung und DIF untersucht wurde. Es wurden 24 Stunden (h) Versuche und 11 h Versuche etabliert, bei denen jeweils nach 0, 6, 12, 18, 24 h inklusive einer 24 h Negativkontrolle (NC) beziehungsweise (bzw.) nach 5, 7, 8, 9, 10, 11 h die Inkubation beendet wurde. Als NC wurde IVIg verwendet, welches ebenfalls intradermal in die Hautproben appliziert wurde. Anhand der HE Färbung wurde eine semiquantitative Histomorphometrie durchgeführt, um das Ausmaß und den Zeitpunkt der Spaltbildung zu identifizieren. Das *scFv* wurde durch eine spezifische DIF Färbung angefärbt und sein Bindungsmuster in der Epidermis dargestellt. Außerdem wurden diese Proben mithilfe zweier indirekten Immunfluoreszenzfärbungen auf die Verteilung von Dsg 1 und Dsg 3 in der Epidermis hin untersucht.

Zur weiteren Untersuchung der PV Pathomechanismen wurde im Anschluss eine Proteomanalyse der Proben der *HSOC* Zeitreihenversuche durchgeführt. Die standardisierte 6plex–*TMT* (engl. *tandem mass tag*) -*TAILS* (engl. *terminal amine isotope labelling of substrates*) ist eine Methode der quantitativen Proteomik. Durch N-terminale Markierungen ermöglicht *TAILS*, die Zugehörigkeit von Peptiden zu Proteinen zu bestimmen und erlaubt gleichzeitig eine Unterscheidung zwischen durch Trypsin entstandenen Peptiden und internen Peptiden aus der Ursprungsprobe.

Je fünf Zeitpunkte aus einem Zeitreihenexperiment (0, 6, 12, 24 h, NC bzw. 5, 7, 8, 9, 10 h) wurden gemeinsam untersucht. Ein Referenzkanal wurde zu gleichen Teilen aus den jeweiligen fünf Proben zusammengefügt. Zuvor wurden die Proteine zum einen mittels *PCT* (engl. *pressure cycling technology*) und zum anderen mittels

einer Ultraschallbehandlung aus den Hautproben isoliert. Im letzten Schritt wurden sowohl *preTAILS*- (gesamtes Proteom der Hautprobe) als auch *TAILS*- (erweitertes Proteom, in dem keine durch Trypsin entstandenen Peptide mehr vorhanden sein sollten) Proben mittels Flüssigchromatographie-Tandem-Massenspektrometrie (LC-MS / MS) gemessen. Die Daten wurden anschließend vom *Proteome Discoverer 2.2.* normalisiert.

Ergebnisse

Die Zeitreihenversuche der *HSOC* zeigten einen ersten signifikanten Anstieg der epidermalen Spaltbildung nach 7 h. Bereits nach 5 bzw. 6 h trat die Spaltbildung in den untersuchten Proben erstmals auf.

Die DIF Färbungen für Px4-3 zeigten ein Honigwaben-artiges Bindungsmuster des *scFv* zwischen den Keratinozyten. Ein ähnliches Muster konnte auch für Dsg 1 und 3 gezeigt werden. Dsg 1 war in den oberflächlicheren epidermalen Schichten anfärbbar, während Dsg 3 erwartungsgemäß in den basalen Schichten aufzufinden war.

Im Anschluss an die MS Messung wurden alle einzigartigen, quantifizierbaren Proteine und Peptide zwischen den *preTAILS* und *TAILS* Analysen verglichen. Wir konnten zeigen, dass *TAILS* die Erfassung des Proteoms durch einzigartige, zuvor nicht identifizierte Proteine und Peptide um ca. 450 Proteine und um ca. 3.000 Peptide pro Experiment erweitert. Außerdem wurde die Überschneidung der Proteine bzw. Peptide zwischen den einzelnen Zeitreihenversuchen ermittelt, um die Vergleichbarkeit der Ergebnisse trotz unterschiedlicher Herkunft der Hautproben einordnen zu können. Zwischen den drei Hautproben pro 24 bzw. 11 h Versuch lag die Überschneidung zwischen 20 und 50 %.

Das identifizierte Proteom wurde zunächst auf die Zusammensetzung der molekularen Proteinfunktionen hin untersucht. Wir stellten fest, dass die katalytischen Funktionen ebenso wie die Bindungsfunktion einen Großteil der identifizierten Proteine ausmachten (ca. 80 %). Die Gruppe der Bindungsfunktion kann zu etwa gleichen Teilen (jeweils ca. 20 %) unterteilt werden in Proteinbindungsfunktion, organisch zyklische Compoundbindungsfunktion und heterozyklische Compoundbindungsfunktion. Zu der Gruppe der Proteinbindungs-

funktion gehören Proteine der Zelladhäsion sowie der Enzym- und Komplementbindung.

Im nächsten Schritt wurden Proteine, die mit der Pathogenese von PV assoziiert sind, in den Ergebnissen der MS Analyse identifiziert. Des Weiteren wurden alle quantifizierbaren Proteine aus den *preTAILS* Analysen geclustert. Es wird deutlich, dass die 5 und 7 h Proben sich am meisten von den anderen Proben bzw. Zeitpunkten unterscheiden und mehrere Gruppen an Proteinen zeigen, die während der Zeit der Spaltbildung hochreguliert werden.

Diskussion

Das Wissen über den Zeitpunkt der intraepidermalen Spaltbildung in der *HSOC* wird große Relevanz im Hinblick auf weitere Testungen von Therapieoptionen und deren Applikationsformen im *HSOC* Modell haben, da die Zeit bis zum Wirkungseintritt nicht größer sein darf als die Zeit bis zum Einsetzen der Spaltbildung.

Das anti-Dsg 1 / Dsg 3 *scFv* wird in Zukunft eine große Relevanz für PV Krankheitsmodelle haben, da es beide Antigene erreicht und sich gut dosieren lässt. Die schnelle, zuverlässige und günstige Herstellung des *scFvs* ist ebenfalls ein großer Vorteil gegenüber Patienten AK.

Die Ergebnisse der Proteomanalysen zeigen eine gesteigerte Abdeckung des Proteoms durch die *TAILS* Methode, auch im Vergleich zu bisher in der Literatur beschriebenen Methoden. Proteine wie Kallikrein und *epidermal growth factor receptor* (EGFR) Kinasen, die bereits zuvor in der Literatur im Zusammenhang mit der PV Pathogenese beschrieben wurden, konnten identifiziert werden. Ihr Verlauf über die Zeit spricht weiterhin für eine Beteiligung am PV Pathomechanismus.

Im weiteren Verlauf wird die bioinformatische Auswertung der Proteomanalyse vertieft werden. Die durch die Clusteranalysen identifizierten Proteine und Peptide, die eine Hochregulierung zwischen 5 und 7 h zeigten, werden genauer untersucht werden. Des Weiteren werden mit Hilfe der genauen Positionen der durch die Clusteranalysen identifizierten Peptide im Masterprotein, sowie der Spaltstellen, die dazugehörigen Proteasen identifiziert werden.

Die hier identifizierten Proteasen und Proteine stellen potentielle Zielstrukturen für zukünftige Therapieoptionen dar und sollten daher in Zukunft noch genauer untersucht werden.

11 ACKNOWLEDGEMENTS

Firstly, I would like to thank my supervisor Prof. Jennifer Hundt. You have been the best supervisor I could have asked for and I am very grateful for your patience, your positive and supportive attitude, the constant sugar uptake and all the long nights in your office (and also on facetime due to the corona virus outbreak).

I want to thank my mentors Dr. Dr. Christoph Hammers and PD Dr. Katja Bieber for their support, as well as Prof. Ralf Ludwig for his input and the helpful ideas.

I would like to thank Dr. Valina from the *Holstentor Privatklinik*, the *Aesthetikum Praxisklinik* in Bremen, the Department of Plastic Surgery at the University Medical Centre Schleswig-Holstein, Lübeck and all their patients for providing the skin used in my experiments.

A huge thank you to the whole Research Training Group 1727 and Prof. Zillikens for providing my scholarship and especially for supporting my internship in Copenhagen. I am very grateful for the back-up and support I received.

I want to thank Prof. Ulrich auf dem Keller for letting me join his group at the Technical University of Denmark in Copenhagen so spontaneously and for providing me with the facilities and help to perform the proteome analyses. I want to thank my mentors Dr. Philipp Kastl and Dr. Farrell McGeoghan for their support and the excellent supervision! Philipp, thank you for taking so much time and patience to help me write a ‘proper’ medical thesis. Also, thank you to Dr. Louise Bundgaard and Dr. Simonas Savickas for your assistance. You all made me feel very welcome in beautiful Copenhagen - tak!

Thank you to the whole Hundt lab group! I am so glad I got to work with every single one of you, I could not have asked for a better team. Nadine Merg, thank you for always keeping everyone’s spirit up and keeping the whole group on track. Also, thank you to Nick Feldmann and Julia Möller for bearing me a hand with some of the experiments.

For many long evenings filled with discussions about terminology and formatting, I want to thank David. You helped me to stay sane through this dissertation and somehow managed to tolerate me. I could not have done it without you.

Last but not least, I want to thank my parents and my sister for their continuous love, encouragement and support not only during the time of this dissertation, but always.

12 CURRICULUM VITAE

Hanna Asmussen
29th August 1996, Bremen

Education:

2012	General Certificate of Secondary Education (GCSE's)
2014	General higher education entrance qualification (Abitur)
2014	Beginning of medical studies, University of Lübeck
2016	First state examination (M1)
2021	Expected graduation from the University of Lübeck

Dissertation:

04/2019 – 09/2019	Research Training Group 1727 "Modulation of Autoimmunity" scholarship
04/2019 – 08/2019	Laboratory time *Lübecker Institut für Experimentelle Dermatologie*
08/2019 – 09/2019	Laboratory internship Technical University of Denmark, Copenhagen
04/2019 – 06/2020	Complete duration of dissertation

Publications and scientific contributions:

11/2019	Poster presentation at the New Developments in Immunology, Inflammation and Infection conference, Research Center Borstel